Functional significance of genes associated with fat distribution

Dissertation
zur Erlangung des akademischen Grades
Dr. rer. nat.

an der Medizinischen Fakultät
der Universität Leipzig

eingereicht von: Dipl. troph. Jacqueline Herold (geb. Krüger)
geboren am: 21.04.1988 in Neu Kaliß

angefertigt an: Universität Leipzig, IFB Adiposity Diseases
Abteilung Endokrinologie, Nephrologie and Rheumatologie

Betreuer: Prof. Dr. rer. med. Peter Kovacs
Dr. rer. nat. Dorit Schleinitz

Beschluss über die Verleihung des Doktorgrads vom: 17. Dezember 2019

Table of content

Abbreviations *4*

Chapter 1 Introduction *7*

1.1. Obesity and fat distribution **7**

1.1.1. Measurement of fat distribution 8

1.1.2. Which factors determine fat distribution? 8

1.2. Genetics of obesity and fat distribution **10**

1.3. Genome wide associations studies (GWAS) **13**

1.4. Candidate genes **15**

1.4.1. Hypoxia inducible factor 3 A (*HIF3A*) 15

1.4.2. Replication initiator 1 (*REPIN1*) 16

1.4.3. Iriquois homeobox 3/5 (*IRX3/5*) 17

1.4.4. Krüppel like factor 13 (*KLF13*) 17

1.5. Aim of the thesis **18**

1.6. References **18**

Chapter 2

Publication: Hypoxia- inducible factor 3A gene expression and methylation in adipose tissue is related to adipose tissue dysfunction *27*

Chapter 3

Publication: Metabolic effects of genetic variation in the human REPIN1 gene *44*

Chapter 4

IRX3 and IRX5 expression in subcutaneous and visceral adipose tissue in obesity *64*

4.1. Abstract **65**

4.2. Introduction **66**

4.3. Material and Methods **66**

4.3.1. Subjects 66

4.3.2. Measurement of human *IRX3 and IRX5* mRNA expression 68

4.3.3. Genotyping of *FTO* SNP rs8050136 68

4.3.4. Statistical analysis 68

4.4. Results and Discussion **69**

4.4.1. Correlation of *IRX3* and *IRX5* mRNA expression with metabolic parameters 69

4.4.2. Differences of *IRX3* and *IRX5* mRNA expression in subcutaneous and visceral adipose tissue 71

4.4.3. Association of rs8050136 with metabolic traits 72

4.5. Summary **73**

4.6. References **74**

Chapter 5

KLF13 is a new candidate gene for the regulation of body fat distribution 76

5.1. Abstract..... 77

5.2. Introduction 78

5.3. Materials and Methods..... 79

5.3.1. Subjects 79
5.3.2. Measurement of *KLF13* 79
5.3.3. Genotyping of rs8042543 79
5.3.4. Cell culture..... 79
5.3.5. siRNA knockdown of *Klf13*..... 80
5.3.6. Lipid staining..... 80
5.3.7. RNA isolation and reverse transcriptase PCR (RT-PCR) analysis..... 81

5.4. Results and Discussion 81

5.4.1. mRNA expression levels in AT correlate with metabolic traits and with rs8042543..... 81
5.4.2. *Klf13* knockdown affects the mRNA expression of *Cebpb* and *Pparg* in adipocytes 84

5.5. Summary..... 89

5.6. References 90

Chapter 6 Zusammenfassung der Arbeit..... 92

Darstellung des eigenen Beitrags zur Publikation „Hypoxia- inducible factor 3A gene expression and methylation in adipose tissue is related to adipose tissue dysfunction“.... 97

Darstellung des eigenen Beitrags zur Publikation „Metabolic effects of genetic variation in the human REPIN1 gene”..... 98

Erklärung über die eigenständige Abfassung der Arbeit..... 99

Curriculum Vitae.....100

Danksagung 104

Abbreviations

% body fat	percentage of body fat
%	percentage
°C	degree Celsius
µm	micrometers
µmol/kg/min	micromol per kilogram per minute
ABSI	A Body Shape Index
ADAMTS9	*a disintegrin-like and metallopeptidase with thrombospondin type 1 motif 9*
adj	adjusted
AGPAT2	*lysophosphatidic acid acyltransferase-β*
AKT1	*AKT serine/threonine kinase 1*
AT	adipose tissue
ATF-4	*activating transcription factor 4*
ATXN1	*ataxin 1*
AU	arbitrary unit
BMI	body mass index
BMP2	*bone morphogenetic protein 2*
Bp	base pairs
BSCL2	*seipin*
C/EBPA	*CCAAT/ enhancer binding protein alpha*
C/EBPB	*CCAAT/ enhancer binding protein beta*
C/EBPγ	*CCAAT/enhancer binding protein gamma*
CAV1	*caveolin 1*
CCL5	*C-C motif chemokine ligand 5*
CGL	congenital generalized lipodystrophy
cm	centimeter
cm^2	square centimeter
CO_2	carbon dioxide
CPEB4	*cytoplasmic polyadenylation element binding protein 4*
CT	computerized tomography
DEPICT	Data-driven Expression Prioritized Integration for Complex Traits
DEXA	dual energy X-ray absorptiometry
DMEM	Dulbecco´s Modified Eagle´s Medium
DNA	desoxy ribonucleic acid
DNM3-PIGC	*dynamin 3-phosphatidylinositol glycan anchor biosynthesis class C*
Epi	epididymal
eQTL	expression quantitative trait loci
et al.	et alii, et aliae, et alia
EWAS	epigenomic wide association study
FBS	fetal bovine serum

FD	fat distribution
FFA	free fatty acids
FML	familial multiple lipomatosis
FPG	fasting plasma glucose
FTO	fat mass and obesity associated
GRAIL	Gene Relationships Among Implicated Loci
GRB14-COBLL1	*growth factor receptor bound protein 14 - cordon-bleu WH2 repeat protein like 1*
GWAS	genome wide associations studies
h	hour
HAART	highly active antiretroviral therapy
HbA1c	glycohemoglobin
HDL	high density lipoprotein
HIF3A	*hypoxia inducible factor 3 alpha*
HIV	human immunodeficiency virus
HMGA2	*high mobility group AT-hook 2*
HOXC13	*homeobox C13*
IBMX	3-isobutyl-1-methylxanthine
Ing	inguinal
IR	insulin resistance
IRX3/5	*iriquois homeobox 3/5*
ITPR2-SSPN	*inositol 1,4,5-trisphosphate receptor type 2- sarcospan*
kDa	kilo dalton
kg/m²	kilogram per square meters
KLF13	*kruppel like factor 13*
LD	linkage disequilibrium
LDL	low density lipoprotein
LHFP	*LHFPL tetraspan subfamily member 6*
LHX2	*LIM homeobox 2*
LMNA	*lamin A/C*
LPP	*LIM domain containing preferred translocation partner in lipoma*
LY86	*lymphocyte antigen 86*
LYPLAL1	*lysophospholipase like 1*
m	meter
MAGENTA	Meta-Analysis Gene-set Enrichment of variaNT Associations
Mb	megabase
MCR4	*melanocortin 4 receptor*
mM	milli Molar
mmol/l	millimol per liter
MRI	magnetic resonance imaging
mRNA	messenger Ribonucleic Acid
ms	milliseconds
NCBI	National Center for Biotechnology Information

NCEP-ATP III	The third Report of the National Cholesterol Education Program of the Expert Panel on Detection, Evaluation, and Treatment of High Blood Cholesterol in Adults
NFE2L3	*nuclear factor, erythroid 2 like 3*
NISCH-STAB1	*nischarin- stabilin 1*
nM	nanomolar
OGTT	oral glucose tolerance test
p	p-value
PBS	phosphate buffered saline
pmol/l	picomol per liter
PPARG	*peroxisome proliferator activated receptor gamma*
PTEN	*phosphatase and tensin*
PTRF	*caveolae associated protein 1*
QTL	quantitative trait locus
R	correlation coefficient
RANTES	*synonym for CCL5 (C-C motif chemokine ligand 5)*
REPIN1	*replication initiator 1*
RREB1	*ras responsive element binding protein 1*
RSPO3	*R-spondin 3*
ScAT	subcutaneous adipose tissue
SHBG	*sex-hormone binding globulin*
siRNA	small interfering ribonucleic acid
SNP	single nucleotide polymorphism
T2D	type 2 diabetes
T3	triiodthyronine
TBOX15-WARS	*T-box 15- tryptophanyl-tRNA synthetase*
TG	triglyceride
TRIB2	*tribbles pseudokinase 2*
unadj.	unadjusted
V	volt
VAT	visceral adipose tissue
VEGFA	*vascular endothelial growth factor A*
WC	waist circumference
WCadjBMI	waist circumference adjusted for body mass index
WHO	world health organisation
WHR	waist-to-hip-ratio
WHRadjBMI	waist-to-hip-ratio adjusted for body mass index
ZNRF3-KREMEN1	*zinc and ring finger 3- kringle containing transmembrane protein 1*

Chapter 1 Introduction

1.1. Obesity and fat distribution

Obesity is a worldwide health problem with more than 650 million obese adults reported in 2016 [1]. According to the World Health Organization (WHO) obesity is an "abnormal or excessive fat accumulation that may impair health" [1]. The most common measurement of obesity is the body mass index (BMI), whereby obesity is defined as a BMI>30 kg/m². One major cause of obesity is the dysbalance between energy intake and expenditure, resulting in storage of triglycerides (TG) in adipose tissue (AT). It is well acknowledged that both genetic and environmental factors play a role in the etiology of this complex heterogeneous disease. There is a strong evidence that obesity is associated with increased individual risk for comorbidities like type 2 diabetes (T2D), fatty liver disease, hypertension or cardiovascular disease [2]. Nevertheless, obesity alone does not necessarily lead to these comorbidities. In the last two decades it has been shown that the AT is not only a passive fuel reservoir, but also an endocrine organ distributed to different sites of the body [3]. Peiris [4] and Björntorp [5] could show very early that anthropometric parameters correlate with fat distribution (FD) and that the body fat is mainly distributed in two fat depots, subcutaneous and visceral AT (ScAT and VAT). If the fat is preferentially stored in VAT (android/"apple" body shape [6]), subjects with obesity are more fragile for complications such as metabolic and cardiovascular diseases (Figure 1). The regional AT distribution appears to be the major mediator between obesity and metabolic disorders in glucose and lipid metabolism [7]. VAT is represented by mesenteric, gonadal, epicardial, retroperitoneal, omental and peri-renal fat pads, while ScAT includes abdominal, gluteal and femoral depots. These fat depots differ in their structure and function, which could, at least partially, explain the higher risk for metabolic and cardiovascular diseases in subjects with excess of VAT [3] (Figure 1).

The AT is constituted of a large number of adipocytes, connective tissue matrix, vascular and neural tissue and other non-adipocyte cells. These non-adipocyte cells are represented by inflammatory cells like macrophages, immune cells, fibroblasts and preadipocytes [8]. The adipocytes are the chief cellular units in AT, serving as the main storage of energy. Smaller adipocytes absorb free fatty acids (FFA) and TG and perform as a buffer in the postprandial time. If the adipocytes become larger they are likely to be more dysfunctional, in particular insulin-resistant and hyperlipolytic [9]. The VAT contains more of the large adipocytes [10], shows increased vascularization and is more innervated compared to the ScAT [8]. The fact that insulin

resistance is positively associated with the amount of VAT can be considered as an important link between obesity and its metabolic sequelae such as cardiovascular diseases [9]. The AT is a very dynamic organ - the lipid excess accrues in increased adipocyte size (hypertrophy) and/or increased number of adipocytes (hyperplasia) and leads to expansion of ScAT and VAT [11].

1.1.1. Measurement of fat distribution

Anthropometric parameters like waist circumference (WC) and waist-to-hip ratio (WHR) are commonly used measures of FD. WC of 102 cm in men and 88 cm in women is considered as a cutoff for a risk of the metabolic syndrome according to the third Report of the National Cholesterol Education Program of the Expert Panel on Detection, Evaluation, and Treatment of High Blood Cholesterol in Adults (NCEP-ATP III) [12]. The WHR is calculated with the WC measured by the approximate midpoint between the lower margin of the last palpable rib and the top of the iliac crest, and the widest circumference measured at the hips and the buttocks (hip) [13].

A more precise assessment of body fat composition is provided by imaging techniques such as dual energy X-ray absorptiometry (DEXA), computerized tomography (CT) or magnetic resonance imaging (MRI) [14]. With CT or MRI scans the visceral and subcutaneous fat area are measured at the level of L4 - L5 or the umbilicus [15], which allow calculating the ratio of VAT to ScAT. This ratio has been reported to correlate with impaired lipid and glucose metabolism in subjects with obesity and allows further categorizing individuals with obesity in visceral obese (>0.4) and subcutaneous obese (<0.4) [16]. In 2012, Krakauer et al. calculated A Body Shape Index (ABSI), which is defined by ABSI = WC (m) / [$BMI^{2/3}$ x height (m) $^{1/2}$] and is reported to be a more adequate index for the evidence of chronic diseases like cardiovascular diseases [17]. However, its use in the clinical practice is limited due to the lack of a robustly defined physiologic cutoff [18].

1.1.2. Which factors determine fat distribution?

Besides genetic factors, sex, age, total body fat content and energy balance are influencing factors for the accumulation of VAT (Figure 1). VAT increases with age independently of BMI in both genders [19]. A close linear correlation was reported between age and the volume of VAT in men [20]. This is also present in women, but weaker in the premenopausal condition while becoming stronger in postmenopausal women [20]. This gender-related difference in VAT accumulation could be one important factor to explain the gender-specific risk of cardiovascular events [21]. It has been shown that the sexual hormones play a role in the fat accumulation. The visceral fat mass in men is negatively correlated with the sex-hormone binding globulin

(SHBG) and testosterone [22], whereas SHBG is further associated with increased levels of circulating insulin [23]. In postmenopausal women, the decreasing estrogen and/or increasing androgens may result in a fat redistribution from the periphery to the intra-abdominal compartments [24]. In addition, changes in endocrine pathways can lead to a shifting from peripheral to central parts of the body, for example in patients with the Cushing´s syndrome manifesting increased cortisol clearance [19].

High energy intake may be associated with an accumulation of VAT due to a dysfunctional AT unable to expand through hyperplasia [25,26], but the overall interrelation between energy intake and the accumulation of fat at particular sites in the body seems to be more complex. Bouchard et al. showed in an experiment with hyper-energetic nutrition in monozygotic twins a correlation of energy intake and ScAT, while the variation in VAT was less than 10 % [27]. But it has also been reported, that during weight loss, people are more prone to loose VAT than ScAT and an explanation could be the higher metabolic activity of VAT compared with ScAT [15]. In line with this, a short-term dietary fructose restriction in children with obesity showed a decrease of VAT and liver fat [28].

In addition, studies suggest that environmental and dietary factors may affect FD directly (Figure 1). Ronn et al. reported in rodents, that bisphenol A (used as part of food packaging) may cause higher liver fat content [29]. Furthermore, the exposure to urban air pollution is responsible for oxidative stress, which is associated with measures of adiposity [30,31]. Air pollution promotes insulin resistance and visceral inflammation in a mouse model [32]. Factors like psychosocial and socioeconomic handicaps, depression and anxiety, alcohol and also smoking activate the respective stress centers. This may result in ´stress-eating´. Other consequences could bethe activation of the sympathetic nervous system as suggested by associations between adrenal hormones and obesity and centralization of body fat [33].

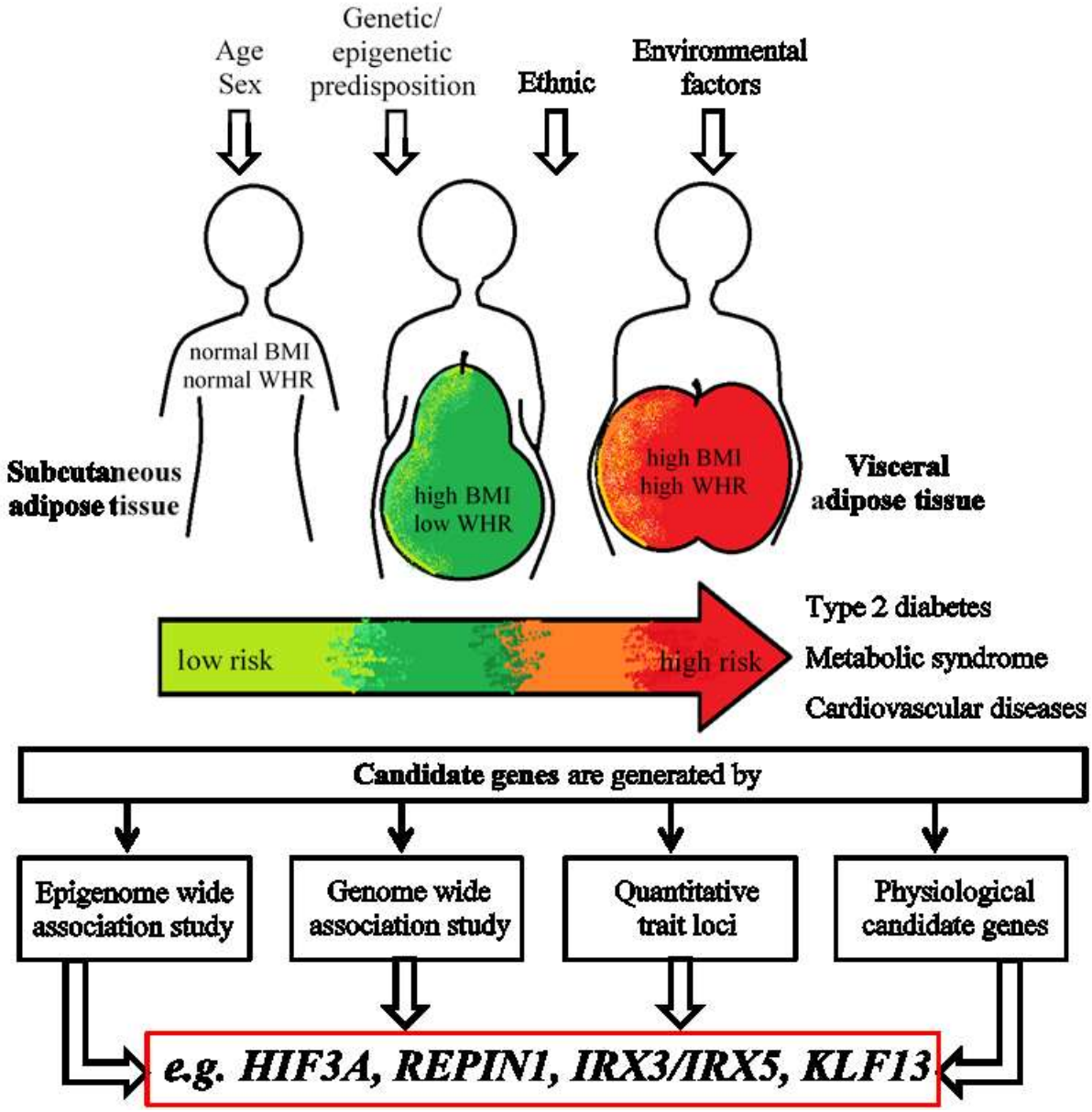

Figure 1. Schema for factors, which influence body fat distribution and approaches to identify novel candidate genes.

1.2. Genetics of obesity and fat distribution

Numerous studies strongly implicate that genetic components play an important role in the development of obesity [34]. However, there is good evidence that not only obesity itself, but also fat distribution is controlled by genetic factors [35] (Figure 1). After accounting for BMI, WHR is heritable with estimates ranging from 22-61 % [36–38]. In a very early work, Bouchard et al. could show that in identical twins the within-pair similarity was particular evident in regard to changes in FD and amount of visceral abdominal fat with significantly more variance among pairs than within pairs [27]. Another example is the Quebec Family Study, which show 56 %

estimated heritability for VAT and only 42 % heritability was estimated for ScAT [39]. This study indicated that the genetic influence on familial aggregation has a greater effect on VAT than on ScAT, independent of the total body fat. Malis et al. supported these findings with a study in young and elderly Danish twins. They reported heritability estimates for WHR to 72-80 %, total fat to 83-86 % and trunk and lower body fat to 81-85 % [40]. Finally, Schousboe et al. estimated the heritability of total body fat percentage among twins in the range of 59-63 % [41].

The genetic influence on FD is also seen in syndromes like lipodystrophy. Lipodystrophy includes a heterogeneous group of disorders characterized by partial or complete absence of AT [42]. The different forms can be divided in acquired or inherited lipodystrophy. The severity of the disease depends on the degree of fat loss. Two major factors causing metabolic dysfunction are believed to be dyslipidemia and alteration of the adipokine profile [43].

The congenital generalized lipodystrophy (CGL) is an autosomal recessive disorder, which is caused by mutations in different genes, all of which are involved in lipid droplet formation and triglyceride synthesis [43], namely *lysophosphatidic acid acyltransferase-β* (*AGPAT2*), *seipin* (*BSCL2*), *caveolin 1* (*CAV1*) and *caveolae associated protein 1* (*PTRF*) [44–47]. *AGPAT2* was reported to affect the adipocyte differentiation via *AKT serine/threonine kinase 1* (*AKT1)* and *peroxisome proliferator activated receptor gamma* (*PPARG)* [48]. The other genes, *BSCL2, CAV1* and *PTFR*, are mainly concerned in vesicle trafficking and affect the formation or maturation of lipid droplets [48]. CGL is characterized by a near-complete lack of body fat from birth or from very young age and these patients have nearly no metabolically active storage fat, but mechanical fat (e.g. orbits, palms and soles) is still existing [48,49]. During the childhood the patients develop symptoms of metabolic syndrome like dyslipidemia, triglyceride accumulation [50] and hyperinsulinemia or T2D [51].

Some of these symptoms are observed in both forms of partial lipodystrophy, the familial partial lipodystrophy (inherited) and the most common acquired form, where patients with human immunodeficiency virus (HIV) receive highly active antiretroviral therapy (HAART) with protease inhibitors [52]. These protease inhibitors decrease the levels of major transcriptions factors, which regulate adipocyte differentiation and function like *CCAAT/enhancer binding protein gamma* (*C/EBPγ)* and *PPARγ* [43]. Altered *PPARγ* activity is also shown in patients with familial partial lipodystrophy type 3 caused by mutations in *PPARγ* [53]. The familial partial lipodystrophy of the Dunnigan type is attributed to mutations in the lamin A/C gene (*LMNA*) [54]. This type is exhibited by gradual loss of ScAT in the trunk and extremities, but the face and neck are not affected [55]. The mutations in *LMNA* affect the nuclear stability and may result in premature cell death of adipocytes [56]. The loss of the ScAT occurs at the time of puberty and

complications such as insulin resistance and increased levels of lipid parameters can develop [57]. It was also shown that variants in *LMNA* were associated with metabolic parameters related to T2D and obesity [58,59], and so it seems that this gene might be involved in the dysfunction of VAT.

Another syndrome with an altered FD is the autosomal-dominant inherited disease familial multiple lipomatosis (FML) [60] with patients manifesting many painless encapsulated subcutaneous lipomas over the torso and limbs. *High mobility group AT-hook 2* (*HMGA2*) was reported to be a possible candidate gene, because it was discovered on a region on chromosome 12q13-15, which is linked to the development in lipomas based on a breakpoint translocation [61]. Another study could show, that *HMGA2* plays a role in the adipocytic cell growth and development [62] and *Hmga2* knockout mice developed a pygmy phenotype with a strong reduction of body weight by affecting the AT [63].

Interestingly, variation in body FD between ethnic groups have been observed among pre-pubertal children. Asian girls and boys were described to have less extremity and/or gynoid fat compared with Caucasian and African-American children of the same sex and age [64] (Figure 1). Another example for ethnic differences in AT distribution is the South African group Khoikhoi, whose women present an increased accumulation of AT in the buttocks [65] .

The genetic heritability of FD patterns cannot be explained only by mutations and single nucleotide polymorphisms (SNPs). Additional factors, like non-coding RNAs and epigenetic modifications like DNA and histone methylation may play an important role (Figure 1). The term “epigenetics” defines heritable changes in gene expression without any changes of the DNA sequence itself [66]. Epigenetic marks are tissue specific and can mediate biological and biochemical processes such as imprinting, which determine expression of alleles according to the maternal or paternal origin and balance the expression [67,68]. Defects in imprinting result in altered gene expression. For instance, a paternal deletion at 15q11-q13 due to imprinting results in the Prader-Willi syndrome, which is among others characterized by severe early onset obesity caused by hyperphagia [69].

The DNA methylation is a post-replication modification and mostly found at cytosines followed by a guanine, the so called CpG sites. Especially methylation/demethylation of CpG sites in the promotor region can affect the gene expression [67]. There is growing evidence that obesity and body FD is also controlled by DNA methylation. For instance, Keller et al. have recently shown depot-specific global DNA methylation levels in ScAT and VAT accompanied by positive correlations between the DNA methylation in ScAT with WC and WHR [70].

1.3. Genome wide associations studies (GWAS)

Genetic loci associated with quantitative traits are referred to as quantitative trait loci (QTL) [71]. QTL mapping is a phenotype-driven method that reveals statistical associations between genotypes and phenotypic values for a quantitative trait of interest. It helps to understand the genetic architecture of trait variation and uncovers new possible candidate genes involved in the regulation of traits of interest [72]. With the development of high-throughput genotyping technologies it became possible to run GWAS, an unbiased approach to identify novel statistically significant loci associated with obesity or body FD [73]. One of the first studies related to body FD showed an association of rs12970134 with WC in subjects of Indian-Asian or European ancestry [74]. This SNP is located near *melanocortin 4 receptor* (*MC4R),* whose mutations are also known to be the major determinants of monogenic obesity [74].

The first meta-analysis of GWAS for WC and WHR was reported from Lindgren et al.[75] who could show that genetic factors play a role in the regulation of WC and WHR. In 2010, Heid et al. published a meta-analysis including 32 GWAS with up to 77,167 participants for WHR adjusted for BMI, which revealed 14 genetic loci (*vascular endothelial growth factor A* [*VEGFA]*, *ADAM metallopeptidase with thrombospondin type 1 motif 9 [ADAMTS9]*, *R-spondin 3 [RSPO3]*, *T-box 15- tryptophanyl-tRNA synthetase [TBX15-WARS]*, *nuclear factor, erythroid 2 like 3 [NFE2L3]*, *lymphocyte antigen 86 [LY86]*, *growth factor receptor bound protein 14 - cordon-bleu WH2 repeat protein like 1 [GRB14-COBLL1]*, *inositol 1,4,5-trisphosphate receptor type 2- sarcospan [ITPR2-SSPN]*, *dynamin 3- phosphatidylinositol glycan anchor biosynthesis class C [DNM3-PIGC]*, *homeobox C13 [HOXC13], zinc and ring finger 3- kringle containing transmembrane protein 1 [ZNRF3-KREMEN1]*, *nischarin- stabilin 1 [NISCH-STAB1]*, *cytoplasmic polyadenylation element binding protein 4 [CPEB4])* including the known locus at *lysophospholipase like 1 (LYPLAL1*) associated with the measurements of FD [38]. Interestingly, seven of these loci revealed stronger effects in women than in men. In 2015, a new meta-analysis of GWAS of WHRadjBMI showed additional loci [76]. In this study, 142,762 individuals of European ancestry from 57 previously described [38] or new GWAS, and further 67,326 European individuals from Metabochip studies were included. As a result the authors identified 49 loci for WHRadjBMI with 33 new loci and nine additional loci in sex-specific analysis, eight were only significant in women and not in men [76]. The 16 previously described variants were confirmed as well. Both reported meta-analyses showed significantly larger heritability and effect estimates in women than in men [38,76]. Furthermore,

Shungin et al. aimed to find a link between central obesity and the higher risk for metabolic disorders and therefore investigated the leading WHRadjBMI SNPs in association for 22 additional traits from the GWAS data [76]. 17 out of the 49 variants showed a significant association with at least one of the metabolic traits (high-density lipoprotein cholesterol [HDL] - 7 SNPs; TG - 5 SNPs; low-density lipoprotein cholesterol [LDL]-2 SNPs; fasting insulin - 3 SNPs). Also, nominal associations ($p<0.05$) were shown with traits like fasting and 2 -h glucose, diastolic and systolic blood pressure, BMI and coronary artery disease [76]. Free available databases were used to assess the functionality of the WHRadjBMI variants and revealed that at eleven of the new loci the lead SNPs were in linkage disequilibrium (LD) with cis-expression quantitative trait loci (eQTL) in ScAT and/or omental AT, liver or blood cell types [76]. Further, the variants were investigated for their location in open chromatin regions in different tissues like AT, liver or blood. At least one variant in seven of the elven loci resided in a putative regulatory element, suggesting its regulatory role in gene expression. Three approaches (GRAIL[77], MAGENTA [78], DEPICT [79]) were used to highlight the related target genes and pathways for the identified loci suggested following members: signaling pathways involving vascular endothelial growth factor (*VEGF*), phosphatase and tensin (PTEN) homologue, the insulin receptor (IR), and peroxisome proliferator-activated receptors (PPARs) [76]. Further, gene sets, which may have a role in body fat regulation like insulin sensitivity and glucose level regulation were highlighted.

It is of note that GWAS of body FD based on more precise measurements such as CT have been recently performed [80]. In one of the first studies of this kind, Fox et al. confirmed previously reported loci (*LYPLAL1* - for VAT/ScAT ratio, *FTO* - ScAT), but also identified a novel variant for VAT near *threonine synthase like 2 (THNSL2)* specifically affecting FD in women only (rs1659258) [80].

Not only cohorts of European ancestry were investigated but also association studies in various ethnic groups were performed in the past. In a study with a cohort of African ancestry, two new loci, associated with WCadjBMI (*LIM homeobox 2 [LHX2]*) and WHRadjBMI (*Ras responsive element binding protein 1 [RREB1]*) were identified and six of the 14 "European" loci were confirmed (*TBX15-WARS2, GRB14, ADAMTS9, LY86, RSPO3, ITPR2-SSPN*) [81]. Hotta et al. investigated the reported SNPs in a cohort of Japanese ancestry and demonstrated that *LYPLAL1* and *NISCH* might influence FD in this population [82].

Additionally, GWAS for other AT related traits like ectopic fat traits (ScAT, VAT,VAT/ScAT ratio etc.) [83], pericardial fat [84] or body fat percentage [85] were performed to demonstrate new loci (e.g. *Ataxin 1 [ATXN1], Tribbles pseudokinase 2 [TRIB2]*) and to confirm some of the reported

loci (e.g. *CPEB4*, *GRB14-COBLL1*). In the last years also epigenome wide associations studies (EWAS) for BMI have been conducted, implicating the close relationship between DNA methylation and obesity [86]. The *hypoxia inducible factor 3A (HIF3A)* was the most prominent gene, whose DNA methylation at corresponding CpG sites showed strong association with BMI [86].

1.4. Candidate genes

Majority of obesity cases are attributed to the polygenic nature of this disease and also the body FD is affected by numerous genetic variants in various genes. Identification and understanding of the causal variants/genes and their mutual interaction is one of the major challenges in functional genetics. Despite the fact that SNPs usually render small effects, they still can play an important role in the complex etiology of diseases and can help to understand the underlying molecular pathomechanisms. Genetic variants and associated loci/genes from GWAS/EWAS and meta-analyses of GWAS provide a powerful resource for further research on individual candidate genes aimed to clarify the underlying molecular mechanisms in the regulation of body FD as well as the causal relationship between abdominal fat accumulation and the higher risk for metabolic diseases [76] (Figure 1).

1.4.1. Hypoxia inducible factor 3 A (*HIF3A*)

Obesity is related to chronic inflammation in AT, which contributes to insulin resistance and impaired glucose and lipid metabolism [87]. The inflammation affects different pathways and metabolic conditions like hypoxia, which can ultimately lead to AT dysfunction. The improved knowledge on combined effects of genetic factors and epigenetic alterations can help to better understand the pathophysiology of obesity and FD. Dick et al. performed a study that showed genome wide significant associations between DNA methylation in blood and BMI [86]. DNA-methylation at three of five CpG sites most strongly associated with BMI were located in intron 1 in *HIF3A.* HIF3A is a component of the hypoxia inducible transcription factor (HIF). HIFs are heterodimeric constructs consisting of hypoxia-regulated α and oxygen-insensitive β subunits and mediating many cellular responses during hypoxia [88]. Whereas family members HIF1α and HIF2α have been extensively investigated in the past, much less is known about HIF3α. In humans, *HIF3A*, the HIF3α encoding gene, is located on chromosome 19q13.2 and is represented by six protein coding transcripts (Ensemble database 13.02.2018). Maynard et al. [89] detected *HIF3A*-transcripts in the heart, placenta, lung and skeletal muscle by using

Northern blot analysis, and Pasanen et al. showed *HIF3A* expression additionally in brain, liver, kidney and pancreas [90]. The biology of HIF3α is very complex due to the different *HIF3A* variants, which are expressed in several tissues, at several time points and are differentially regulated by hypoxia and other factors [91]. The HIF3A mRNA and protein levels increase during hypoxia in a tissue-specific manner mediated by *HIF1A* and/or *HIF2A* [92,93]. On the other hand it was demonstrated that one *HIF3A* variant serves as a negative regulator of HIF1/2α [94]. There are also oxygen-independent regulation pathways as has been shown by insulin or 2-deoxy-D-glucose treatments resulting in higher *HIF3A* mRNA levels [95]. Furthermore, oleic and linoleic acid can bind to the Per-Arnt-Sim (PAS)-B domain of HIF3A [96] and drive its regulation.

HIF3A is a potential candidate gene based not only on the results from the above mentioned EWAS [97] but also on the corresponding biological pathways. In my study, I conducted mRNA expression and DNA methylation analyses of the reported CpG sites in human VAT and ScAT. Furthermore, the genotypes of *HIF3A* polymorphisms rs8102595 and rs3826795 were analyzed for associations with anthropometric and metabolic parameters.

1.4.2. Replication initiator 1 (*REPIN1*)

In 1998 Kovacs et al. reported a QTL for serum fasting insulin, TG and body weight in rats on chromosome 4 [98]. One of the most plausible candidate genes within this locus is the zinc finger protein replication initiator 1 (REPIN1). The human *REPIN1* is located on chromosome 7 and consists of four exons including one coding. Eleven protein coding transcripts are listed in the Ensembl database, four of them are annotated in the NCBI reference sequence (RefSeq). The transcription results in a 64 kDa Protein composed of 567 or 624 amino acids (NM_013400, NM_001099696, NM_014374, NM_001099695, Ensemble database 13.02.2018). REPIN1 is ubiquitously expressed with highest expression reported in liver and AT [99]. Repin1 has been extensively investigated in liver and AT-specific knock-out mouse models [100,101]. Briefly, the liver- as well as the AT-specific model show a metabolic healthier phenotype compared with the wildtype mice. The *repin1* knockout mice are more insulin sensitive, have reduced AT mass and an improved lipid metabolism represented by lower LDL and total cholesterol levels [100,101]. In another study it was shown that *Repin1* knockdown in 3T3-L1 cells results in smaller adipocytes, reduced basal but revised insulin stimulated glucose uptake, and changes in mRNA expression of genes which are involved in adipogenesis, lipid uptake and lipid droplet formation [102]. All these data were generated in mice, whereas human data are lacking so far. Therefore, in the present study I investigated the role of genetic variation within human *REPIN1* on glucose and lipid metabolism.

1.4.3. Iriquois homeobox 3/5 (*IRX3/5*)

In 2007, the most significant hit in the GWAS for obesity, especially for BMI, was reported within the *fat mass and obesity associated gene (FTO*) locus [103]. Independent studies confirmed different common variants (i.e. rs9939609 [104], rs9930506 [103]) in intron 1 of the *FTO* and their associations with BMI in the general population [104–106]. On the other hand Klöting et al. demonstrated an inverse relationship of *FTO* mRNA expression and BMI in human AT [107]. In 2014, Smemo et al. showed that *FTO* has a long range connection to *iroquios homebox 3 (IRX3)* [108]. The obesity related region in intron 1 of *FTO* interacts directly with the promotor of *IRX3* [108]. In line with this, *Irx3* deficient mice exhibited a 25-30 % reduced body weight through the loss of fat mass [108]. Consistently, Claussnitzer et al. demonstrated a link between *FTO* variants and *IRX3* and *IRX5* [109]. With the help of different bioinformatic tools (i.e. Roadmap Epigenomics [110], ENCODE [111]) they found *IRX3* and *IRX5* as the genes most likely affected by the obesity-associated *FTO*-variants. They confirmed this in *in vitro* studies and showed that both genes were affected by the risk alleles of the *FTO*-variants in human adipocytes [109]. *IRX3* is located on chromosome 16 and has one protein-coding transcript (NM_024336). This transcript contains four coding exons that are translated into a 501 amino acid protein. *IRX5* displays four protein coding transcripts according to the Ensembl database but only one possesses an NCBI RefSeq entry (NM_005853). This transcript with three coding exons results in a protein with 482 amino acids.

In the present study I analyzed the mRNA expression levels of *IRX3* and *IRX5* in VAT and ScAT and tested for associations with a representative FTO variant and metabolic traits.

1.4.4. Krüppel like factor 13 (*KLF13*)

Shungin et al. reported in their GWAS 49 loci, which were associated with WHRadjBMI. 16 were reported before, 33 loci were new and one of these was the Krüppel like factor 13 (*KLF13*) loci [76]. *KLF13* is located on chromosome 15 in humans. Three protein coding transcripts are described in the Ensembl database, one of them is annotated in the NCBI reference sequence (RefSeq). The transcript is composed by 288 amino acids (NM_015995, Ensemble database 15.10.2018) in two coding exons. *KLF13* belongs to the KLF family, which include 17 members (KLF1 - 17) [112]. The *KLF´*s have three highly conserved Cy_2/His_2 zinc fingers and they bind to GC- and CACCC- boxes of DNA [113,112]. The fingers are connected by the characteristic Krüppel-link, which is a seven-amino acid spacer TGEKP(Y/F)X [114]. Most of the *KLF´s* are widely expressed but the mechanisms are not totally defined, although it is known that multiple members of the *KLF* family regulated the same processes but with opposing effects [115]. *KLF´s*

can also regulate other family members; for example the expression of *KLF3* is regulated by *KLF1* in erythroid cells [116].

In this study I analyzed the mRNA expression levels in VAT and ScAT of *KLF13* and tested the reported SNP rs8042543 for association with metabolic traits. Moreover, I investigated the role of *KLF13* in AT biology by employing its knockdown in epididymal and inguinal murine cells.

1.5. Aim of the thesis

In the last decades obesity and related diseases grew to a global health problem. One of the main predictors of obesity associated comorbidities is the body FD. Similar to obesity, there is good evidence that the body FD is controlled by genetic factors. Recent advances in high throughput genotyping and sequencing technologies allowed identification of candidate genes, which are involved in the polygenic regulation of FD. GWAS and EWAS uncovered multiple genetic variants, associated with measures of body fat composition like WHR and BMI, which are now targeted in detailed functional analyses.

This thesis aims to clarify the role of *HIF3A, REPIN1, IRX3*, *IRX5* and *KLF13* as novel candidate genes in the pathogenesis of the human body FD (Figure 1).

1.6. References

1 World Health Organization. Obesity and overweight. http://www.who.int/mediacentre/factsheets/fs311/en/.

2 Blüher M. Adipose tissue dysfunction in obesity. *Experimental and clinical endocrinology & diabetes : official journal, German Society of Endocrinology [and] German Diabetes Association* 2009; **117**: 241–250; doi:10.1055/s-0029-1192044.

3 Lee M-J, Wu Y, Fried SK. Adipose tissue heterogeneity: implication of depot differences in adipose tissue for obesity complications. *Molecular aspects of medicine* 2013; **34**: 1–11; doi:10.1016/j.mam.2012.10.001.

4 Peiris AN, Sothmann MS, Hoffmann RG, Hennes MI, Wilson CR, Gustafson AB *et al.* Adiposity, fat distribution, and cardiovascular risk. *Annals of internal medicine* 1989; **110**: 867–872; dio: 10.7326/0003-4819-110-11-867

5 Björntorp P. Metabolic implications of body fat distribution. *Diabetes care* 1991; **14**: 1132–1143.

6 Vague J. La différenciation sexuelle; facteur déterminant des formes de l'obésité. *La Presse medicale* 1947; **55**: 339.
7 Bouchard C, Després JP, Mauriège P. Genetic and nongenetic determinants of regional fat distribution. *Endocrine reviews* 1993; **14**: 72–93; doi:10.1210/edrv-14-1-72.
8 Ibrahim MM. Subcutaneous and visceral adipose tissue: structural and functional differences. *Obesity reviews : an official journal of the International Association for the Study of Obesity* 2010; **11**: 11–18; doi:10.1111/j.1467-789X.2009.00623.x.
9 Frayn KN. Visceral fat and insulin resistance--causative or correlative? *The British journal of nutrition* 2000; **83 Suppl 1**: S71-7.
10 Misra A, Vikram NK. Clinical and pathophysiological consequences of abdominal adiposity and abdominal adipose tissue depots. *Nutrition (Burbank, Los Angeles County, Calif.)* 2003; **19**: 457–466; doi:10.1016/S0899-9007(02)01003-1.
11 Ferranti S de, Mozaffarian D. The perfect storm: obesity, adipocyte dysfunction, and metabolic consequences. *Clinical chemistry* 2008; **54**: 945–955; doi:10.1373/clinchem.2007.100156.
12 Executive Summary of The Third Report of The National Cholesterol Education Program (NCEP) Expert Panel on Detection, Evaluation, And Treatment of High Blood Cholesterol In Adults (Adult Treatment Panel III). *JAMA* 2001; **285**: 2486–2497.
13 World Health Organization. Waist Circumference and Waist–Hip Ratio: Report of a WHO Expert Consultation, 2011.
14 Seabolt LA, Welch EB, Silver HJ. Imaging methods for analyzing body composition in human obesity and cardiometabolic disease. *Annals of the New York Academy of Sciences* 2015; **1353**: 41–59; doi:10.1111/nyas.12842.
15 Wajchenberg BL. Subcutaneous and visceral adipose tissue: their relation to the metabolic syndrome. *Endocrine reviews* 2000; **21**: 697–738; doi:10.1210/edrv.21.6.0415.
16 Fujioka S, Matsuzawa Y, Tokunaga K, Tarui S. Contribution of intra-abdominal fat accumulation to the impairment of glucose and lipid metabolism in human obesity. *Metabolism: clinical and experimental* 1987; **36**: 54–59; doi:10.1016/0026-0495(87)90063-1;
17 Krakauer NY, Krakauer JC. A new body shape index predicts mortality hazard independently of body mass index. *PloS one* 2012; **7**: e39504; doi:10.1371/journal.pone.0039504.
18 Ji M, Zhang S, An R. Effectiveness of A Body Shape Index (ABSI) in predicting chronic diseases and mortality: a systematic review and meta-analysis. *Obesity reviews : an official journal of the International Association for the Study of Obesity* 2018; **19**: 737–759; doi:10.1111/obr.12666.
19 Wajchenberg BL. Subcutaneous and visceral adipose tissue: Their relation to the metabolic syndrome. *Endocrine reviews* 2000; **21**: 697–738; dio:10.1210/edrv.21.6.0415
20 Matsuzawa Y, Nakamura T, Shimomura I, Kotani K. Visceral fat accumulation and cardiovascular disease. *Obesity research* 1995; **3 Suppl 5**: 645S-647S.
21 Lemieux S, Després JP, Moorjani S, Nadeau A, Thériault G, Prud'homme D *et al.* Are gender differences in cardiovascular disease risk factors explained by the level of visceral adipose tissue? *Diabetologia* 1994; **37**: 757–764.

22 Seidell JC, Björntorp P, Sjöström L, Kvist H, Sannerstedt R. Visceral fat accumulation in men is positively associated with insulin, glucose, and C-peptide levels, but negatively with testosterone levels. *Metabolism: clinical and experimental* 1990; **39**: 897–901; doi:10.1016/0026-0495(90)90297-P
23 Haffner SM, Katz MS, Stern MP, Dunn JF. The relationship of sex hormones to hyperinsulinemia and hyperglycemia. *Metabolism: clinical and experimental* 1988; **37**: 683–688; doi:10.1016/0026-0495(88)90091-1
24 Goss AM, Darnell BE, Brown MA, Oster RA, Gower BA. Longitudinal associations of the endocrine environment on fat partitioning in postmenopausal women. *Obesity (Silver Spring, Md.)* 2012; **20**: 939–944; doi:10.1038/oby.2011.362.
25 Smith U. Abdominal obesity: a marker of ectopic fat accumulation. *The Journal of clinical investigation* 2015; **125**: 1790–1792; doi:10.1172/JCI81507.
26 Schleinitz D, Böttcher Y, Blüher M, Kovacs P. The genetics of fat distribution. *Diabetologia* 2014; **57**: 1276–1286; doi:10.1007/s00125-014-3214-z.
27 Bouchard C, Tremblay A, Després JP, Nadeau A, Lupien PJ, Thériault G *et al.* The response to long-term overfeeding in identical twins. *The New England journal of medicine* 1990; **322**: 1477–1482; doi:10.1056/NEJM199005243222101.
28 Schwarz J-M, Noworolski SM, Erkin-Cakmak A, Korn NJ, Wen MJ, Tai VW *et al.* Effects of Dietary Fructose Restriction on Liver Fat, De Novo Lipogenesis, and Insulin Kinetics in Children With Obesity. *Gastroenterology* 2017; **153**: 743–752; doi:10.1053/j.gastro.2017.05.043.
29 Rönn M, Kullberg J, Karlsson H, Berglund J, Malmberg F, Orberg J *et al.* Bisphenol A exposure increases liver fat in juvenile fructose-fed Fischer 344 rats. *Toxicology* 2013; **303**: 125–132; doi:10.1016/j.tox.2012.09.013.
30 Ponticiello BG, Capozzella A, Di Giorgio V, Casale T, Giubilati R, Tomei G *et al.* Overweight and urban pollution: preliminary results. *The Science of the total environment* 2015; **518-519**: 61–64; doi:10.1016/j.scitotenv.2015.02.084.
31 Charles LE, Burchfiel CM, Violanti JM, Fekedulegn D, Slaven JE, Browne RW *et al.* Adiposity measures and oxidative stress among police officers. *Obesity (Silver Spring, Md.)* 2008; **16**: 2489–2497; doi:10.1038/oby.2008.395.
32 Sun Q, Yue P, Deiuliis JA, Lumeng CN, Kampfrath T, Mikolaj MB *et al.* Ambient air pollution exaggerates adipose inflammation and insulin resistance in a mouse model of diet-induced obesity. *Circulation* 2009; **119**: 538–546; doi:10.1161/CIRCULATIONAHA.108.799015.
33 Björntorp P. Do stress reactions cause abdominal obesity and comorbidities? *Obesity reviews : an official journal of the International Association for the Study of Obesity* 2001; **2**: 73–86; doi:10.1046/j.1467-789x.2001.00027.x
34 Lyon HN, Hirschhorn JN. Genetics of common forms of obesity: a brief overview. *The American journal of clinical nutrition* 2005; **82**: 215S-217S; doi:10.1093/ajcn/82.1.215S.
35 Zillikens MC, Yazdanpanah M, Pardo LM, Rivadeneira F, Aulchenko YS, Oostra BA *et al.* Sex-specific genetic effects influence variation in body composition. *Diabetologia* 2008; **51**: 2233–2241; doi:10.1007/s00125-008-1163-0.

36 Rose KM, Newman B, Mayer-Davis EJ, Selby JV. Genetic and behavioral determinants of waist-hip ratio and waist circumference in women twins. *Obesity research* 1998; **6**: 383–392; doi:10.1002/j.1550-8528.1998.tb00369.x
37 Selby JV, Newman B, Quesenberry CP, Fabsitz RR, Carmelli D, Meaney FJ *et al.* Genetic and behavioral influences on body fat distribution. *International journal of obesity* 1990; **14**: 593–602.
38 Heid IM, Jackson AU, Randall JC, Winkler TW, Qi L, Steinthorsdottir V *et al.* Meta-analysis identifies 13 new loci associated with waist-hip ratio and reveals sexual dimorphism in the genetic basis of fat distribution. *Nature genetics* 2010; **42**: 949–960; doi:10.1038/ng.685.
39 Pérusse L, Després JP, Lemieux S, Rice T, Rao DC, Bouchard C. Familial aggregation of abdominal visceral fat level: results from the Quebec family study. *Metabolism: clinical and experimental* 1996; **45**: 378–382; doi:10.1016/S0026-0495(96)90294-2
40 Malis C, Rasmussen EL, Poulsen P, Petersen I, Christensen K, Beck-Nielsen H *et al.* Total and regional fat distribution is strongly influenced by genetic factors in young and elderly twins. *Obesity research* 2005; **13**: 2139–2145; doi:10.1038/oby.2005.265.
41 Schousboe K, Visscher PM, Erbas B, Kyvik KO, Hopper JL, Henriksen JE *et al.* Twin study of genetic and environmental influences on adult body size, shape, and composition. *International journal of obesity and related metabolic disorders : journal of the International Association for the Study of Obesity* 2004; **28**: 39–48; doi:10.1038/sj.ijo.0802524.
42 Garg A, Agarwal AK. Lipodystrophies: disorders of adipose tissue biology. *Biochimica et biophysica acta* 2009; **1791**: 507–513; doi:10.1016/j.bbalip.2008.12.014.
43 Vegiopoulos A, Rohm M, Herzig S. Adipose tissue: between the extremes. *The EMBO journal* 2017; **36**: 1999–2017; doi:10.15252/embj.201696206.
44 Agarwal AK, Arioglu E, Almeida S de, Akkoc N, Taylor SI, Bowcock AM *et al.* AGPAT2 is mutated in congenital generalized lipodystrophy linked to chromosome 9q34. *Nature genetics* 2002; **31**: 21–23; doi:10.1038/ng880.
45 Magré J, Delépine M, Khallouf E, Gedde-Dahl T, van Maldergem L, Sobel E *et al.* Identification of the gene altered in Berardinelli-Seip congenital lipodystrophy on chromosome 11q13. *Nature genetics* 2001; **28**: 365–370; doi:10.1038/ng585.
46 Kim CA, Delépine M, Boutet E, El Mourabit H, Le Lay S, Meier M *et al.* Association of a homozygous nonsense caveolin-1 mutation with Berardinelli-Seip congenital lipodystrophy. *The Journal of clinical endocrinology and metabolism* 2008; **93**: 1129–1134; doi:10.1210/jc.2007-1328.
47 Hayashi YK, Matsuda C, Ogawa M, Goto K, Tominaga K, Mitsuhashi S *et al.* Human PTRF mutations cause secondary deficiency of caveolins resulting in muscular dystrophy with generalized lipodystrophy. *The Journal of clinical investigation* 2009; **119**: 2623–2633; doi:10.1172/JCI38660.
48 Patni N, Garg A. Congenital generalized lipodystrophies--new insights into metabolic dysfunction. *Nature reviews. Endocrinology* 2015; **11**: 522–534; doi:10.1038/nrendo.2015.123.

49 Garg A, Fleckenstein JL, Peshock RM, Grundy SM. Peculiar distribution of adipose tissue in patients with congenital generalized lipodystrophy. *The Journal of clinical endocrinology and metabolism* 1992; **75**: 358–361; doi:10.1210/jcem.75.2.1639935.

50 BERARDINELLI W. An undiagnosed endocrinometabolic syndrome: report of 2 cases. *The Journal of clinical endocrinology and metabolism* 1954; **14**: 193–204; doi:10.1210/jcem-14-2-193.

51 van Maldergem L, Magré J, Khallouf TE, Gedde-Dahl T, Delépine M, Trygstad O *et al.* Genotype-phenotype relationships in Berardinelli-Seip congenital lipodystrophy. *Journal of Medical Genetics* 2002; **39**: 722–733; doi:10.1136/jmg.39.10.722

52 Blümer RM, van Vonderen MG, Sutinen J, Hassink E, Ackermans M, van Agtmael MA *et al.* Zidovudine/lamivudine contributes to insulin resistance within 3 months of starting combination antiretroviral therapy. *AIDS (London, England)* 2008; **22**: 227–236; doi:10.1097/QAD.0b013e3282f33557.

53 Agarwal AK, Garg A. A novel heterozygous mutation in peroxisome proliferator-activated receptor-gamma gene in a patient with familial partial lipodystrophy. *The Journal of clinical endocrinology and metabolism* 2002; **87**: 408–411; doi:10.1210/jcem.87.1.8290.

54 Shackleton S, Lloyd DJ, Jackson SN, Evans R, Niermeijer MF, Singh BM *et al.* LMNA, encoding lamin A/C, is mutated in partial lipodystrophy. *Nature genetics* 2000; **24**: 153–156; doi:10.1038/72807.

55 Garg A, Peshock RM, Fleckenstein JL. Adipose tissue distribution pattern in patients with familial partial lipodystrophy (Dunnigan variety). *The Journal of clinical endocrinology and metabolism* 1999; **84**: 170–174; doi:10.1210/jcem.84.1.5383.

56 Nolis T. Exploring the pathophysiology behind the more common genetic and acquired lipodystrophies. *Journal of human genetics* 2014; **59**: 16–23; doi:10.1038/jhg.2013.107.

57 Cao H, Hegele RA. Nuclear lamin A/C R482Q mutation in canadian kindreds with Dunnigan-type familial partial lipodystrophy. *Human molecular genetics* 2000; **9**: 109–112.

58 Wegner L, Andersen G, Sparsø T, Grarup N, Glümer C, Borch-Johnsen K *et al.* Common variation in LMNA increases susceptibility to type 2 diabetes and associates with elevated fasting glycemia and estimates of body fat and height in the general population: studies of 7,495 Danish whites. *Diabetes* 2007; **56**: 694–698; doi:10.2337/db06-0927.

59 Hegele RA, Cao H, Harris SB, Zinman B, Hanley AJ, Anderson CM. Genetic variation in LMNA modulates plasma leptin and indices of obesity in aboriginal Canadians. *Physiological genomics* 2000; **3**: 39–44; doi:10.1152/physiolgenomics.2000.3.1.39.

60 Keskin D, Ezirmik N, Celik H. Familial multiple lipomatosis. *The Israel Medical Association journal : IMAJ* 2002; **4**: 1121–1123.

61 Fedele M, Battista S, Manfioletti G, Croce CM, Giancotti V, Fusco A. Role of the high mobility group A proteins in human lipomas. *Carcinogenesis* 2001; **22**: 1583–1591.

62 Ashar HR, Fejzo MS, Tkachenko A, Zhou X, Fletcher JA, Weremowicz S *et al.* Disruption of the architectural factor HMGI-C: DNA-binding AT hook motifs fused in lipomas to distinct transcriptional regulatory domains. *Cell* 1995; **82**: 57–65.

63 Zhou X, Benson KF, Ashar HR, Chada K. Mutation responsible for the mouse pygmy phenotype in the developmentally regulated factor HMGI-C. *Nature* 1995; **376**: 771–774; doi:10.1038/376771a0.

64 He Q, Horlick M, Thornton J, Wang J, Pierson RN, Heshka S *et al.* Sex-specific fat distribution is not linear across pubertal groups in a multiethnic study. *Obesity research* 2004; **12**: 725–733; doi:10.1038/oby.2004.85.
65 Ersek RA, Bell HN, Salisbury AV. Serial and superficial suction for steatopygia (Hottentot bustle). *Aesthetic plastic surgery* 1994; **18**: 279–282.
66 Egger G, Liang G, Aparicio A, Jones PA. Epigenetics in human disease and prospects for epigenetic therapy. *Nature* 2004; **429**: 457–463; doi:10.1038/nature02625.
67 Herrera BM, Keildson S, Lindgren CM. Genetics and epigenetics of obesity. *Maturitas* 2011; **69**: 41–49; doi:10.1016/j.maturitas.2011.02.018.
68 Reik W, Walter J. Imprinting mechanisms in mammals. *CURRENT OPINION IN GENETICS & DEVELOPMENT* 1998; **8**: 154–164; doi:10.1016/S0959-437X(98)80136-6
69 Shapira NA, Lessig MC, He AG, James GA, Driscoll DJ, Liu Y. Satiety dysfunction in Prader-Willi syndrome demonstrated by fMRI. *Journal of neurology, neurosurgery, and psychiatry* 2005; **76**: 260–262; doi:10.1136/jnnp.2004.039024.
70 Keller M, Kralisch S, Rohde K, Schleinitz D, Dietrich A, Schön MR *et al.* Global DNA methylation levels in human adipose tissue are related to fat distribution and glucose homeostasis. *Diabetologia* 2014; **57**: 2374–2383; doi:10.1007/s00125-014-3356-z.
71 Grisel JE. Quantitative trait locus analysis. *Alcohol research & health : the journal of the National Institute on Alcohol Abuse and Alcoholism* 2000; **24**: 169–174.
72 Ishikawa A. A Strategy for Identifying Quantitative Trait Genes Using Gene Expression Analysis and Causal Analysis. *Genes* 2017; **8;** doi:10.3390/genes8120347.
73 Fehlert E, Wagner R, Ketterer C, Böhm A, Machann J, Fritsche L *et al.* Genetic determination of body fat distribution and the attributive influence on metabolism. *Obesity (Silver Spring, Md.)* 2017; **25**: 1277–1283; doi:10.1002/oby.21874.
74 Chambers JC, Elliott P, Zabaneh D, Zhang W, Li Y, Froguel P *et al.* Common genetic variation near MC4R is associated with waist circumference and insulin resistance. *Nature genetics* 2008; **40**: 716–718; doi:10.1038/ng.156.
75 Lindgren CM, Heid IM, Randall JC, Lamina C, Steinthorsdottir V, Qi L *et al.* Genome-wide association scan meta-analysis identifies three Loci influencing adiposity and fat distribution. *PLoS Genetics* 2009; **5**: e1000508; doi:10.1371/journal.pgen.1000508.
76 Shungin D, Winkler TW, Croteau-Chonka DC, Ferreira T, Locke AE, Mägi R *et al.* New genetic loci link adipose and insulin biology to body fat distribution. *Nature* 2015; **518**: 187–196; doi:10.1038/nature14132.
77 Raychaudhuri S, Plenge RM, Rossin EJ, Ng ACY, Purcell SM, Sklar P *et al.* Identifying relationships among genomic disease regions: predicting genes at pathogenic SNP associations and rare deletions. *PLoS Genetics* 2009; **5**: e1000534; doi:10.1371/journal.pgen.1000534.
78 Segrè AV, Groop L, Mootha VK, Daly MJ, Altshuler D. Common inherited variation in mitochondrial genes is not enriched for associations with type 2 diabetes or related glycemic traits. *PLoS Genetics* 2010; **6;** doi:10.1371/journal.pgen.1001058.
79 Pers TH, Karjalainen JM, Chan Y, Westra H-J, Wood AR, Yang J *et al.* Biological interpretation of genome-wide association studies using predicted gene functions. *Nature communications* 2015; **6**: 5890; doi:10.1038/ncomms6890.

80 Fox CS, Liu Y, White CC, Feitosa M, Smith AV, Heard-Costa N *et al.* Genome-wide association for abdominal subcutaneous and visceral adipose reveals a novel locus for visceral fat in women. *PLoS Genetics* 2012; **8**: e1002695; doi:10.1371/journal.pgen.1002695.
81 Liu C-T, Monda KL, Taylor KC, Lange L, Demerath EW, Palmas W *et al.* Genome-wide association of body fat distribution in African ancestry populations suggests new loci. *PLoS Genetics* 2013; **9**: e1003681; doi:10.1371/journal.pgen.1003681.
82 Hotta K, Kitamoto A, Kitamoto T, Mizusawa S, Teranishi H, So R *et al.* Replication study of 15 recently published Loci for body fat distribution in the Japanese population. *Journal of atherosclerosis and thrombosis* 2013; **20**: 336–350; doi:10.5551/jat.14589
83 Chu AY, Deng X, Fisher VA, Drong A, Zhang Y, Feitosa MF *et al.* Multiethnic genome-wide meta-analysis of ectopic fat depots identifies loci associated with adipocyte development and differentiation. *Nature genetics* 2017; **49**: 125–130; doi:10.1038/ng.3738.
84 Fox CS, White CC, Lohman K, Heard-Costa N, Cohen P, Zhang Y *et al.* Genome-wide association of pericardial fat identifies a unique locus for ectopic fat. *PLoS Genetics* 2012; **8**: e1002705; doi:10.1371/journal.pgen.1002705.
85 Lu Y, Day FR, Gustafsson S, Buchkovich ML, Na J, Bataille V *et al.* New loci for body fat percentage reveal link between adiposity and cardiometabolic disease risk. *Nature communications* 2016; **7**: 10495; doi:10.1038/ncomms10495.
86 Dick KJ, Nelson CP, Tsaprouni L, Sandling JK, Aïssi D, Wahl S *et al.* DNA methylation and body-mass index: a genome-wide analysis. *The Lancet* 2014; **383**: 1990–1998; doi:10.1016/S0140-6736(13)62674-4.
87 Glass CK, Olefsky JM. Inflammation and lipid signaling in the etiology of insulin resistance. *Cell metabolism* 2012; **15**: 635–645; doi:10.1016/j.cmet.2012.04.001.
88 Yang S-L, Wu C, Xiong Z-F, Fang X. Progress on hypoxia-inducible factor-3: Its structure, gene regulation and biological function (Review). *Molecular medicine reports* 2015; **12**: 2411–2416; doi:10.3892/mmr.2015.3689.
89 Maynard MA, Qi H, Chung J, Lee EHL, Kondo Y, Hara S *et al.* Multiple splice variants of the human HIF-3 alpha locus are targets of the von Hippel-Lindau E3 ubiquitin ligase complex. *The Journal of biological chemistry* 2003; **278**: 11032–11040; doi:10.1074/jbc.M208681200.
90 Pasanen A, Heikkilä M, Rautavuoma K, Hirsilä M, Kivirikko KI, Myllyharju J. Hypoxia-inducible factor (HIF)-3alpha is subject to extensive alternative splicing in human tissues and cancer cells and is regulated by HIF-1 but not HIF-2. *The international journal of biochemistry & cell biology* 2010; **42**: 1189–1200; doi:10.1016/j.biocel.2010.04.008.
91 Duan C. Hypoxia-inducible factor 3 biology: complexities and emerging themes. *American journal of physiology. Cell physiology* 2016; **310**: C260-9; doi:10.1152/ajpcell.00315.2015.
92 Li QF, Wang XR, Yang YW, Lin H. Hypoxia upregulates hypoxia inducible factor (HIF)-3alpha expression in lung epithelial cells: characterization and comparison with HIF-1alpha. *CELL RESEARCH* 2006; **16**: 548–558; doi:10.1038/sj.cr.7310072.
93 Tanaka T, Wiesener M, Bernhardt W, Eckardt K-U, Warnecke C. The human HIF (hypoxia-inducible factor)-3alpha gene is a HIF-1 target gene and may modulate hypoxic gene induction. *The Biochemical journal* 2009; **424**: 143–151; doi:10.1042/BJ20090120.

94 Maynard MA, Evans AJ, Shi W, Kim WY, Liu F-F, Ohh M. Dominant-negative HIF-3 alpha 4 suppresses VHL-null renal cell carcinoma progression. *Cell cycle (Georgetown, Tex.)* 2007; **6**: 2810–2816; doi:10.4161/cc.6.22.4947.

95 Heidbreder M, Qadri F, Jöhren O, Dendorfer A, Depping R, Fröhlich F *et al.* Non-hypoxic induction of HIF-3alpha by 2-deoxy-D-glucose and insulin. *BIOCHEMICAL AND BIOPHYSICAL RESEARCH COMMUNICATIONS* 2007; **352**: 437–443; doi:10.1016/j.bbrc.2006.11.027.

96 Fala AM, Oliveira JF, Adamoski D, Aricetti JA, Dias MM, Dias MVB *et al.* Unsaturated fatty acids as high-affinity ligands of the C-terminal Per-ARNT-Sim domain from the Hypoxia-inducible factor 3α. *SCIENTIFIC REPORTS* 2015; **5**: 12698; doi:10.1038/srep12698.

97 Dick KJ, Nelson CP, Tsaprouni L, Sandling JK, Aïssi D, Wahl S *et al.* DNA methylation and body-mass index. A genome-wide analysis. *The Lancet* 2014; **383**: 1990–1998; doi:10.1016/S0140-6736(13)62674-4.

98 Kovács P, Klöting I. Quantitative trait loci on chromosomes 1 and 4 affect lipid phenotypes in the rat. *ARCHIVES OF BIOCHEMISTRY AND BIOPHYSICS* 1998; **354**: 139–143; doi:10.1006/abbi.1998.0686.

99 Klöting N, Wilke B, Klöting I. Triplet repeat in the Repin1 3'-untranslated region on rat chromosome 4 correlates with facets of the metabolic syndrome. *Diabetes/metabolism research and reviews* 2007; **23**: 406–410; doi:10.1002/dmrr.713.

100 Hesselbarth N, Kunath A, Kern M, Gericke M, Mejhert N, Rydén M *et al.* Repin1 deficiency in adipose tissue improves whole-body insulin sensitivity, and lipid metabolism. *International journal of obesity (2005)* 2017; **41**: 1815–1823; doi:10.1038/ijo.2017.172.

101 Kern M, Kosacka J, Hesselbarth N, Brückner J, Heiker JT, Flehmig G *et al.* Liver-restricted Repin1 deficiency improves whole-body insulin sensitivity, alters lipid metabolism, and causes secondary changes in adipose tissue in mice. *Diabetes* 2014; **63**: 3295–3309; doi:10.2337/db13-0933.

102 Ruschke K, Illes M, Kern M, Klöting I, Fasshauer M, Schön MR *et al.* Repin1 maybe involved in the regulation of cell size and glucose transport in adipocytes. *BIOCHEMICAL AND BIOPHYSICAL RESEARCH COMMUNICATIONS* 2010; **400**: 246–251; doi:10.1016/j.bbrc.2010.08.049.

103 Scuteri A, Sanna S, Chen W-M, Uda M, Albai G, Strait J *et al.* Genome-wide association scan shows genetic variants in the FTO gene are associated with obesity-related traits. *PLoS Genetics* 2007; **3**: e115; doi:10.1371/journal.pgen.0030115.

104 Frayling TM, Timpson NJ, Weedon MN, Zeggini E, Freathy RM, Lindgren CM *et al.* A common variant in the FTO gene is associated with body mass index and predisposes to childhood and adult obesity. *Science (New York, N.Y.)* 2007; **316**: 889–894; doi:10.1126/science.1141634.

105 Dina C, Meyre D, Gallina S, Durand E, Körner A, Jacobson P *et al.* Variation in FTO contributes to childhood obesity and severe adult obesity. *Nature genetics* 2007; **39**: 724–726; doi:10.1038/ng2048.

106 Tönjes A, Zeggini E, Kovacs P, Böttcher Y, Schleinitz D, Dietrich K *et al.* Association of FTO variants with BMI and fat mass in the self-contained population of Sorbs in Germany.

European journal of human genetics : EJHG 2010; **18**: 104–110; doi:10.1038/ejhg.2009.107.

107 Klöting N, Schleinitz D, Ruschke K, Berndt J, Fasshauer M, Tönjes A *et al.* Inverse relationship between obesity and FTO gene expression in visceral adipose tissue in humans. *Diabetologia* 2008; **51**: 641–647; doi:10.1007/s00125-008-0928-9.

108 Smemo S, Tena JJ, Kim K-H, Gamazon ER, Sakabe NJ, Gómez-Marín C *et al.* Obesity-associated variants within FTO form long-range functional connections with IRX3. *Nature* 2014; **507**: 371–375; doi:10.1038/nature13138.

109 Claussnitzer M, Dankel SN, Kim K-H, Quon G, Meuleman W, Haugen C *et al.* FTO Obesity Variant Circuitry and Adipocyte Browning in Humans. *The New England journal of medicine* 2015; **373**: 895–907; doi:10.1056/NEJMoa1502214.

110 Kundaje A, Meuleman W, Ernst J, Bilenky M, Yen A, Heravi-Moussavi A *et al.* Integrative analysis of 111 reference human epigenomes. *Nature* 2015; **518**: 317–330; doi:10.1038/nature14248.

111 ENCODE Project Consortium. An integrated encyclopedia of DNA elements in the human genome. *Nature* 2012; **489**: 57–74; doi:10.1038/nature11247.

112 Suske G, Bruford E, Philipsen S. Mammalian SP/KLF transcription factors: bring in the family. *Genomics* 2005; **85**: 551–556; doi:10.1016/j.ygeno.2005.01.005.

113 Kaczynski J, Cook T, Urrutia R. Sp1- and Krüppel-like transcription factors. *Genome biology* 2003; **4**: 206; dio:10.1186/gb-2003-4-2-206

114 Dang DT, Pevsner J, Yang VW. The biology of the mammalian Krüppel-like family of transcription factors. *The international journal of biochemistry & cell biology* 2000; **32**: 1103–1121; doi10.1016/S1357-2725(00)00059-5

115 Pearson R, Fleetwood J, Eaton S, Crossley M, Bao S. Krüppel-like transcription factors: a functional family. *The international journal of biochemistry & cell biology* 2008; **40**: 1996–2001; doi:10.1016/j.biocel.2007.07.018.

116 Funnell APW, Maloney CA, Thompson LJ, Keys J, Tallack M, Perkins AC *et al.* Erythroid Krüppel-like factor directly activates the basic Krüppel-like factor gene in erythroid cells. *Molecular and cellular biology* 2007; **27**: 2777–2790; doi:10.1128/MCB.01658-06.

Chapter 2

Publication: *Hypoxia- inducible factor 3A* gene expression and methylation in adipose tissue is related to adipose tissue dysfunction

Authors: Susanne Pfeiffer*, Jacqueline Krüger*, Anna Maierhofer, Yvonne Böttcher, Nora Klöting, Nady El Hajj, Dorit Schleinitz, Michael R. Schön, Arne Dietrich, Mathias Fasshauer, Tobias Lohmann, Mariam Dreßler, Michael Stumvoll, Thomas Haaf, Matthias Blüher & Peter Kovacs

*These authors contributed equally to this work

Accepted: 26.05.2016

Published: 27.06.2016

Scientific Reports 6, Article number: 27969; doi:10.1038/srep27969

www.nature.com/scientificreports

SCIENTIFIC REPORTS

OPEN

Hypoxia-inducible factor 3A gene expression and methylation in adipose tissue is related to adipose tissue dysfunction

Received: 20 November 2015
Accepted: 26 May 2016
Published: 27 June 2016

Susanne Pfeiffer[1,*], Jacqueline Krüger[2,*], Anna Maierhofer[3], Yvonne Böttcher[2], Nora Klöting[1,2], Nady El Hajj[3], Dorit Schleinitz[2], Michael R. Schön[4], Arne Dietrich[2,5], Mathias Fasshauer[1,2], Tobias Lohmann[6], Miriam Dreßler[6], Michael Stumvoll[1], Thomas Haaf[3], Matthias Blüher[1] & Peter Kovacs[2]

Recently, a genome-wide analysis identified DNA methylation of the *HIF3A* (*hypoxia-inducible factor 3A*) as strongest correlate of BMI. Here we tested the hypothesis that *HIF3A* mRNA expression and CpG-sites methylation in adipose tissue (AT) and genetic variants in *HIF3A* are related to parameters of AT distribution and function. In paired samples of subcutaneous AT (SAT) and visceral AT (VAT) from 603 individuals, we measured *HIF3A* mRNA expression and analyzed its correlation with obesity and related traits. In subgroups of individuals, we investigated the effects on *HIF3A* genetic variants on its AT expression (N = 603) and methylation of CpG-sites (N = 87). *HIF3A* expression was significantly higher in SAT compared to VAT and correlated with obesity and parameters of AT dysfunction (including CRP and leucocytes count). *HIF3A* methylation at cg22891070 was significantly higher in VAT compared to SAT and correlated with BMI, abdominal SAT and VAT area. Rs8102595 showed a nominal significant association with AT *HIF3A* methylation levels as well as with obesity and fat distribution. *HIF3A* expression and methylation in AT are fat depot specific, related to obesity and AT dysfunction. Our data support the hypothesis that HIF pathways may play an important role in the development of AT dysfunction in obesity.

Obesity and its associated comorbidities constitute an evolving health burden worldwide[1]. Obesity is closely related to chronic inflammation in adipose tissue, liver and skeletal muscle[2], which may contribute to chronic systemic inflammation, insulin resistance, and deterioration in glucose and lipid metabolism[3]. Upon weight gain, adipocyte hypertrophy may lead to hypoxia in adipose tissue which is considered as a causative factor in adipose tissue dysfunction[4–7]. It has been recently shown that adipose tissue expression of *hypoxia inducible factor (HIF) 1A* (*HIF1A*) increases in mice exposed to high fat diet[4]. In states of relative adipose tissue hypoxia, induction of HIF1α[5,6] stimulates accumulation of macrophages in adipose tissue[4,7] and the production of adipocyte-derived pro-inflammatory cytokines. HIFs are heterodimeric transcription factors that mediate hypoxia response in various tissues[6]. They consist of an oxygen-labile α-subunit and a constitutively expressed β-subunit. Three existing isoforms of the α-subunit, HIF1α, HIF2α and HIF3α, allow the formation of transcription factors with different functions upon dimerizing with HIF1β. Multiple isoforms of HIF3α exist[8]. HIF3α is capable of activating certain target genes independent or in collaboration with HIF1α, suggesting a role of HIF3α in glucose and amino acid metabolism, apoptosis, proteolysis, p53 signaling and PPAR signaling. In addition, HIF3α has been shown to play a role in adipocyte differentiation[9,10].

[1]Department of Medicine, Dermatology und Neurology, Department of Endocrinology und Nephrology, University of Leipzig, Leipzig, Germany. [2]Leipzig University Medical Center, IFB AdiposityDiseases, University of Leipzig, Leipzig, Germany. [3]Institute of Human Genetics, University of Würzburg, Würzburg, Germany. [4]Clinic of Visceral Surgery, Städtisches Klinikum Karlsruhe, Karlsruhe, Germany. [5]Department of Surgery, University of Leipzig, Leipzig, Germany. [6]Municipal Clinic Dresden-Neustadt, Dresden, Germany. *These authors contributed equally to this work. Correspondence and requests for materials should be addressed to P.K. (email: peter.kovacs@medizin.uni-leipzig.de)

Recent genome-wide analysis of DNA methylation in whole blood and human adipose tissue revealed an association of methylation at three CpG sites in intron 1 of *HIF3A* with BMI[11–13]. In addition, two single nucleotide polymorphisms (SNPs) rs8102595 and rs3826795, have been shown to be associated with methylation at these sites, yet to be independent of BMI[11]. The strong relationship of *HIF3A* methylation and obesity was also shown in neonates[14]. Furthermore, gene-diet interactions between the methylation-associated SNP rs3826795 and vitamin B intake were recently reported, providing a potential causal link between the epigenetic status and obesity[15].

Further investigation of the relationship between HIFs and development of obesity-associated comorbidities might reveal important insights in pathophysiological processes concerning AT inflammation and/or insulin resistance in the etiology of obesity related metabolic diseases. We therefore tested the hypothesis that expression of *HIF3A* in human subcutaneous and visceral adipose tissue is related to obesity, parameters of fat distribution and adipose tissue function. We further assessed the relationship between the AT expression, genetic variation (rs8102595 and rs3826795) and methylation of CpG-sites in *HIF3A*.

Material and Methods

Study participants. A total of 288 Caucasian men and 577 women were included in the study (Table 1). According to the ADA criteria, 343 subject were diagnosed with type 2 diabetes (T2D) and 484 had normal glucose tolerance (NGT)[16]. Paired samples of visceral adipose tissue and subcutaneous adipose tissue were obtained from 603 individuals following open abdominal surgery for gastric banding, cholecystectomy, weight reduction surgery, abdominal injuries or explorative laparotomy. Patients with end-stage malignant diseases were excluded from the study. All adipose tissue samples were frozen immediately in liquid nitrogen after explantation and stored at −80 °C. Six-hundred and three subjects (mean age 50 ± 14 years, mean BMI 43.6 ± 13.0 kg/m^2) were included into adipose tissue *HIF3A* mRNA expression analysis. DNA methylation analysis was performed in a subgroup of 87 subjects (mean age 58 ± 15 years, mean BMI 32.9 ± 12.7 kg/m^2). Genotyping was done in 548 individuals overlapping with adipose tissue biopsy donors (mean age 50 ± 14 years, mean BMI 34.6 ± 13.6 kg/m^2).

Phenotypic characterization including anthropometric measurements, body fat analysis (bioimpedance analyses or dual-energy X-ray absorptiometry) and metabolic parameters such as fasting plasma glucose and insulin, a 75-g oral glucose tolerance test (oGTT), HbA1c, lipoprotein-, triglyceride-, free fatty acid- and adipokine serum concentrations was performed as previously described[17,18]. Measurement of abdominal visceral and subcutaneous fat areas (N = 245) was performed using computed tomography (CT) or MRI scans. All subjects had a stable weight, defined as the absence of fluctuations of >2% of body weight for at least 3 months before surgery. In addition, adipocytes and cells of the stromal vascular fraction were isolated from adipose tissue samples of 35 subjects (18 men, 17 women). Adipocytes were isolated by collagenase (1 mg/ml) digestion. To determine cell size distribution and adipocyte number, aliquots of adipocytes were fixed with osmic acid and counted in a Coulter counter as previously described[19]. The study was approved by the ethics committee of the University of Leipzig (approval number: 159-12-21052012) and all subjects gave written informed consent. All methods were carried out in accordance with the approved guidelines.

Analysis of human *HIF3A* mRNA expression. Briefly, human *HIF3A* mRNA expression was measured by qRT-PCR using TaqMan Gene Expression Assay (Applied Biosystems, Darmstadt, Germany). Total RNA was isolated from adipose tissue samples using the Qiacube System (Qiagen, Hilden, Germany), and 2 µg RNA were reverse transcribed with standard reagents (Life Technologies). Further details including PCR conditions are provided in the Supplemental material. The following Gene Expression Assay was used: Hs00541709_M1 (tagging the transcripts NM_022462.4, NM_152794.3, NM_152795.3, NM_152796.4). *HIF3A* mRNA expression was calculated relative to the mRNA expression of *hypoxanthine guanine phosphoribosyltransferase 1 (HPRT1)*, determined by the assay Hs01003267_M1 (Applied Biosystems, Darmstadt, Germany). Expression of *HIF3A* and *HPRT1* mRNA were quantified by using the second derivative maximum method of the TaqMan Software (Applied Biosystems).

For expression analysis of *HIF3A* in adipocytes and stromal vascular fraction, total RNA was isolated from adipocytes and stromal vascular fraction extracted from 35 paired samples of subcutaneous and visceral adipose tissue. 300 ng RNA were reverse transcribed with standard reagents and from each RT-PCR, 23.5 µl was amplified in a 40 µl PCR using the Taqman Gene Expression Assay and the TaqMan Fast Advanced Mastermix according to the manufacturer's instruction. *HIF3A* mRNA expression was calculated relative to the mRNA expression of *HPRT1* mRNA or *18S rRNA*, determined by the assay Hs01003267_m1 (Applied Biosystems, Darmstadt, Germany).

DNA extraction and bisulfite conversion. Briefly, genomic DNA was extracted using the DNeasy Blood and Tissue Kit (Qiagen, Hilden, Germany) and bisulfite conversion was performed using the Epitect Bisulfite Kit (Qiagen, Hilden, Germany) according to the manufacturer's protocol.

Determining CpG methylation levels. PCR and sequencing primers were designed using the PyroMark Assay Design 2.0 software (Qiagen, Hilden, Germany). DNA fragments were amplified from bisulfite-converted DNA using forward primer 5′-TGGTTGAAGGGTTATTTAGGG-3′and biotinylated reverse primer 5′-ACTCTATCCCACCCCTTTT-3′. The PCR reaction mixture and cycler program are provided in the Supplementary material. Bisulfite pyrosequencing was performed on a PyroMark Q96MD pyrosequencing system (Qiagen) using the PyroMark Gold Q96 CDT reagent kit (Qiagen) and the Pyro Q-CpG software (Qiagen). Percentage of methylation at eleven individual CpG sites within intron 1 of *HIF3A* were determined using three different sequencing primers (Assay 1: 5′-TTTAGGGGGTGTAGG-3′; Assay 2: 5′-GGTGAGATGATTTTATAGGAA-3′; Assay 3: 5′-GTTAAGAGGGGTTTTTATT-3′). Assay 1 included seven CpGs, Assay 2 only one CpG and Assay 3 three CpGs. The sixth CpG site in Assay 1, the CpG site in Assay 2 and

	Total	Lean	Overweight	Obese	NGT	T2D	CRP<5
N	865	88	73	704	484	343	347
Men/Women	288/577	40/48	36/37	212/492	155/329	124/219	129/218
Age (years)	49 ± 13	62 ± 15[aaa]	62 ± 14	46 ± 11[ccc]	47 ± 15[ddd]	51 ± 10	49 ± 13
BMI (kg/m2)	44.3 ± 12.6	22.1 ± 2.3[aaa]	27.2 ± 1.3[bbb]	48.9 ± 9.0[ccc]	40.9 ± 12.9[eee]	49.4 ± 10.8	41.8 ± 11.7[aaa]
Body weight (kg)	129 ± 39	63 ± 9[aaa]	78 ± 9[bbb]	142 ± 30[ccc]	119 ± 41[ddd]	143 ± 33	122 ± 38[aaa]
Height (m)	1.6 ± 0.1	1.68 ± 0.09	1.69 ± 0.09	1.69 ± 0.09	1.69 ± 0.1	1.69 ± 0.1	1.70 ± 0.09
Waist (cm)	126.8 ± 26.2	77.0 ± 13.7[aaa]	96.8 ± 13.8[bbb]	137.1 ± 19.7[ccc]	116.2 ± 28.2[eee]	142.6 ± 22.0	124.0 ± 27.9
Hip (cm)	129.1 ± 28.7	86.3 ± 9.7[aaa]	102.4 ± 11.4[bbb]	141.5 ± 21.0[ccc]	126.0 ± 30.3[eee]	135.7 ± 24.7	127.0 ± 28.5
WHR	0.95 ± 0.13	0.90 ± 0.11[aa]	0.94 ± 0.08	0.97 ± 0.14	0.91 ± 0.12[eee]	1.05 ± 0.08	0.95 ± 0.13
Visceral Fat area (cm^2)	240 ± 172	45 ± 29[aaa]	119 ± 60[bbb]	313 ± 154[ccc]	177 ± 142[eee]	392 ± 150	209 ± 175
SC fat area (cm^2)	1093 ± 789	52 ± 26[aaa]	273 ± 171[bbb]	1509 ± 559[ccc]	992 ± 817[eee]	1386 ± 671	920 ± 814[e]
CT ratio (vis/sc)	0.4 ± 0.5	1.9 ± 0.9[aaa]	0.5 ± 0.3[bb]	0.2 ± 0.1[ccc]	0.3 ± 0.4	0.5 ± 0.7	0.4 ± 0.5
Body Fat (%)	41.4 ± 11.5	19.0 ± 3.5	24.3 ± 3.9	45.1 ± 8.0	38.5 ± 13.0	44.3 ± 9.4	39.1 ± 11.0
CRP (mg/dl)	11.4 ± 14.4	14.9 ± 22.9	9.1 ± 13.1	11.2 ± 13.1	11.2 ± 15.6	12.1 ± 13.2	2.4 ± 1.5
IL-6 (pg/ml)	6.0 ± 5.2	2.2 ± 3.3	2.8 ± 2.4	7.0 ± 5.3	5.2 ± 4.6	7.5 ± 6.0	4.1 ± 1.3
HbA1c (%)	6.1 ± 1.2	5.3 ± 0.4	5.7 ± 0.6	6.1 ± 1.2	5.5 ± 0.5	6.9 ± 1.4	6.0 ± 1.0
oGTT2h (mmol/l)	7.0 ± 2.6	6.0 ± 1.0	6.1 ± 0.9	7.4 ± 2.9	6.3 ± 1.0	14.8 ± 5.9	6.6 ± 1.7
FPG (mmol/l)	6.5 ± 2.5	5.5 ± 1.0	5.9 ± 1.5	6.7 ± 2.7	5.4 ± 1.0	8.1 ± 3.2	6.1 ± 2.1
FPI (pmol/)	123.1 ± 133.8	10.8 ± 20.6	68.0 ± 92.5	146.4 ± 137.2	62.4 ± 70.8	206.2 ± 156.4	109.7 ± 121.7
GIR (µmol/kg/min)	75.1 ± 33.4	102.5 ± 18.5	77.7 ± 25.8	56.9 ± 31.2	90.6 ± 21.4	30.5 ± 23.5	85.3 ± 28.3
Total cholesterol (mmol/l)	4.9 ± 1.0	5.1 ± 0.8	5.0 ± 1.1	4.9 ± 1.0	4.9 ± 1.0	4.9 ± 1.0	4.9 ± 1.0
HDL-C (mmol/l)	1.2 ± 0.3	1.7 ± 0.5	1.4 ± 0.3	1.1 ± 0.3	1.3 ± 0.4	1.1 ± 0.3	1.2 ± 0.4
LDL-C (mmol/l)	3.1 ± 0.9	2.8 ± 1.0	3.2 ± 0.8	3.1 ± 0.9	3.1 ± 0.9	3.0 ± 0.8	3.1 ± 0.9
FFA (mmol/l)	0.5 ± 0.4	0.2 ± 0.2	0.3 ± 0.3	0.6 ± 0.3	0.3 ± 0.3	0.8 ± 0.3	0.5 ± 0.3
TG (mmol/l)	1.8 ± 1.1	1.1 ± 0.4[aaa]	1.2 ± 0.5	1.9 ± 1.1[ccc]	1.4 ± 0.9[eee]	2.1 ± 1.1	1.8 ± 1.1
Leptin (ng/ml)	39.3 ± 24.2	4.8 ± 3.7[aaa]	12.4 ± 7.0[bbb]	45.4 ± 21.8[ccc]	37.1 ± 23.9	41.2 ± 25.0	35.6 ± 22.7[c]
Adiponectin (µg/ml)	6.9 ± 4.4	14.3 ± 6.2[aaa]	8.8 ± 3.5[bbb]	6.0 ± 3.3[ccc]	8.5 ± 4.7[eee]	4.9 ± 3.1	7.1 ± 4.2
Albumin (g/L)	28.1 ± 18.9	32.9 ± 7.7	34.4 ± 13.2	26.9 ± 20.2	27.1 ± 18.8	28.6 ± 19.6	29.5 ± 20.0
ALAT (µkat/l)	0.6 ± 0.5	0.4 ± 0.3[aaa]	0.5 ± 0.3	0.7 ± 0.5[ccc]	0.6 ± 0.4[d]	0.7 ± 0.5	0.7 ± 0.4
ASAT (µkat/l)	0.6 ± 2.3	0.4 ± 0.3	0.4 ± 0.2	0.6 ± 2.5	0.6 ± 3.0	0.6 ± 0.5	0.5 ± 0.3
gGT (µkat/l)	0.9 ± 1.5	1.0 ± 1.4	1.0 ± 1.5	0.8 ± 1.3	0.8 ± 1.0[d]	1.0 ± 1.7	0.7 ± 0.9[e]
TSH (mU/l)	1.9 ± 7.9	1.5 ± 2.1	1.5 ± 1.9	2.1 ± 8.8	1.7 ± 1.8	2.3 ± 12.4	1.4 ± 1.0
fT3 (pg/ml)	4.6 ± 0.9	4.5 ± 1.0	4.4 ± 0.7	4.7 ± 0.9[c]	4.5 ± 0.9	4.7 ± 0.9	4.6 ± 0.9
fT4 (pmol/l)	17.1 ± 1.4	17.2 ± 3.3	17.5 ± 3.2	16.9 ± 3.5	16.9 ± 3.4[d]	17.4 ± 3.4	17.6 ± 3.3[e]
Leucocytes/nl	8.1 ± 2.7	7.5 ± 3.2	7.4 ± 3.1	8.2 ± 2.6[c]	2.1 ± 0.5	2.1 ± 0.5	7.4 ± 2.2[e]
Erythrocytes (Mio/µl)	4.7 ± 0.8	4.6 ± 2.7	4.3 ± 0.9	4.7 ± 0.4	4.7 ± 1.0	4.7 ± 0.4	4.7 ± 0.4
Thrombocytes (10^3/l)	260 ± 81	252 ± 108	241 ± 71	261 ± 79	261 ± 73	259 ± 88	232 ± 66[e]

Table 1. Anthropometric and metabolic characteristics of study participants. Data are means ± SD; [a,b,c,d,e]$p < 0.05$, [aa,bb,cc,dd,ee]$p < 0.01$, [aaa,bbb,ccc,ddd,eee]$p < 0.001$ for comparison between (a) lean and obese, (b) lean and overweight, (c) overweight and obese, (d) type 2 diabetes subjects (T2D) and subjects with normal glucose tolerance (NGT) and (e) CRP < 5 and the entire cohort. 51 subjects with type 1 diabetes or impaired glucose tolerance were not considered for group comparison. BMI – Body Mass Index, WHR – waist-to-hip ratio, sc - subcutaneous, TG – Triglycerides, ALAT – alanine aminotransferase, ASAT - aspartate aminotransferase, gGT - Gamma-glutamyl transferase, TSH – thyroid-stimulating hormone, fT3 – free triiodothyronine, fT4 – free tetraiodothyronine, CRP – C-reactive protein, IL-6 – Interleukin 6, HbA1c – Glycohemoglobin, oGTT – oral Glucose Tolerance Test, FPG – Fasting plasma glucose, FPI – Fasting plasma insulin, GIR – Glucose infusion rate during the steady state of an euglycemic hyperinsulinemic clamp, HDL-C – high Density Lipoprotein Cholesterol, LDL-C – Low Density Lipoprotein Cholesterol, FFA – Free Fatty Acids.

the third CpG site in Assay 3 correspond to the CpG sites on the 450 K array reported elsewhere[11]. In our experience, the average methylation difference between technical replicates is approximately one percentage point.

Genotyping of *HIF3A* SNPs. Genomic DNA was extracted from blood using the Quick Gene DNA whole blood Kit (Kurabo, Japan). Genotyping of the two previously reported SNPs rs8102595 (A/G) and rs3826795 (G/A)[11] was performed using the TaqMan SNP Genotyping assay (Applied Biosystems; C _29247492_10; C_31640839_10). To assess genotyping reproducibility, a random ~5% selection of the sample were re-genotyped for all SNPs; all genotypes matched initial designated genotypes. Potential functional significance of the studied genetic variants was checked using the Regulome Database, which includes public datasets from GEO, the ENCODE project, and published literature[20].

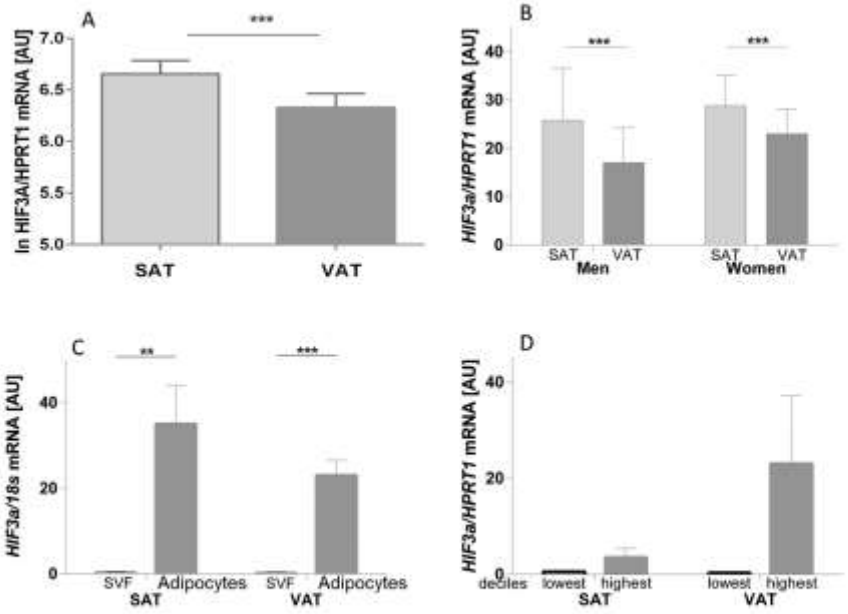

Figure 1. ***HIF3A*** **mRNA expression in human subcutaneous (SAT, n = 584) and visceral (VAT, n = 588) adipose tissue.** In the entire study cohort (**A**), but also in subgroups of men (SAT, n = 108; VAT, n = 110) and women (SAT, n = 231; VAT, n = 230) (Subjects with T2D were excluded from analysis) (**B**). Expression of *HIF3A* is significantly higher in subcutaneous (SAT) compared to visceral (VAT) adipose tissue. **(C)** *HIF3A* mRNA expression in adipocytes (n = 35) and cells of the stromal vascular fraction (SVF). *HIF3A* is significantly higher expressed in adipocytes compared to cells of the SVF in both compartments **(D)** *HIF3A* mRNA expression in relation to adipocyte cell size in subcutaneous (SAT) and visceral (VAT) adipose tissue. Individuals were categorized by mean SAT and VAT adipocyte size into deciles. Comparison of *HIF3A* mRNA expression between individuals with the lowest versus highest mean adipocyte size decile reveals that *HIF3A* is more highly expressed in subjects with higher mean adipocyte volume. Data are presented as means ± SEM. $^{**}p < 0.01$, $^{***}p < 0.001$, AU-arbitrary units.

Statistical Analyses. All non-normally distributed parameters were logarithmically transformed to approximate a normal distribution. To analyze differences in *HIF3A* methylation/expression levels between visceral and subcutaneous adipose tissue, paired two-tailed t-tests were applied. To test for group differences (e.g. lean vs. obese, NGT vs. T2D) two tailed *t-tests* were used. Pearson's correlation coefficients were used to assess bivariate correlation with phenotypes related to obesity, fat distribution and glucose and insulin homeostasis. Linear regression models were used to control for confounders such as age, gender and BMI. To test SNPs for genetic associations with mRNA expression, DNA methylation and metabolic traits, linear regression analysis adjusted for respective covariates was applied. Association studies on type 2 diabetes (T2D) and obesity (lean with BMI < 25 kg/m^2 vs. obese with BMI ≥ 30 kg/m^2) were done using logistic regression analyses. P-values ≤ 0.05 were considered to provide nominal evidence for association. Two-sided p-values are reported without adjustments for multiple testing. The analysis of associations with quantitative traits was restricted to nondiabetic subjects to avoid diabetes status or treatment masking potential effects of the variants on these parameters. Statistical analyses were performed using SPSS statistics version 20.0.1 (SPSS, Inc., Chicago, IL, USA).

Results

HIF3A **mRNA expression is fat depot related.** Analysis of paired subcutaneous and visceral adipose tissue samples revealed significantly higher *HIF3A* mRNA expression in subcutaneous compared to visceral adipose tissue (Fig. 1A). The fat depot differences in *HIF3A* expression could be confirmed in both genders (Fig. 1B). There was no significant difference in both subcutaneous and visceral adipose tissue *HIF3A* mRNA expression between individuals with normal glucose tolerance (NGT) and with type 2 diabetes (Supplementary Figure).

We further analyzed the contribution of adipocytes and stromal vascular fraction cells on whole adipose tissue *HIF3A* mRNA expression. Analysis of visceral and subcutaneous stromal vascular fraction showed significantly higher *HIF3A* mRNA levels in subcutaneous compared to visceral stromal vascular fraction ($p < 0.05$) (subcutaneous 0.56 ± 0.84 and visceral 0.37 ± 0.57). In paired samples of adipocytes and stromal vascular fraction cells we found significantly higher *HIF3A* expression in adipocytes compared to stromal vascular fraction cells both in subcutaneous and visceral fat compartments (Fig. 1C). There was no significant fat depot-related difference in *HIF3A* mRNA expression of isolated adipocytes. We further sought to determine *HIF3A* mRNA expression

	HIF3A mRNA Expression in subcutaneous adipose tissue			*HIF3A* mRNA Expression in visceral adipose tissue		
	r	p-value	adj. p-value	r	p-value	adj. p-value
Age (years)	−0.23	4.61×10^{-3}	**0.032**	−0.237	3.08×10^{-3}	0.076
BMI (kg/m²)	0.239	2.86×10^{-3}	**0.017**[a]	0.283	5.46×10^{-5}	$\mathbf{8.84 \times 10^{-4}}$[a]
Body weight (kg)	0.235	5.56×10^{-3}	0.467[a]	0.263	5.45×10^{-4}	0.280[a]
Height (m)	0.044	0.458	0.467	0.001	0.983	0.538
Waist (cm)	0.472	8.41×10^{-8}	**0.010**	0.515	1.89×10^{-10}	**0.048**
Hip (cm)	0.387	2.13×10^{-5}	0.425	0.442	6.73×10^{-7}	0.628
WHR	0.172	0.067	**0.018**	0.139	0.135	**0.033**
Visceral fat area (cm²)	0.391	3.19×10^{-5}	0.636	0.442	1.71×10^{-6}	0.479
SC fat area (cm²)	0.392	2.99×10^{-5}	0.240	0.465	4.06×10^{-7}	0.604
CT ratio (sc/vis)	−0.259	7.04×10^{-4}	0.165	−0.319	7.80×10^{-6}	0.325
Body fat (%)	0.324	0.017	0.055[a]	0.442	8.23×10^{-6}	**0.013**[a]
CRP (mg/dl)	−0.138	0.021	$\mathbf{1.8 \times 10^{-3}}$	−0.153	0.010	$\mathbf{3.19 \times 10^{-4}}$
Leucocytes/nl	−0.127	0.032	$\mathbf{3.05 \times 10^{-3}}$	−0.133	0.024	$\mathbf{1.13 \times 10^{-3}}$
Met Blood (%)	0.054	0.720	0.618	0.023	0.876	0.772
Met SAT (%)	−0.054	0.687	0.482	−0.088	0.498	0.345
Met VAT (%)	0.060	0.648	0.667	−0.045	0.729	0.757
Leptin mRNA sc	0.227	2.82×10^{-4}	$\mathbf{2.37 \times 10^{-4}}$	0.216	5.28×10^{-4}	$\mathbf{1.41 \times 10^{-3}}$
Leptin mRNA vis	0.117	0.063	**0.043**	0.195	2.0×10^{-3}	$\mathbf{2.60 \times 10^{-3}}$
PPARG mRNA sc	0.001	0.977	0.939	0.002	0.967	0.878
PPARG mRNA vis	0.050	0.253	0.439	0.111	0.010	**0.023**

Table 2. Correlation analyses of subcutaneous and visceral adipose tissue *HIF3A* mRNA expression with metabolic parameters, methylation levels and mRNA expression of *leptin* and *PPARG*. r - correlation coefficient (Pearson adj. – p-value adjusted to age, sex and BMI), [a]adjusted for sex and age; BMI – Body Mass Index, WHR – waist-to-hip ratio, sc - subcutaneous, CRP – C-reactive protein, Met Blood (%)/Met SAT (%)/Met VAT (%) - Methylation of cg22891070 in *HIF3A* in blood/SAT/VAT.

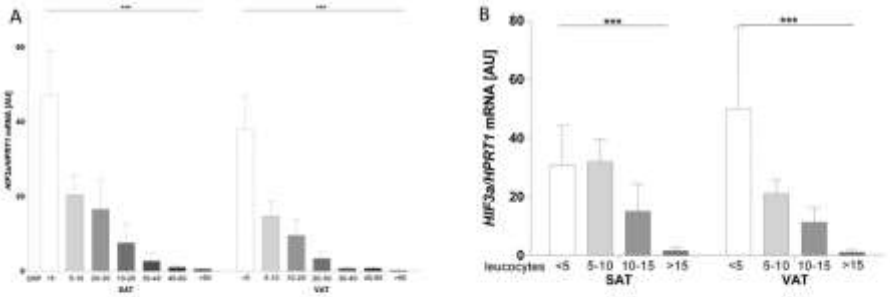

Figure 2. *HIF3A* mRNA expression in subcutaneous and visceral adipose tissue in relation to CRP serum concentration categories (n = 318) and leucocyte counts (n = 326). A significant inverse relationship between both CRP level (**A**) and leucocyte count (**B**) and expression of *HIF3A* in both compartments can be observed. Data are presented as means ± SEM. ***p < 0.001, AU-arbitrary units.

in relation to adipocyte cell size. Comparison of *HIF3A* mRNA expression between individuals with the lowest versus highest mean adipocyte size decile reveals that *HIF3A* is more highly expressed in subjects with higher mean adipocyte volume (Fig. 1D).

***HIF3A* mRNA expression in adipose tissue correlates with parameters of obesity, systemic inflammation, glucose metabolism and mRNA expression of genes regulating adipogenesis (*leptin*, *PPARG*).** *HIF3A* mRNA expression in visceral and subcutaneous adipose tissue correlated significantly with BMI, body weight, waist and hip circumferences, abdominal visceral and subcutaneous fat area, %body fat, free fatty acid, triglyceride, alanine aminotransferase (ALAT), leptin serum concentrations and with the mRNA expression of *Leptin* (Table 2 and Supplementary Table 1). Furthermore, there were significant inverse correlations between subcutaneous and visceral adipose tissue *HIF3A* expression and age, CT ratio, adiponectin and C-reactive protein (CRP) serum concentrations (Fig. 2A) and leucocyte count (Fig. 2B). Only in visceral adipose tissue, *HIF3A* expression correlated with fasting plasma insulin, thyroid-stimulating hormone (TSH),

	rs8102595			rs3826795		
	A/A	A/G + G/G	p-value	A/A+ A/G	G/G	p-value
N	446	95		208	336	
Men/Women	151/295	32/63		73/135	110/226	
Age	52.83 ± 15.79	55.48 ± 15.44	0.482	49.56 ± 15.31	50.72 ± 14.69	0.278
BMI (kg/m²)	43.48 ± 13.74	42.51 ± 13.50	0.239	43.64 ± 14.04	42.93 ± 13.32	0.908
Body weight (kg)	126.86 ± 42.81	124.57 ± 40.14	0.680	128.42 ± 45.54	124.60 ± 41.15	0.769
Height (m)	1.69 ± 0.09	1.69 ± 0.9	0.628	1.69 ± 0.09	1.69 ± 0.09	0.763
Waist (cm)	124.26 ± 29.98	121.84 ± 30.09	0.798	124.46 ± 30.43	122.85 ± 29.87	0.935
Hip (cm)	130.53 ± 28.99	128.59 ± 28.38	0.851	129.54 ± 28.38	130.08 ± 29.56	0.676
WHR	0.95 ± 0.13	0.96 ± 0.16	0.316	0.96 ± 0.16	0.94 ± 0.12	0.921
VAT area (cm²)	242.93 ± 173.84	237.02 ± 159.92	0.575	256.05 ± 183.40	228.98 ± 159.97	0.674
SAT area (cm²)	1095.74 ± 795.48	1129.73 ± 819.78	0.536	1122.85 ± 774.80	1094.46 ± 817.64	0.902
VAT mean	123.00 ± 20.82	122.08 ± 20.60	0.999	119.69 ± 25.71	124.66 ± 17.25	**0.014**
SAT mean	127.37 ± 19.89	127.51 ± 17.42	0.486	126.50 ± 19.04	127.99 ± 19.84	0.334
VAT max	209.23 ± 58.51	230.21 ± 96.06	0.060	210.73 ± 74.84	213.66 ± 63.47	0.109
SAT max	214.28 ± 70.88	249.22 ± 110.69	$\mathbf{1.23 \times 10^{-3}}$	224.71 ± 80.22	217.94 ± 79.94	0.987
CT ratio (vis/sc)	0.47 ± 0.63	0.38 ± 0.30	0.922	0.40 ± 0.42	0.48 ± 0.66	0.826
Body fat (%)	41.95 ± 11.35	42.26 ± 11.72	0.496	41.15 ± 11.88	42.57 ± 11.11	0.607
CRP (mg/dl)	12.04 ± 15.09	11.20 ± 16.05	0.935	13.09 ± 15.67	11.34 ± 15.49	0.198
Leucocytes/nl	8.21 ± 2.88	8.08 ± 2.50	0.743	8.42 ± 3.22	8.00 ± 2.48	0.155
Blood Met (%)	20.99 ± 8.07	22.31 ± 5.11	0.143	21.43 ± 7.36	21.27 ± 7.56	0.811
Met SAT (%)	11.95 ± 5.86	16.34 ± 6.54	**0.011**	13.56 ± 7.38	12.69 ± 5.83	0.784
Met VAT (%)	17.04 ± 5.61	19.69 ± 6.10	**0.038**	18.20 ± 4.41	17.46 ± 6.18	0.401
SAT *HIF3A* mRNA	21.08 ± 72.62	7.43 ± 40.53	0.209	11.58 ± 49.82	22.60 ± 76.47	0.660
VAT *HIF3A* mRNA	23.92 ± 106.19	10.45 ± 50.03	0.073	16.80 ± 82.25	24.09 ± 106.69	0.729

Table 3. Association of rs8102595 and rs3826795 with anthropometric and metabolic characteristics, mRNA expression and DNA methylation. Due to the low minor allele frequency (MAF) of the studied polymorphisms, subjects homozygous for the minor alleles (n = 3 for rs8102595, n = 16 for rs3826795) were combined with heterozygous groups (i.e. dominant mode of inheritance was used for statistical analyses). p-value adjusted for age, gender and BMI and diabetes status; BMI – Body Mass Index, WHR – waist-to-hip ratio, SAT – subcutaneous adipose tissue, VAT- visceral adipose tissue CRP – C-reactive protein, Met Blood (%)/Met SAT (%)/Met VAT (%) - Methylation of cg22891070 in *HIF3A* in blood/SAT/VAT, *HIF3A* mRNA – mRNA expression of *HIF3A* in subcutaneous/visceral adipose tissue.

high density lipoprotein (HDL)-cholesterol, gamma glutamyltransferase and the mRNA expression with PPARG ($p < 0.05$; Table 2).

After adjusting for age and gender, correlations between visceral and subcutaneous adipose tissue *HIF3A* mRNA expression and BMI, but also between visceral *HIF3A* mRNA expression and %body fat remained significant (Table 2). Correlations between subcutaneous and visceral adipose tissue *HIF3A* mRNA expression and waist, WHR, CRP level, leucocyte count and *leptin* mRNA expression remained significant after adjusting for age, gender and BMI (Table 2). After adjusting for covariates, free fatty acids only correlated with subcutaneous *HIF3A* mRNA expression and visceral *HIF3A* mRNA levels correlated with visceral mRNA expression of PPARG. In both fat depots, we found decreased *HIF3A* mRNA expression with increasing subcategories of both CRP serum concentrations and leucocyte counts (Fig. 2). To avoid a potential bias of systemic inflammation on *HIF3A* expression and its associations with anthropometric and metabolic traits, we performed correlation analyses only in individuals with CRP < 5mg/dl; however, the data remained unchanged (data not shown).

Association of rs8102595 and rs3826795 with *HIF3A* DNA methylation, mRNA expression and metabolic traits. In the present study, we included 2 SNPs (rs8102595 and rs3826795) which have previously been shown to be associated with DNA methylation in a large cohort including >2000[11]. Both studied polymorphisms were in Hardy-Weinberg Equilibrium ($p > 0.05$) with following minor allele frequencies: rs8102595-10.8%, rs3826795-21.6%. There was no significant association between the SNPs and *HIF3A* mRNA expression in any of the two adipose tissue depots (Table 3). However, rs8102595 was nominally associated with *HIF3A* DNA methylation in visceral and subcutaneous adipose tissue ($p < 0.05$ after adjusting for age, gender and BMI; Table 3). Subjects carrying the minor allele (G) had a higher *HIF3A* DNA methylation in visceral adipose tissue, which was in line with the lower *HIF3A* mRNA expression in visceral adipose tissue (albeit not significant). Association analyses with parameters of obesity and fat distribution revealed a nominal association between rs3826795 and total cholesterol and the mean fat cell size of visceral adipose tissue (Supplementary Table 2). Rs8102595 showed an association with HDL-cholesterol, glucose infiltration rate and maximum fat cell size of subcutaneous adipose tissue (Table 3 and Supplementary Table 2).

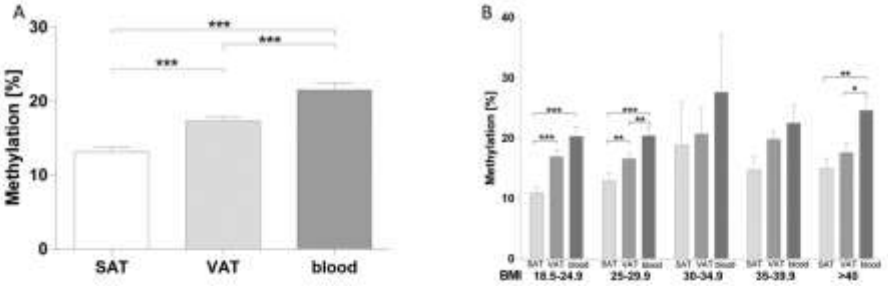

Figure 3. Methylation of cg22891070 in *HIF3A* in different tissues and in relation to BMI (n = 87). The *HIF3A* locus is significantly higher methylated in blood compared to SAT and VAT **(A)** The difference in methylation levels can be observed for all BMI groups **(B)** Methylation levels are higher in subjects with increased BMI **(B)**. Data are presented as means ± SEM. *p < 0.05, **p < 0.01, ***p < 0.001.

***HIF3A* DNA methylation in blood, subcutaneous and visceral adipose tissue.** Methylation measured at the CpG site in Assay 2, corresponds to the published cg22891070, which has been reported to show the strongest correlation to BMI[11]. In our study, *HIF3A* DNA methylation at cg22891070 was significantly higher in blood (20.84 ± 7.74%) compared to subcutaneous (12.83 ± 6.82%; $p < 0.001$) and visceral adipose tissue (17.28 ± 5.61%; $p < 0.001$), whereas *HIF3A* DNA methylation in visceral adipose tissue was significantly higher than in subcutaneous adipose tissue ($p < 0.001$; Fig. 3A). In addition, DNA methylation at cg22891070 in visceral adipose tissue correlated significantly with hip ($p < 0.01$, $r = 0.614$), subcutaneous ($p < 0.01$, $r = 0.651$) and visceral fat mass ($p < 0.05$, $r = 0.468$) and inversely with the CT-ratio ($p < 0.01$, $r = -0.653$). Correlations between methylation in visceral adipose tissue and subcutaneous fat mass ($p < 0.01$), CT ratio ($p < 0.01$), hip ($p < 0.01$) and adiponectin ($p < 0.05$, $r = -0.187$) remained significant even after adjusting for age, gender and BMI. Furthermore, methylation of cg22891070 in subcutaneous adipose tissue correlated with CT ratio ($p < 0.05$, $r = -0.571$) and age ($p < 0.05$, $r = -0.268$). After adjusting for gender and BMI the correlation remained significantly for age ($p = 0.032$). Albeit not significant, in all analyzed tissues, obese individuals displayed a higher methylation of cg22891070 compared to lean and overweight individuals (Fig. 3B). The analyses including other tested CpG sites did not reveal correlations beyond those observed for cg22891070 (data not shown).

Discussion

Recent studies revealed an association between BMI and methylation of *HIF3A* in whole blood and in adipose tissue[11–13]. It has been proposed that the HIF-system could play a role in mechanisms involved in the pathophysiology of adipose tissue-inflammation, obesity-induced insulin resistance and the etiology of obesity related diseases. We therefore sought to further elucidate the relationship between *HIF3A* mRNA expression in visceral and subcutaneous adipose tissue and obesity, but also methylation of CpG-sites in *HIF3A*. In summary, we show that *HIF3A* gene expression and methylation in adipose tissue are fat depot specific, and related to obesity and adipose tissue dysfunction.

We investigated the methylation and expression of *HIF3A* in two distinct fat depots, subcutaneous and visceral adipose tissue. We show that higher *HIF3A* mRNA expression in both subcutaneous and visceral adipose tissue is associated with higher BMI and obesity related traits. HIF3A has been shown to accelerate 3T3-L1 adipocyte differentiation and to induce the expression of adipocyte related genes[9]. Interestingly, we found higher adipose tissue *HIF3A* mRNA expression in individuals of the highest decile of mean adipocyte size (for both depots) compared to the lowest decile. This may suggest that *HIF3A* is involved in the determination of adipocyte size and may thereby contribute to adipose tissue expandability. Our results further support the hypothesis that expression of *HIF3A* might be induced in states of metabolic excess and mediate mechanisms involved in adipogenesis. Moreover, based on our data, the expression of *HIF3A* seems to be more pronounced in adipocytes compared to the stromal vascular fraction independent of the fat depot. To this end, adipocytes isolated from subcutaneous adipose tissue displayed higher expression levels of *HIF3A* than those isolated from visceral adipose tissue. Thus, the major proportion of *HIF3A* expression in adipose tissue might be attributed to primary adipocytes, which further supports the proposed regulatory role of HIF3A in adipogenesis. In further support of this, we found a positive correlation between the mRNA expression of *HIF3A* and *leptin* (in both visceral and subcutaneous adipose tissue) as well as *PPARG* (in visceral adipose tissue), two genes involved in the regulation of adipogenesis.

It is noteworthy, that *HIF3A* expression inversely correlated with CRP level and leucocyte count, suggesting down-regulation of the *HIF3A* expression in inflammatory states. Chronic inflammation in adipose tissue, liver and skeletal muscle are commonly associated with obesity[2], which results in secondary pathologies like insulin resistance, hyperinsulinemia and glucose intolerance[3,21]. Obesity promoted relative hypoxia in adipocytes stimulates HIF1A-induction[5,6], which then triggers the inflammation process by mediating the production of adipocyte-derived chemokines and adipose tissue macrophage accumulation[4,7]. HIF3A can inhibit HIF1A mediated signaling under certain circumstances[22]. The observed reduced expression of *HIF3A* in inflammatory states may facilitate increased HIF1A signaling, which in turn could activate an inflammatory cascade within adipose tissue.

HIF3A mRNA expression is regulated at different levels. Transcription of *HIF3A* can be induced by HIF1 via hypoxia response elements (HREs) in the promoter region and protein stability of HIF3α can be regulated in dependency of oxygen supply via the oxygen-dependent degradation domain (ODD)[22–24]. *HIF3A* expression has further been shown to be regulated by micro RNA (miRNA), thus to be modified on a post-transcriptional level[25]. These different mechanisms can supplement one another in fine tuning of *HIF3A* expression. We hypothesize that the complex regulation of *HIF3A* expression can be influenced by DNA methylation in various ways by interfering with different mechanisms of regulation. An association between BMI and methylation at three CpG-sites in intron 1 of *HIF3A* in whole blood and in adipose tissue has recently been identified by employing genome-wide DNA-methylation analyses[11–13]. In contrast, we did not find a correlation between BMI and *HIF3A* methylation. This may be due to the smaller sample size and a different composition of our cohort, which is characterized by a relatively high BMI (32.9 kg/m^2), and thus, strongly differing from the previously reported cohorts with average BMI ranging between 24.2 and 28.3 kg/m^2. Rönn *et al.* were able to replicate the association between methylation of *HIF3A* and BMI in a female cohort only[12] and Demerath *et al.* showed *HIF3A* methylation to be associated with BMI only in one of three cohorts investigated[13]. Considering multiple isoforms of HIF3α[8], it is plausible that methylation might be transcript-specific; yet, one would expect to observe consistent results upon expression analysis of the same transcript.

It is of note that the CpG sites at the *HIF3A* locus that were associated with BMI are situated within regions of open chromatin, suggesting that these sites lie in a regulatory region[11,26]. However, this regulation appears more complex than being dependent on methylation only. It is plausible that methylation of *HIF3A* results in altered expression profiles, networking with mechanisms in different stages of regulation. Yet, a linear effect between methylation and expression even of the same transcript cannot be confirmed.

Methylation analysis of *HIF3A* in our cohort revealed significant differences between methylation in blood, subcutaneous and visceral adipose tissue, being strongest in blood and weakest in subcutaneous adipose tissue. Since *HIF3A* mRNA expression in subcutaneous adipose tissue is higher than in visceral adipose tissue, it is possible that methylation could together with other regulatory mechanisms, cause a decrease in the expression of *HIF3A*. In line with this, rs8102595 was nominally associated with DNA methylation at cg22891070 in subcutaneous and visceral adipose tissue; thus supporting data by Dick *et al.*[11] reporting associations of 2 SNPs (rs8102595 and rs3826795) with DNA methylation. Based on the Regulome Database[20], rs3826795 might affect the binding of transcription factors POLR2A and SIN3A, and rs8102595 might influence DNA-protein binding. However, considering the lack of associations of the two SNPs with BMI, changes in *HIF3A* methylation seem to be mediated by obesity rather than promoting obesity itself[11]. It is also of note, that we did not observe an association between the SNPs and *HIF3A* mRNA expression in any of the two adipose tissue depots. We have to point out however, that the availability of the biomaterial (adipose tissue and blood samples) only allowed including 548 subjects for genotyping and for subsequent genotype-expression association analyses, which may have resulted in the lack of statistical power for correlation analyses.

In contrast to previous studies mostly investigating subcutaneous adipose tissue, the present study reveals mRNA expression and DNA methylation differences between subcutaneous and visceral adipose tissue. The two depots consist of different histological and biochemical compounds. The depot-specific expression of *HIF3A* may be important for the different functioning of the different depots. Whereas visceral adipose tissue is more vascular, innervated and contains a higher number of inflammatory and immune cells, subcutaneous adipose tissue has a higher preadipocyte differentiating capacity and a lower percentage of large adipocytes[27]. As *HIF3A* mRNA expression is higher in subcutaneous adipose tissue, possibly due to differences in methylation, this contributes to our assumption that HIF3α might be involved in preadipocyte differentiation, and that this process may be regulated by methylation, along with other factors. It is noteworthy that recently, we observed diminished hydroxymethylation levels in subcutaneous adipose tissue, as a measure of potential de-methylation mechanisms, which might be related to the higher number of pre-adipocytes in subcutaneous adipose tissue[28].

We found methylation of *HIF3A* in both compartments to be correlated inversely with fat distribution, and methylation in VAT correlated significantly with subcutaneous fat mass. This suggests that methylation occurs rather in subjects with a preponderance of subcutaneous fat. We also detected an inverse association between age and methylation in subcutaneous adipose tissue, which leads to the assumption that the modification is dynamic and changes during lifetime.

Finally, it has to be acknowledged that the CpG site cg22891070 presented in our study is located between the 2 previously reported CpG islands[11]. Various *HIF3A* transcripts with different functions have been reported[22] and it is also likely that they can be specifically affected by the methylation. Since the expression assay used in the present study tagged all potential *HIF3A* transcripts, we were not able to link cg22891070 to a specific transcript. However, in our own datasets based on genome-wide expression arrays (unpublished data) transcript variants 2 (NM_022462.4) and 3 (NM_152795.3) seem to be predominantly expressed in adipose tissue. Since Pasanen *et al.*[22] suggested no functional relevance of the variant 3, it remains to be determined whether transcript variant 2 appears functionally relevant in adipose tissue.

In conclusion, our data suggest that *HIF3A* expression and methylation in adipose tissue is related to its dysfunction, making HIF3A an important factor involved in the complex etiology of obesity and associated comorbidities. HIF3A might function as an accelerator of adipogenesis in situations of excess of energetic supply and might contribute to the etiology of secondary obesity-induced pathologies by allowing a stronger induction of HIF1α-mediated proinflammatory signaling.

References

1. Swinburn, B. A. *et al.* The global obesity pandemic: shaped by global drivers and local environments. *Lancet* **378,** 804–814 (2011).
2. Glass, C. K. & Olefsky, J. M. Inflammation and lipid signaling in the etiology of insulin resistance. *Cell Metab.* **15,** 635–645 (2012).
3. Shu, C. J., Benoist, C. & Mathis, D. The immune system's involvement in obesity-driven type 2 diabetes. *Semin. Immunol.* **24,** 436–442 (2012).

4. Lee, Y. S. *et al.* Increased adipocyte O_2 consumption triggers HIF-1α, causing inflammation and insulin resistance in obesity. *Cell* **157,** 1339–1352 (2014).
5. Greer, S. N., Metcalf, J. L., Wang, Y. & Ohh, M. The updated biology of hypoxia-inducible factor. *EMBO J.* **31,** 2448–2460 (2012).
6. Majmundar, A. J., Wong, W. J. & Simon, M. C. Hypoxia-inducible factors and the response to hypoxic stress. *Mol. Cell* **40,** 294–309 (2010).
7. Gonsalves, C. S. & Kalra, V. K. Hypoxia-mediated expression of 5-lipoxygenase-activating protein involves HIF-1alpha and NF-kappaB and microRNAs 135a and 199a-5p. *J. Immunol.* **184,** 3878–3888 (2010).
8. Hara, S., Hamada, J., Kobayashi, C., Kondo, Y. & Imura, N. Expression and characterization of hypoxia-inducible factor (HIF)-3alpha in human kidney: suppression of HIF-mediated gene expression by HIF-3alpha. *Biochem. Biophys. Res. Commun.* **287,** 808–813 (2001).
9. Heidbreder, M. *et al.* Non-hypoxic induction of HIF-3alpha by 2-deoxy-D-glucose and insulin. *Biochem. Biophys. Res. Commun.* **352,** 437–443 (2007).
10. Hatanaka, M. *et al.* Hypoxia-inducible factor-3alpha functions as an accelerator of 3T3-L1 adipose differentiation. *Biological & pharmaceutical bulletin* **32,** 1166–1172 (2009).
11. Demerath, E. W. *et al.* Epigenome-wide association study (EWAS) of BMI, BMI change and waist circumference in African American adults identifies multiple replicated loci. *Human Molecular Genetics* **24,** 4464–4479 (2015).
12. Rönn, T. *et al.* Impact of age, BMI and HbA1c levels on the genome-wide DNA methylation and mRNA expression patterns in human adipose tissue and identification of epigenetic biomarkers in blood. *Human Molecular Genetics* **24,** 3792–3813 (2015).
13. Dick, K. J. *et al.* DNA methylation and body-mass index: a genome-wide analysis. *Lancet* **383,** 1990–1998 (2014).
14. Pan, H. *et al.* HIF3A association with adiposity: the story begins before birth. *Epigenomics* **7,** 1–13 (2015).
15. Huang, T. *et al.* DNA methylation variants at HIF3A locus, B vitamins intake, and long-term weight change: gene-diet interactions in two US cohorts. *Diabetes* **64,** 3146–3154 (2015).
16. American Diabetes Association. Diagnosis and classification of diabetes mellitus. *Diabetes care* **29** Suppl 1, S43–8 (2006).
17. Blüher, M. *et al.* Fas and FasL expression in human adipose tissue is related to obesity, insulin resistance, and type 2 diabetes. *The Journal of clinical endocrinology and metabolism* **99,** E36–44 (2014).
18. Klöting, N. *et al.* Insulin-sensitive obesity. *American journal of physiology. Endocrinology and metabolism* **299,** E506–15 (2010).
19. Blüher, M. *et al.* Adipose tissue selective insulin receptor knockout protects against obesity and obesity-related glucose intolerance. *Developmental cell* **3,** 25–38 (2002).
20. Boyle, A. P. *et al.* Annotation of functional variation in personal genomes using RegulomeDB. *Genome research* **22,** 1790–1797 (2012).
21. Lee, Y. S. *et al.* Inflammation is necessary for long-term but not short-term high-fat diet-induced insulin resistance. *Diabetes* **60,** 2474–2483 (2011).
22. Pasanen, A. *et al.* Hypoxia-inducible factor (HIF)-3alpha is subject to extensive alternative splicing in human tissues and cancer cells and is regulated by HIF-1 but not HIF-2. *The international journal of biochemistry & cell biology* **42,** 1189–1200 (2010).
23. Tanaka, T., Wiesener, M., Bernhardt, W., Eckardt, K.-U. & Warnecke, C. The human HIF (hypoxia-inducible factor)-3alpha gene is a HIF-1 target gene and may modulate hypoxic gene induction. *Biochem. J.* **424,** 143–151 (2009).
24. Heikkilä, M., Pasanen, A., Kivirikko, K. I. & Myllyharju, J. Roles of the human hypoxia-inducible factor (HIF)-3α variants in the hypoxia response. *Cellular and molecular life sciences: CMLS* **68,** 3885–3901 (2011).
25. Gits, C. M. M. *et al.* MicroRNA response to hypoxic stress in soft tissue sarcoma cells: microRNA mediated regulation of HIF3α. *BMC cancer* **14,** 429 (2014).
26. Cockerill, P. N. Structure and function of active chromatin and DNase I hypersensitive sites. *The FEBS journal* **278,** 2182–2210 (2011).
27. Ibrahim, M. M. Subcutaneous and visceral adipose tissue: structural and functional differences. *Obesity reviews: an official journal of the International Association for the Study of Obesity* **11,** 11–18 (2010).
28. Rohde, K. *et al.* DNA 5-hydroxymethylation in human adipose tissue differs between subcutaneous and visceral adipose tissue depots. *Epigenomics* **7,** 911–920 (2015).

Acknowledgements

We thank all those who participated in the study. This work was supported by grants from the IFB AdiposityDiseases (ADI-K50D and ADI-K7-45 to Y.B. and AD2-060E to P.K.) funded by the Federal Ministry of Education and Research (BMBF), Germany, FKZ: 01EO1501. This project was further supported by grants from the Collaborative Research Center funded by the German Research Foundation (CRC 1052; B01, B03, B04 to M.B., P.K. and N.K. respectively) and individual grant (HA 1374/15-1 to T.H.), by the Kompetenznetz Adipositas (Competence network for Obesity) funded by the German Federal Ministry of Education and Research (German Obesity Biomaterial Bank; FKZ 01GI1128) and by the German Diabetes Foundation (Deutsche Diabetes-Stiftung). Dorit Schleinitz is funded by the Boehringer Ingelheim Foundation.

Author Contributions

S.P., J.K., A.M. and N.E.H. performed mRNA expression and DNA methylation experiments; Y.B., N.K., T.H. and P.K. designed the study; M.R.S., A.D., M.F., T.L., M.D. and M.B. collected and provided biomaterial and clinical phenotypes; S.P., J.K., D.S., M.S., M.B. and P.K. wrote the manuscript.

Additional Information

Supplementary information accompanies this paper at http://www.nature.com/srep

Competing financial interests: The authors declare no competing financial interests.

How to cite this article: Pfeifer, S. *et al. Hypoxia-inducible factor 3A* gene expression and methylation in adipose tissue is related to adipose tissue dysfunction. *Sci. Rep.* **6**, 27969; doi: 10.1038/srep27969 (2016).

Hypoxia-inducible factor 3A gene expression and methylation in adipose tissue is related to adipose tissue dysfunction

Susanne Pfeiffer[1*], Jacqueline Krüger[2*], Anna Maierhofer[3], Yvonne Böttcher[2], Nora Klöting[1,2], Nady El Hajj[3], Dorit Schleinitz[2], Michael R. Schön[4], Arne Dietrich[2,5], Mathias Fasshauer[1,2], Tobias Lohmann[6], Miriam Dreßler[6], Michael Stumvoll[1], Thomas Haaf[3], Matthias Blüher[1], Peter Kovacs[2]

[1]Department of Medicine, Dermatology und Neurology, Department of Endocrinology und Nephrology, University of Leipzig, Leipzig, Germany
[2]Leipzig University Medical Center, IFB AdiposityDiseases, University of Leipzig, Leipzig, Germany
[3]Institute of Human Genetics, University of Würzburg, Würzburg, Germany
[4]Clinic of Visceral Surgery, Städtisches Klinikum Karlsruhe, Karlsruhe, Germany
[5]Department of Surgery, University of Leipzig, Leipzig, Germany
[6]Municipal Clinic Dresden-Neustadt, Dresden, Germany

Supplemental Material

Material and Methods

Analysis of human *HIF3A* mRNA expression

Briefly, human *HIF3*α mRNA expression was measured by qRT-PCR using TaqMan Gene Expression Assay (Applied Biosystems, Darmstadt, Germany), and fluorescence was detected on a TaqMan Quant Studio 6 Flex Real-Time PCR-System (Applied Biosystems, Darmstadt, Germany). Total RNA was isolated from AT samples using the Qiacube System (Qiagen, Hilden, Germany), and 2 µg RNA were reverse transcribed with standard reagents (Life Technologies). From each RT-PCR, 2µl was amplified in a 20µl PCR using the Taqman Gene Expression Assay (Applied Biosystems, Darmstadt, Germany) and the TaqMan Fast Advanced Mastermix (Applied Biosystems, Darmstadt, Germany). Samples were incubated in the Quant Studio 6 Flex Real-Time PCR-System (Applied Biosystems, Darmstadt, Germany)

for an initial denaturation at 95°C for 20s, followed by 45 PCR cycles, each cycle consisting of 95°C for 1s and 60°C for 20s. The following Gene Expression Assay was used: Hs00541709_M1 (tagging the transcripts NM_022462.4, NM_152794.3, NM_152795.3 and NM_152796.4). *HIF3A* mRNA expression was calculated relative to the mRNA expression of *HPRT1* mRNA, determined by a premixed assay on demand for *HPRT1* mRNA (Hs01003267_M1, Applied Biosystems, Darmstadt, Germany). Expression of *HIF3A* and *HPRT1* mRNA were quantified by using the second derivative maximum method of the TaqMan Software (Applied Biosystems).

For expression analysis of *HIF3A* in adipocytes and SVF, total RNA was isolated from adipocytes and SVF extracted from paired samples of SAT and VAT. 305 ng RNA were reverse transcribed with standard reagents and from each RT-PCR, 23.5µl was amplified in a 40µl PCR using the Taqman Gene Expression Assay and the TaqMan Fast Advanced Mastermix according to the manufacturer's instruction. *HIF3A* mRNA expression was calculated relative to the mRNA expression of *hypoxanthine guanine phosphoribosyltransferase 1 (HPRT1)* mRNA or *18S rRNA* (for isolated adipocytes only), determined by a premixed assay on demand (Hs01003267_m1; Applied Biosystems, Darmstadt, Germany).

DNA extraction and bisulfite conversion

Genomic DNA was extracted using the DNeasy Blood and Tissue Kit (Qiagen, Hilden, Germany) and bisulfite conversion was performed using the Epitect Bisulfite Kit (Qiagen, Hilden, Germany) according to the manufacturer's protocol. PCRs were carried out to amplify DNA fragments for pyrosequencing. The following primers were used (Metabion, Martiensried, Germany): Forward 5'-TGGTTGAAGGGTTATTTAGGG-3'; reverse carrying a biotin label at its 5'-end 5'-ACTCTATCCCACCCCTTTT-3'. The PCR reaction mixture for pyrosequencing consisted of 5 µl 10x PCR buffer with $MgCl_2$ (Roche Diagnostics,

Mannheim, Germany), 1 µl (10 mM dNTPs) PCR Grade Nucleotide Mix (Roche Diagnostics), 2.5 µl (10 pmol/µl) of forward and reverse primer (Metabion, München-Planegg, Germany), 0.4 µl (5 U/µl) FastStart Taq DNA Polymerase (Roche Diagnostics), 2 µl of bisulfite-converted DNA and 36.6 µl PCR-grade water. Amplifications were performed with an initial denaturation step at 95°C for 5 min, 38 cycles of 95°C for 30 s, 60°C for 30 s, and 72°C for 45 s, and a final extension step at 72°C for 5 min.

Results

Supplementary Table 1. Correlation analyses between subcutaneous and visceral adipose tissue *HIF3A* mRNA expression and study parameters.

	HIF3A mRNA Expression in subcutaneous adipose tissue			*HIF3A* mRNA Expression in visceral adipose tissue		
	r	p-value	adj. p-value	r	p-value	adj. p-value
Age (years)	-0.23	$4.61x10^{-5}$	**0.032**	-0.237	$3.08x10^{-5}$	0.076
BMI (kg/m²)	0.239	$2.86x10^{-5}$	**0.017**[a]	0.283	$5.46x10^{-7}$	**$8.84x10^{-4}$**[a]
Body weight (kg)	0.235	$5.56x10^{-5}$	0.467[a]	0.263	$5.45x10^{-6}$	0.280[a]
Height (m)	0.044	0.458	0.467	0.001	0.983	0.538
Waist (cm)	0.472	$8.41x10^{-9}$	**0.010**	0.515	$1.89x10^{-10}$	**0.048**
Hip (cm)	0.387	$2.13x10^{-5}$	0.425	0.442	$6.73x10^{-7}$	0.628
WHR	0.172	0.067	**0.018**	0.139	0.135	**0.033**
Visceral fat area (cm²)	0.391	$3.19x10^{-5}$	0.636	0.442	$1.71x10^{-6}$	0.479
SC fat area (cm²)	0.392	$2.99x10^{-5}$	0.240	0.465	$4.06x10^{-7}$	0.604
CT ratio (sc/vis)	-0.259	$7.04x10^{-3}$	0.165	-0.319	$7.80x10^{-4}$	0.325
Body fat (%)	0.324	0.017	0.055[a]	0.442	$8.23x10^{-4}$	**0.013**
CRP (mg/dl)	-0.138	0.021	**$1.8x10^{-3}$**	-0.153	0.010	**$3.19x10^{-4}$**
FPG (mmol/l)	0.077	0.200	0.180	0.017	0.770	0.784
FPI (pmol/l)	0.130	0.181	0.161	0.250	$8.21x10^{-3}$	0.634
Total Cholesterol (mmol/l)	-0.017	0.827	0.673	-0.010	0.891	0.586
HDL-C (mmol/l)	-0.138	0.141	0.913	-0.211	0.022	0.602
LDL-C	0.109	0.249	0.896	0.111	0.236	0.802
FFA (mmol/l)	0.442	$1.99x10^{-5}$	**$8.97x10^{-3}$**	0.401	$1.43x10^{-4}$	0.063
TG (mmol/l)	0.218	$3.40x10^{-3}$	0.085	0.196	$7.63x10^{-3}$	0.262
Leptin (ng/ml)	0.413	$2.14x10^{-5}$	0.866	0.461	$1.78x10^{-6}$	0.918
Adiponectin (µg/ml)	-0.290	$3.47x10^{-3}$	0.415	-.0348	$4.09x10^{-4}$	0.241
Albumin (g/L)	-0.328	0.072	0.159	-0.217	0.225	**0.015**
ALAT (µkat/l)	0.176	$3.31x10^{-3}$	0.303	0.135	0.023	0.980
gGT (µkat/l)	-0.101	0.095	0.226	-0.148	0.014	**0.040**
TSH (mU/l)	0.091	0.153	0.850	0.128	0.043	0.471
Leucocytes/nl	-0.127	0.032	**$3.05x10^{-3}$**	-0.133	0.024	**$1.13x10^{-3}$**
Met Blood (%)	0.054	0.720	0.618	0.023	0.876	0.772
Met SAT (%)	-0.054	0.687	0.482	-0.088	0.498	0.345
Met VAT (%)	0.060	0.648	0.667	-0.045	0.729	0.757

r - correlation coefficient (Pearson adj. – p-value adjusted to age, gender and BMI, [a] adjusted for gender and age; BMI – Body Mass Index, WHR – waist-to-hip ratio, sc - subcutaneous,

CRP – C-reactive protein, FPI – Fasting plasma insulin, HDL-C – high Density Lipoprotein Cholesterol, FFA – Free Fatty Acids, TG – Triglycerides, ALAT – alanine aminotransferase, gGT -Gamma-glutamyl transferase, TSH – thyroid-stimulation hormone, Met Blood (%)/ Met SAT (%) / Met VAT (%) - Methylation of cg22891070 in *HIF3A* in blood / SAT/ VAT

Supplementary Table 2. Association of rs8102595 and rs3826795 with anthropometric and metabolic characteristics, mRNA expression and DNA methylation.

	rs8102595			rs3826795		
	A/A	A/G + G/G	p-value	A/A+ A/G	G/G	p-value
N	446	95		208	336	
Men/Women	151/295	32/63		73/135	110/226	
Age	52.83±15.79	55.48±15.44	0.482	49.56±15.31	50.72±14.69	0.278
BMI (kg/m²)	43.48±13.74	42.51±13.50	0.239	43.64±14.04	42.93±13.32	0.908
Body weight (kg)	126.86±42.81	124.57±40.14	0.680	128.42±45.54	124.60±41.15	0.769
Height (m)	1.69±0.09	1.69±0.9	0.628	1.69±0.09	1.69±0.09	0.763
Waist (cm)	124.26±29.98	121.84±30.09	0.798	124.46±30.43	122.85±29.87	0.935
Hip (cm)	130.53±28.99	128.59±28.38	0.851	129.54±28.38	130.08±29.56	0.676
WHR	0.95±0.13	0.96±0.16	0.316	0.96±0.16	0.94±0.12	0.921
VAT area (cm²)	242.93±173.84	237.02±159.92	0.575	256.05±183.40	228.98±159.97	0.674
SAT area (cm²)	1095.74±795.48	1129.73±819.78	0.536	1122.85±774.80	1094.46±817.64	0.902
VAT mean	123.00±20.82	122.08±20.60	0.999	119.69±25.71	124.66±17.25	**0.014**
SAT mean	127.37±19.89	127.51±17.42	0.486	126.50±19.04	127.99±19.84	0.334
VAT max	209.23±58.51	230.21±96.06	0.060	210.73±74.84	213.66±63.47	0.109
SAT max	214.28±70.88	249.22±110.69	**$1.23x10^{-3}$**	224.71±80.22	217.94±79.94	0.987
CT ratio (vis/sc)	0.47±0.63	0.38±0.30	0.922	0.40±0.42	0.48±0.66	0.826
Body fat (%)	41.95±11.35	42.26±11.72	0.496	41.15±11.88	42.57±11.11	0.607
CRP (mg/dl)	12.04±15.09	11.20±16.05	0.935	13.09±15.67	11.34±15.49	0.198
IL-6 (pg/ml)	6.05±5.24	5.17±3.71	0.880	6.16±4.54	5.79±5.39	0.286
HbA1C (%)	6.07±1.11	5.82±0.86	0.443	6.00±1.10	6.02±1.05	0.766
oGTT2h (mmol/l)	6.99±2.41	7.49±3.97	0.663	7.57±3.40	6.74±2.22	0.064
FPG (mmol/l)	6.34±2.17	5.83±0.98	0.827	6.34±2.45	6.22±1.77	0.904
FPI (pmol/)	131.78±141.75	107.18±98.96	0.297	124.28±118.40	127.54±145.26	0.729
GIR (µmol/kg/min)	75.66±33.87	65.78±35.86	**0.042**	73.75±33.57	73.58±35.24	0.567
Total cholesterol (mmol/l)	4.87±0.99	4.72±097	0.130	4.99±1.06	4.75±0.93	**0.019**
HDL-C (mmol/l)	1.24±0.41	1.22±0.46	**0.027**	1.25±0.40	1.23±0.42	0.418
LDL-C (mmol/l)	3.11±0.94	3.02±1.12	0.143	3.19±1.02	3.01±0.93	0.167
FFA (mmol/l)	0.58±0.41	0.54±0.39	0.525	0.57±0.43	0.57±0.39	0.076
TG (mmol/l)	1.65±0.89	1.49±0.66	0.654	1.69±0.96	1.58±0.78	0.444
Leptin (ng/ml)	37.12±22.14	40.64±23.96	0.313	35.43±21.13	39.15±23.34	0.655
Adiponectin (µg/ml)	7.93±4.97	6.59±3.36	0.091	7.17±4.67	8.11±4.75	0.095
Albumin (g/l)	40-95±9.62	40.59±9.43	0.648	39.37±10.74	41.84±8.40	0.086
ALAT (µkat/l)	0.65±0.50	0.58±0.49	0.360	0.65±0.53	0.62±0.47	0.767
ASAT (µkat/l)	0.71±3.18	0.52±0.31	0.382	0.89±0.65	0.54±0.28	0.742
gGT (µkat/l)	0.89±1.65	0.81±0.77	0.679	0.85±1.33	0.88±1.64	0.960
TSH (mU/l)	2.317±10.87	1.735±2.64	0.296	2.96±15.74	1.73±2.06	0.071

fT3 (pg/ml)	4.66±0.99	4.71±0.81	0.348	4.76±1.03	4.62±0.92	0.609
fT4 (pmol/l)	17.15±3.47	17.81±3.63	0.354	16.78±2.68	17.65±3.71	0.222
Blood Met (%)	20.99±8.07	22.31±5.11	0.143	21.43±7.36	21.27±7.56	0.811
Met SAT (%)	11.95±5.86	16.34±6.54	**0.011**	13.56±7.38	12.69±5.83	0.784
Met VAT (%)	17.04±5.61	19.69±6.10	**0.038**	18.20±4.41	17.46±6.18	0.401
SAT *HIF3α* mRNA	21.08±72.62	7.43±40.53	0.209	11.58±49.82	22.60±76.47	0.660
VAT *HIF3α* mRNA	23.92±106.19	10.45±50.03	0.073	16.80±82.25	24.09±106.69	0.729
Leucoytes/nl	8.21±2.88	8.08±2.50	0.743	8.42±3.22	8.00±2.48	0.155
Erythrocytes (Mio/µl)	4.79±1.05	4.62±0.50	0.230	4.65±0.59	4.82±1.16	0.237
Thrombocytes x10^9/l	257.94±82.94	291.52±101.69	0.089	261.59±75.91	263.98±93.83	0.762

Due to the low minor allele frequency (MAF) of the studied polymorphisms, subjects homozygous for the minor alleles (n=3 for rs8102595, n=16 for rs3826795) were combined with heterozygous groups (i.e. dominant mode of inheritance was used statistical analyses).
p-value adjusted for age, gender and BMI and diabetes status; BMI – Body Mass Index, WHR – waist-to-hip ratio, SAT – subcutaneous adipose tissue, CRP – C-reactive protein, IL-6 – Interleukin 6, HbA1c – Glycohemoglobin, oGTT – oral Glucose Tolerance Test, FPG – Fasting plasma glucose, FPI – Fasting plasma insulin, GIR – Glucose infusion rate during the steady state of an euglycemic hyperinsulinemic clamp, HDL-C – high Density Lipoprotein Cholesterol, LDL-C – Low Density Lipoprotein Cholesterol , FFA – Free Fatty Acids, TG – Triglycerides, ALAT – alanine aminotransferase, ASAT - aspartate aminotransferase, gGT - Gamma-glutamyl transferase, TSH – thyroid-stimulation hormone, fT3 – free triiodothyronine, fT4 – free tetraiodothyronine, Met Blood (%)/ Met Sc (%) / Met Visc (%) - Methylation of cg22891070 in *HIF3A* in blood / SAT / VAT, *HIF3a* mRNA – mRNA expression of *HIF3A* in subcutaneous/visceral adipose tissue.

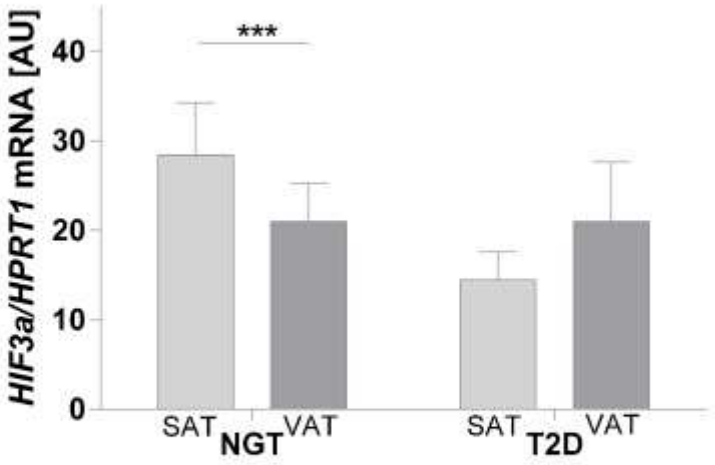

Supplementary Figure: Fat depot-related *HIF3A* mRNA expression pattern is distinct in individuals with either normal glucose tolerance (NGT; SAT, n=316; VAT, n=242) or type 2 diabetes (T2D; SAT, n=318; VAT, n=245)

Chapter 3

Publication: Metabolic effects of genetic variation in the human *REPIN1* gene

Authors: Jacqueline Krüger*, Claudia Berger*, Kerstin Weidle, Dorit Schleinitz, Anke Tönjes, Michael Stumvoll, Matthias Blüher, Peter Kovacs#, Nora Klöting#

* These authors contributed equally to this work

Accepted: 17.04.2018

Published: 18.06.2018,

International Journal of Obesity. doi: 10.1038/s41366-018-0123-0

International Journal of Obesity
https://doi.org/10.1038/s41366-018-0123-0

ARTICLE

Genetics and Epigenetics

Metabolic effects of genetic variation in the human *REPIN1* gene

Jacqueline Krüger[1] · Claudia Berger[1,2] · Kerstin Weidle[1] · Dorit Schleinitz[1] · Anke Tönjes[3] · Michael Stumvoll[3] · Matthias Blüher[3] · Peter Kovacs[1] · Nora Klöting[1]

Received: 17 January 2018 / Revised: 6 April 2018 / Accepted: 17 April 2018

Abstract

Background Replication initiator 1 (Repin1) is a zinc finger protein highly expressed in liver and adipose tissue. The *Repin1* resides within a quantitative trait locus (QTL) for body weight and triglyceride levels in the rat, and its hepatic deletion in mice results in improved insulin sensitivity and lower body weight. Here, we analyzed whether genetic variation within the *Repin1* affects parameters of glucose and lipid metabolism.

Methods We sequenced *REPIN1* in 48 non-related Caucasian subjects. We discovered a 12 base pair deletion (12 bp del; rs3832490), which was subsequently genotyped in two well-characterized cohorts ($N = 3013$) to test for associations with metabolic traits. Functional consequences of the variant were investigated in HepG2 cells in vitro.

Results In human cohorts, we show that the 12 bp del associates with improved glucose metabolism (lower fasting plasma glucose, fasting plasma insulin, and HOMA IR). Cells transfected with the plasmid carrying the 12 bp del variant are characterized by increased *GLUT2* and fatty acid translocase *CD36* expression and more lipid droplets.

Conclusion Our data suggest that genetic variation in human *REPIN1* plays a role in glucose and lipid metabolism by differentially affecting the expression of REPIN1 target genes including glucose and fatty acid transporters.

Introduction

It is well acknowledged that obesity and related traits are influenced by genetic factors. Despite recent advances in high throughput technologies which led to the identification of numerous genetic variants associated with complex metabolic traits including obesity [1], the genetic architecture of these phenotypes is far from being fully understood. In particular, identification of target genes within the loci associated with phenotypes of interest and understanding their functional consequences remains a challenging task. The replication initiator 1 (*Repin1*) residing on rat chromosome 4 within a quantitative trait locus (QTL) for body weight, serum fasting insulin, and triglycerides does represent such a gene [2, 3]. A single nucleotide polymorphism (SNP) in the coding region and a triplet repeat (TTT) in the 3′-untranslated region (UTR) in the *Repin1* have been shown to be associated with altered metabolism in rat strains [3], thus rendering *Repin1* a plausible candidate for the respective QTL.

Repin1 is a replication initiation-region protein 60 kDa (RIP60) firstly described in a study investigating DNA-binding proteins involved in replication activation of the Chinese hamster dihydrofolate reductase gene (*dhfr*) [4]. Moreover, Repin1 is a polydactyl zinc finger protein containing 15 zinc finger (ZF) DNA-binding motifs, and these are organized in three zinc finger hand clusters, cluster Z1 includes ZFs 1–5, cluster Z2 includes ZFs 6–8, and cluster Z3 includes ZFs 9–15 [5]. The clusters have different affinities to bind DNA [5]. Repin1 is ubiquitously expressed with the highest levels in adipose tissue and liver [3]. In humans, *REPIN1* comprises four exons and maps on

These authors contributed equally: Jacqueline Krüger, Claudia Berger.

Electronic supplementary material The online version of this article (https://doi.org/10.1038/s41366-018-0123-0) contains supplementary material, which is available to authorized users.

✉ Peter Kovacs
peter.kovacs@medizin.uni-leipzig.de

✉ Nora Klöting
nora.kloeting@medizin.uni-leipzig.de

[1] Leipzig University Medical Center, IFB Adiposity Diseases, University of Leipzig, 04103 Leipzig, Germany

[2] German Diabetes Center Leipzig, University of Leipzig, 04103 Leipzig, Germany

[3] Department of Medicine, University of Leipzig, 04103 Leipzig, Germany

Published online: 18 June 2018

chromosome 7q36.1. Recent studies suggest that Repin1 plays a role in the adipocyte biology. In 3T3-L1 cells, a *Repin1* knockdown resulted in smaller lipid droplets and lower palmitate uptake, as well as improved glucose transport [6]. Furthermore, a whole-body *Repin1* deletion in *db/db* and BL/6N mice improved insulin sensitivity and chronic hyperglycemia, most likely due to reduced fat mass and lower adipose tissue inflammation [7, 8]. Both liver- and adipose tissue-specific *Repin1* knockout mice (*LRep1*$^{-/-}$) exhibit improved whole-body insulin sensitivity, accompanied with significantly lower triglyceride content in the liver and secondary changes in adipose tissue [8, 9]. Altogether, these data point to a crucial role of Repin1 in lipid and glucose metabolism in mice. Since a balance between storage and release of lipids by adipose tissue is essential for maintenance of normal energy homeostasis [10], Repin1 might also be considered as a factor contributing to ectopic lipid accumulation in peripheral tissues, such as liver, pancreas, or skeletal muscle under conditions of energy surplus.

Here, we tested for the first time the hypothesis that genetic variants within the *REPIN1* are associated with alterations in glucose and lipid metabolism. We sequenced the *REPIN1* in 48 non-related Caucasian subjects and identified a 12 base pair deletion, which was subsequently genotyped in two well-characterized cohorts ($N = 3013$). Functional consequences of this variant were investigated in HepG2 cells in vitro.

Material and methods

Subjects

Informed consent was given by all the participants and the study was approved by the Ethics Committee at the University of Leipzig.

Leipzig cohort

The Leipzig cohort was recruited at the University Hospital of Leipzig, Germany, and includes 1982 subjects (1098 women and 884 men); 578 subjects had normal glucose tolerance (NGT, BMI 26.6 ± 5.9 kg/m^2), 176 subjects had an impaired glucose tolerance (IGT, BMI = 30.5 ± 5.9 kg/m^2), and 1093 subjects had type 2 diabetes (T2D, BMI 30.4 ± 6.1 kg/m^2) according to the American Diabetes Association (ADA) criteria from 2010 [11]. The remaining subjects had type 1 diabetes or latent autoimmune diabetes of adults (LADA) and were excluded from further analysis. About 557 individuals were lean (BMI 23.1 ± 1.6 kg/m^2), 736 were overweight (BMI 27.3 ± 1.4 kg/m^2), and 689 subjects had obesity (BMI 35.4 ± 5.9 kg/m^2). Anthropometric and metabolic measurements included BMI, % body fat, waist to hip ratio (WHR), glucose, insulin, cholesterol, triglycerides, and free fatty acids serum concentrations. In addition, the participants without prior T2D diagnosis underwent an oral glucose tolerant test (oGTT). The main characteristics of the cohort are given in Table 1.

For a small subgroup ($N = 20$), subcutaneous and visceral adipose tissue were removed and adipocytes were isolated by collagenase (1 mg/ml) digestion. To investigate cell size and adipocyte number, aliquots of adipocytes were fixed with osmic acid and counted in a Coulter counter as previously described [12].

Sorbs cohort

The self-contained population of Sorbs in Germany had undergone extensive phenotyping as recently described elsewhere [13–15]. Briefly, it included standardized questionnaires to assess past medical history, family history, and collection of anthropometric data. The cohort includes 614 women and 417 men, had a mean age of 48 ± 16 years, and mean BMI 26.9 ± 4.9 kg/m^2. Among the 1031 subjects, 397 were lean (BMI 22.4 ± 1.7 kg/m^2), 400 were overweight (BMI 27.4 ± 1.4 kg/m^2), and 234 subjects had obesity (BMI 33.9 ± 3.8 kg/m^2). Anthropometric parameters (body weight, BMI, % body fat, WHR) and metabolic parameters (lipids, oGTT, HOMA IR) were available for analyses. The main characteristics of the cohort are given in Table S1.

In both cohorts, blood samples were deep-frozen and stored at −80 °C. Glucose was assessed by the Hexokinase method (Automated Analyzer Modular, Roche Diagnostics, Mannheim, Germany) and serum insulin was measured using the AutoDELFIA Insulin assay (PerkinElmer Life and Analytical Sciences, Turku, Finland). Total serum cholesterol and TG concentrations were measured by standard enzymatic methods (CHOD-PAP and GPO-PAP; Roche Diagnostics). Serum LDL-cholesterol and HDL-cholesterol concentrations were determined using commercial homogeneous direct measurement methods (Roche Diagnostics). All assays were performed in an automated clinical chemistry analyzer (Hitachi/ Roche Diagnostics) at the Institute of Laboratory Medicine, University Hospital Leipzig.

Sequencing

The *REPIN1* (four exons, exon–intron boundaries, 5′ and 3′ UTRs based on NCBI reference NM_013400.3) was sequenced in 48 non-related Caucasian subjects (27 subject with T2D and 21 controls, 23 women and 25 men). Sequencing was performed using the Big Dye® Terminator (Applied Biosystems, Inc., Foster City, CA) on an

Table 1 Association of the 12 bp deletion (rs3832490) with type 2 diabetes and obesity

rs3832490	NGT	T2D	MAF NGT vs. T2D	Unadjusted *p*-value	Adjusted[a] p-value add model (OR [95% CI])	Adjusted[b] p-value dom model (OR [95% CI])
Case Control Study for T2D in Sorbs cohort						
wt/wt	774 (85.1%)	99 (90.85)	0.076/0.059	$\mathbf{6.0 \times 10^{-4}}$	0.088 (0.643 [0.347–1.191]	**0.042** (0.472 [0.229–0.974])
wt/del	133 (14.3%)	7 (6.4%)				
del/del	3 (0.3%)	3 (2.8%)				
Case Control Study for T2D in the Leipzig cohort						
wt/wt	491 (87.5%)	967 (89.6%)	0.062/0.053	0.226	0.393 (0.816 [0.512–1.300])	0.292 (0.774 [0.481–1.246])
wt/del	70 (12.5%)	110 (10.2%)				
del/del	0 (0%)	2 (0.2%)				
Case Control Study for T2D in the combined cohort						
wt/wt	1203 (86.2%)	1064 (89.6%)	0.069/0.054	**0.013**	**0.010** (0.665 [0.487–0.908])	$\mathbf{5.89 \times 10^{-3}}$ (0.635 [0.459–0.877])
wt/del	189 (13.5%)	118 (9.9%)				
del/del	3 (0.2%)	5 (0.4%)				

rs3832490	BMI <25 kg/m^2 lean	BMI > 30 kg/m^2 obese	MAF lean vs. obese	Unadjusted *p*-value	Adjusted[b] p-value add model (OR [95% CI])	Adjusted[b] p-value dom model (OR [95% CI])
Case Control Study for obesity in the combined cohort						
wt/wt	816 (87.0%)	792 (88.7%)	0.066/0.058	0.526	0.314 (0.857 [0.635–1.157])	0.300 (0.848 [0.621–1.158])
wt/del	119 (12.7%)	98 (11.0%)				
del/del	3 (0.3%)	3 (0.3%)				

NGT subjects with normal glucose tolerance, *T2D* subjects with type 2 diabetes, *MAF* minor allele frequency, *BMI* body mass index, *OR* odds ratio for the minor allele,wt- *REPIN1* wildtype variant, del- *REPIN1* 12 bp deleetion variant, underlined values are the adjusted p-values and bold p-values indicate statistical significance

[a]Adjusted for sex, age, and BMI

[b]Adjusted for sex and age; dom model—dominant model of inheritance for the minor allele

automated DNA capillary sequencer (ABI PRISM® 3100 Avant; Applied Biosystems, Inc., Foster City, CA). Sequence information and polymerase chain reaction (PCR) conditions for all oligonucleotide primers used for variant screening are provided in Supplemental Table S2.

Genotyping of SNPs

SNPs were genotyped in both study cohorts by employing the TaqMan SNP Genotyping assay system according to the manufacturer's protocol and by using the ABI PRISM® 7500 Sequence Detecting System (Applied Biosystems, Inc., Foster City, CA). To limit genotyping errors, a random ~5% selection of samples was re-genotyped; all genotypes matched initially designated genotypes.

Genotyping of the 12 bp deletion variant in humans

Sequencing revealed a 12 bp del (CCGCCAGGGGCC/–) in exon 4 of *REPIN1* (Figure S1). Screening for the deletion in both study cohorts was done by restriction fragment length polymorphism (RFLP). DNA was amplified by PCR and the corresponding product (564 bp) was subsequently digested with the enzyme *Apa*I. The experimental protocol including PCR conditions and primer sequences is provided in Supplemental Table S3. Briefly, the digestion with *Apa*I resulted in 3 fragments (99 bp, 143 bp, 322 bp) in wildtype homozygous subjects, two fragments (230 bp and 322 bp) in homozygous carriers of the deletion, and four fragments (99 bp, 143 bp, 230 bp, 322 bp) in heterozygous subjects. The products were visualized using gel electrophoresis (Figure S2).

Cloning and expression of recombinant REPIN1 wildtype and 12 bp deletion variants

REPIN1 constructs, which consist of the coding sequence of exon 4 with (deletion) or without 12 bp del (wildtype) and a size of 1.7 kb, were cloned into the pNTAP-β-vector (InterPlay Mammalian TAP System, Agilent Technologies, Waldbronn, Germany). Subsequently, hepatocellular carcinoma cells (HepG2) were transfected with the eukaryotic expression vectors for the *REPIN1* wildtype and deletion or with the empty vector. For transfection of HepG2, cells GeneJammer Transfection Reagent (Agilent Technologies, Waldbronn, Germany) was used. Cells were grown until 80% confluence in a 6-well plate with growth medium (RPMI-1640 medium (Biochrom GmbH, Berlin, Germany), supplemented with 10% fetal bovine serum (FBS, AppliChem, Darmstadt, Germany), 100 units/ml of penicillin (Biochrom GmbH, Berlin, Germany) and 100 mg/ml of streptomycin (Biochrom GmbH, Berlin, Germany)). Three microliters of transfection reagent was mixed with 97 µl of serum-free and antibiotic-free RPIM 1640 medium and incubated for 5 min. Afterwards 1 µg of wt or 12 bp del variant plasmid was added to the transfection solution and incubated for 45 min at room temperature in two different approaches. The different plasmids contained the wt variant of the 4th exon of REPIN1 or the 4th exon with the deletion of 12 bp.

The transfection mixture was added dropwise to one well of the 6-well plate. In addition, three negative controls were conducted: a cell control, a reagent control, and a DNA control. Twenty-four hours after transfection, the medium was changed to selection medium (growth medium supplemented with 50 mg/ml Geneticin (AppliChem, Darmstadt, Germany)). The medium was replaced twice a week until the control cells died. The successful transfection was verified by growth with selection media containing Geneticin and by PCR with a *REPIN1* specific primer pair (fw: AGATTCACAAGCGATCCGAG, rw: ACTTCTGGCTGAAGGCT
TTG) and restriction digestion with *Apa*I. After amplification and digestion, the reactions were visualized using Gelred (GeneOn GmbH, Ludwigshafen, Germany) staining in 1% agarose gels. For the cells carrying the *REPIN1* plasmid with the 12 bp del, only two fragments were detected (Fig. 1a). The overexpression was confirmed by qPCR (Lightcycler) using a specific *REPIN1* probe and calculated relative to *18S rRNA* (both Applied Biosystems, Hs00274221_s1, Hs99999901_s1, Warrington, GB) (Fig. 1b).

Cell culture and in vitro assays

HepG2 cell line was purchased from American Type Culture Collection (Manassas, VA, USA). The cells were cultured at 37 °C in humidified air with 5% CO_2 in RPMI-1640 medium (Biochrom GmbH, Berlin, Germany), supplemented with 10% FBS (AppliChem, Darmstadt, Germany), 100 units/ml of penicillin (Biochrom GmbH, Berlin, Germany), 100 mg/ml of streptomycin (Biochrom GmbH, Berlin, Germany), and 50 mg/ml Geneticin (AppliChem, Darmstadt, Germany).

Measurement of glycerol, triglyceride, and retinol-binding protein (RBP4) concentrations

Glycerol concentration was measured by using the *Adipolysis Assay Kit* (Merck/Millipore, Darmstadt, Germany). Cells were cultivated in 6-well plates to reach 80% confluence and afterwards harvested, washed, and lysed in sucrose buffer. *Free Glycerol Assay Reagent* was added to samples, standard, and blank and absorption was detected at 560 nm. Glycerol concentration was calculated with the provided standard curve. The protein level of the cells was taken as reference.

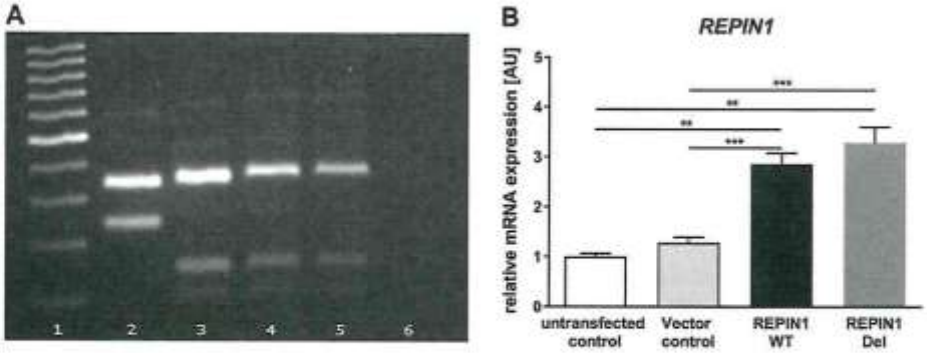

Fig. 1 A: Agarose gel after transfecting HepG2 cells with *REPIN1* 12 bp del- and wildtype plasmid. 1-100 bp Ladder, 2-12 bp del, 3-wild-type, 4-untransfected control, 5-vector control, 6-negative control. B: Gene expression of *REPIN1* in HepG2 cells after transfection with empty vector (vector control), different *REPIN1*plasmids or in untransfected cells. Expression was related to 18S rRNA. $^{*}p < 0.05$, $^{**}p < 0.01$, $^{***}p < 0.005$

Triglyceride concentration in cells was determined using the *LabAssay™ Triglyceride (GPO-DAOS method)-Kit* (Wako Chemicals, Neuss, Germany). Cells were harvested, washed, lysed in sucrose buffer, mixed with color reagent, and measured at 620 nm. The protein level of the cells was taken as reference.

RBP4 concentration was measured by *RBP4 (human) Competitive ELISA Kit* (Adipogen, Seoul, South Korea). Cells were grown in a 6-well plate and the medium was taken after 48 h incubation. ELISA was performed with the medium according to the manufacturer's protocol.

Lipid staining

HepG2 cells were grown in 24-well plates for 24 h, washed and incubated with 30 µl/ml AdipoRed™ (Lonza, Basel, CH) in phosphate buffered saline (PBS) (wo Ca^{2+}/wo Mg^{2+} pH 7.4). Nuclei were counterstained with Hoechst (1 µg/ml in MilliQ water) to normalize the AdipoRed signal. To quantify the lipid staining, the fluorescence was measured at the FLUOstar OPTIMA (BMG LABTECH) and the amount of AdipoRed/Hoechst was analyzed.

RNA isolation and reverse transcriptase PCR (RT-PCR) analysis

Total RNA from the cultured cells was isolated using QIAzol reagent (Qiagen, Hilden, D) according to the manufacturer's instructions. cDNA was synthesized from 2 µg of total RNA, using Superscript II Reverse Transcriptase (Invitrogen, Darmstadt, Germany). RT-generated cDNAs were amplified and measured by qPCR using Lightcycler (Roche, Germany) with selective primers (Supplemental Table S4), purchased from Biomers (Ulm, Germany). Specific mRNA expression was calculated relative to *18S rRNA* which was used as reference due to its resistance to glucose-dependent regulation [16]. mRNA expression was quantified by using the second derivative maximum method.

FACS analysis

Cells were grown, starved for 24 h of glucose, and stimulated with 25 mmol/l glucose for 16 h. After harvesting, cells were washed with PBS and incubated with human GLUT2 PE-conjugated antibody (10 µl/10^6 cells, R&D systems, Minneapolis, USA) for 20 min at 4 °C in the dark. Cells were fixed with Fix & Perm® Reagent A (Molecular Probes by Life Technologies, Frederick, Maryland, USA) for 10 min at room temperature, washed, and re-suspended in PBS. Positive cells were counted at the flow cytometer (Beckton Dickinson, Heidelberg, Germany) based to 100,000 cells.

Statistical analysis

Prior to the analyses, all non-normally distributed parameters were logarithmically transformed to approximate a normal distribution. To test the 12 bp del for genetic association with metabolic traits, linear regression models adjusted for covariates were used. Logistic regression analyses were done for case control studies for T2D (NGT vs. T2D) and obesity (lean vs. obese). For these analyses, two models of inheritance were considered. In the additive model, homozygotes for the major allele, heterozygotes and homozygotes for the minor allele (12 bp del) were coded to a continuous numeric variable for genotype (as 0, 1, 2). A dominant model for the minor allele was defined as contrasting genotypic groups including homozygotes for the minor alleles and heterozygotes vs. subjects homozygous for the major allele. The analysis of associations of the variants with quantitative traits was done under linear

Table 2 Association of the 12 bp deletion (rs3832490) with metabolic traits in the Sorbs

rs3832490	wt/wt	wt/del	del/del	*p*-Value
N	702	119	3	
Sex (m/f)	285/427	48/71	–/3	
BMI (kg/m^2)	26.4 ± 4.6	26.8 ± 4.8	22.4 ± 1.7	0.670[a]
WHR	0.86 ± 0.11	0.87 ± 0.09	0.81 ± 0.03	0.352
Body fat (%)	20.9 ± 11.3	20.9 ± 9.3	13.1 ± 2.7	0.275[a]
Traits related to glucose metabolism				
Fasting plasma glucose (mmol/l)	5.3 ± 0.5	5.3 ± 0.5	4.6 ± 0.2	0.264
Fasting plasma insulin (pmol/l)	39.1 ± 24.0	37.3 ± 20.9	18.5 ± 10.1	0.183
120 min plasma glucose (mmol/l)	5.4 ± 1.7	5.4 ± 1.85	5.2 ± 1.1	0.478
HOMA B	65.3 ± 43.8	61.5 ± 32.6	54.3 ± 41.9	0.505
HOMA IR	1.3 ± 0.9	1.3 ± 0.8	0.53 ± 0.3	0.163
Traits related to obesity				
Total cholesterol (mmol/l)	5.3 ± 1.0	5.3 ± 1.0	5.6 ± 1.5	0.843
LDL cholesterol (mmol/l)	3.37 ± 0.9	3.39 ± 0.9	3.61 ± 0.9	0.926
HDL cholesterol (mmol/l)	1.65 ± 0.39	1.69 ± 0.44	2.07 ± 0.6	0.219
Triglycerides (mmol/l)	1.25 ± 0.8	1.24 ± 0.9	0.71 ± 0.2	0.302

The data are given as mean ± standard deviation; *p*-value adjusted for sex, age and BMI

BMI body mass index, *WHR* waist-to-hip-ratio, *HOMA IR* homeostatic model assessment for insulin resistance, *HOMAR B* homeostatic model assessment for β-cell function, *LDL cholesterol* low-density lipoprotein cholesterol, *HDL cholesterol* high-density lipoprotein cholesterol, *FFA* free fatty acids

[a]Adjusted for sex and age

regression in non-diabetic subjects to avoid diabetes status or treatment interfering with potential effects of the variants on these parameters. For the in vitro analyses, data are given as means ± standard error of the mean (SEM). Data sets were analyzed for statistical significance using a two-tailed unpaired *t*-test.

p-Values ≤0.05 were considered to provide nominal evidence for association and are provided without correction for multiple testing. Statistical analyses were performed using SPSS statistics version 20.0.1 (SPSS, Inc., Chicago, IL, USA) and GraphPad Prism 6.05 (GraphPad Software, La Jolla, USA).

Results

Sequencing of REPIN1

Sequencing of the *REPIN1* revealed 12 variants within the coding region, which fell into 9 linkage disequilibrium groups (L.D.) All SNPs were in Hardy Weinberg equilibrium. One of the variants, the 12 bp deletion (rs3832490) resides in exon 4 and predicts a protein sequence lacking four amino acids (PPGA) at position P356_A359del without causing a frame shift (see Figure S1).

Three of 48 sequenced subjects were heterozygote carriers of the 12 bp del, which was further confirmed by genotyping via RFLP.

The 12 bp del as well as eight polymorphisms (rs3735170, rs10278590, rs10229175, rs9640161, rs4725336, rs17173703, rs1051760, rs6971465; Figure S3) representing the remaining L.D. groups were genotyped for association analyses.

Association studies

Association analyses of the 12 bp deletion (rs3832490) with T2D and obesity

In the Sorbs cohort, rs3832490 was associated with T2D. The frequency of carriers of the 12 bp del (homozygous and heterozygous) was significantly higher in subjects with NGT compared with patients with T2D ($p < 0.05$ after adjusting for age, sex, and BMI in a dominant model of inheritance for the minor allele; Table 1). Albeit not significant, the genotype distribution in subjects with NGT and with T2D was similar in the Leipzig cohort (Supplementary table S5). Finally, a combined analysis including both cohorts rendered a significant association with T2D ($p = 5.89 \times 10^{-3}$; after adjusting for age, sex, and BMI) (Table 2).

In a case control study for obesity, comparing lean (BMI < 25 kg/m^2) with obese (BMI > 30 kg/m^2) subjects, no association was observed in both cohorts (Table 1, Supplemental Table S5).

Table 3 Association of the 12 bp deletion (rs3832490) with metabolic traits in the Leipzig cohort

rs3832490	wt/wt	wt/del	*p*-Value
N	491	70	
Sex (m/f)	166/325	24/46	
BMI (kg/m^2)	26.6 ± 5.9	26.4 ± 5.7	0.817[a]
WHR	0.88 ± 0.14	0.89 ± 0.13	0.437
Body fat (%)	24.9 ± 7.7	20.6 ± 1.9	**7.15×10^{-3}**[a]
Traits related to glucose metabolism			
Fasting plasma glucose (mmol/l)	5.2 ± 0.5	5.2 ± 0.5	0.831
Fasting plasma insulin (pmol/l)	48.4 ± 81.4	50.8 ± 101.9	0.211
120 min plasma glucose (mmol/l)	5.9 ± 0.9	6.1 ± 0.8	**0.047**
HOMA B	94.0 ± 226.1	78.7 ± 140.5	0.338
HOMA IR	1.6 ± 2.8	1.7 ± 3.7	0.304
HbA1c (%)	5.3 ± 0.4	5.4 ± 0.3	0.564
Traits related to obesity			
Total cholesterol (mmol/l)	4.9 ± 0.9	4.7 ± 0.6	0.172
LDL cholesterol (mmol/l)	2.9 ± 0.9	2.5 ± 0.6	0.070
HDL cholesterol (mmol/l)	1.3 ± 0.4	1.4 ± 0.5	0.794
Triglycerides (mmol/l)	1.3 ± 0.6	1.1 ± 0.3	0.319
FFA (mmol/l)	0.29 ± 0.24	0.24 ± 0.18	0.758
Max. adipocyte vis (µm)	289.7 ± 120.5	209.8 ± 37.6	**0.011**
Max. adipocyte sc (µm)	305.9 ± 142.2	205.5 ± 51.4	**9.1×10^{-3}**

The data are given as mean±standard deviation; *p*-value adjusted for sex, age, and BMI, bold p-values indicate statistical significance

BMI body mass index, *WHR* waist-to-hip-ratio, *HOMA IR* homeostatic model assessment for insulin resistance, *HOMAR B* homeostatic model assessment for β-cell function, *LDL cholesterol* low-density lipoprotein cholesterol, *HDL cholesterol* high-density lipoprotein cholesterol, *FFA* free fatty acids

[a]Adjusted for sex and age

Association of the 12 bp deletion (rs3832490) with metabolic traits

There were no significant associations of the 12 bp deletion (rs3832490) with any of the studied metabolic traits, most likely due to the weak statistical power, given the low frequency of the variant. It is noteworthy, however, that the three Sorbs homozygous for the deletion had lower fasting plasma glucose, HOMA B as well as HOMA IR, when compared with the non-carriers of the variant. The three subjects had also a lower BMI, WHR, and % body fat (Table 2). Interestingly, the same subjects had higher mean HDL cholesterol and lower serum triglycerides, but on the other hand they manifested higher LDL cholesterol as well as higher total cholesterol.

No homozygous carriers of the *REPIN1* deletion variant were found in the Leipzig cohort. The analyses showed an association of the variant with percentage body fat, with heterozygous carriers having less body fat and smaller maximum of adipocyte size in subcutaneous and visceral adipose tissue (all $p < 0.05$ after adjusting for age and sex; Table 3). But there is also a strong and significant correlation between the body fat and the adipocyte size in the Leipzig cohort with $r = 0.728$ (6.1×10^{-4}) and $r = 0.540$ (2.9×10^{-4}) in visceral and subcutaneous adipose tissue, respectively.

Association of genetic variation in REPIN1 with metabolic traits

In addition to the 12 bp del (rs3832490), we genotyped eight SNPs representing major linkage disequilibrium groups within the *REPIN1*. In the Leipzig cohort, four of the eight tested SNPs (rs1051760, rs6971465, rs10278590, and rs17173703, Supplemental Table S6) showed nominal association with glucose infusion rate (GIR) during hyperinsulinemic–euglycemic clamp ($p < 0.05$ adjusted for age, sex, and BMI). In addition, rs1051760, rs3735170, and rs17173703 exhibited an association with HbA1c (Supplemental Table S6). Moreover, rs17173703 was associated with total and LDL cholesterol, whereas rs9640161 and rs10229175 showed associations with serum triglycerides

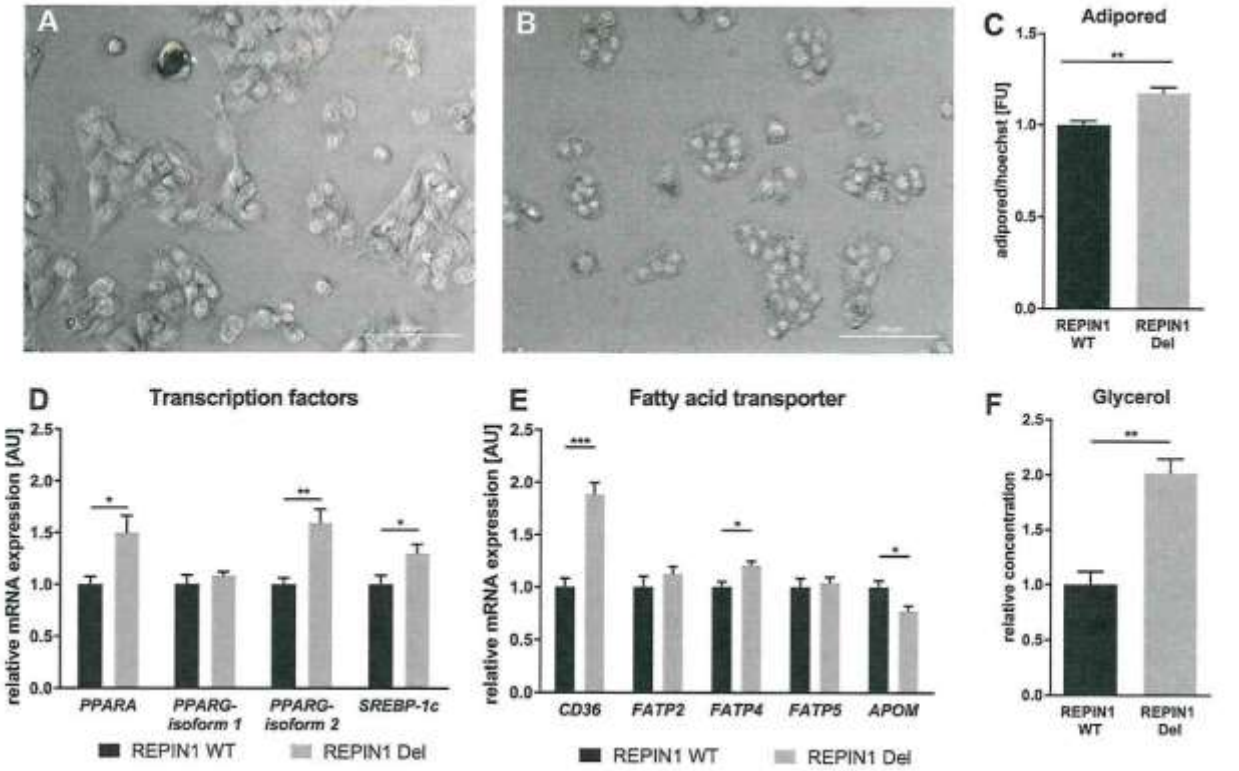

Fig. 2 A: *REPIN1* 12 bp deletion transfected HepG2 cells after incubation with AdipoRed and Hoechst. Lipid droplets are seen in red in the cytoplasm of the cells, nuclei in blue, scale bar 100 µm. B: *REPIN1* wildtype transfected HepG2 cells after incubation with AdipoRed and Hoechst. Lipid droplets are seen in red in the cytoplasm of the cells, nuclei in blue, scale bar 100 µm. C: Quantification of lipid droplets by measuring the fluorescence signal of AdipoRed normalized to the fluorescence signal of Hoechst. AdipoRed stains the triglycerides of the lipid droplets and a higher fluorescence signal was detected in the *REPIN1* 12 bp del cells. D: Relative mRNA expression of transcription factors related to *18S RNA*: Peroxisome Proliferator Activated Receptor A (*PPARA*), *PPARG -isoform 2* and Sterol regulatory element-binding protein 1c (*SREBP-1C*) are significantly higher expressed in *REPIN1* 12 bp del cells than in control. No differences are in *PPARG-isoform 1*. E: Expression levels of the fatty acid transporter related to *18S RNA*: significant higher expression of *CD36* and fatty acid transport protein 4 (*FATP4*) in 12 bp del compared to controls while apolipoprotein M (*APOM*) is lower expressed. In *FATP2* and *FATP5*expression are no differences. F: Measurement of glycerol levels of the cells. *REPIN1* 12 bp del cells have a significant higher concentration of glycerol in relation to protein level compared to control. $*p < 0.05$, $**p < 0.01$, $***p < 0.005$

(Supplemental Table S6). No significant associations were found in the Sorbs cohort for any variant (Supplemental Table S7).

Functional analysis of the 12 bp deletion in REPIN1 in HepG2 cells

Cloning and expression of the recombinant REPIN1 wildtype and 12 bp del variant

Figure 1a shows the result of the gel electrophoresis after PCR and *Apa*I digestion with the two bands for the deletion and three bands for the wildtype *REPIN1* overexpressing cells. mRNA expression of *REPIN1* was 190% higher in wildtype and 230% higher in cells expressing the variant with deletion than in untransfected cells or the vector control. However, there was no significant difference between the del and wt variant ($p = 0.40$). Consistently, the protein levels were comparable between the wt and 12 bp del variant as well (data not shown).

No difference between untransfected and vector control was found (Fig. 1b).

Lipid staining and cell differentiation

Given the previously reported role of Repin1 in regulation of key genes of glucose and lipid metabolism [9], we investigated the effects of the 12 bp del on intracellular lipid content, as well as expression of fatty acid and glucose transporter genes. The intracellular lipid droplets can be assessed by the lipophilic AdipoRed assay. As indicated by these assays, HepG2 cells transfected with the *REPIN1* 12 bp del variant (Fig. 2a) seemed to have more stained lipid droplets than the cells transfected with the wildtype variant (Fig. 2b). Consistently, after quantification using AdipoRed and Hoechst, cells carrying the 12 bp del had significantly

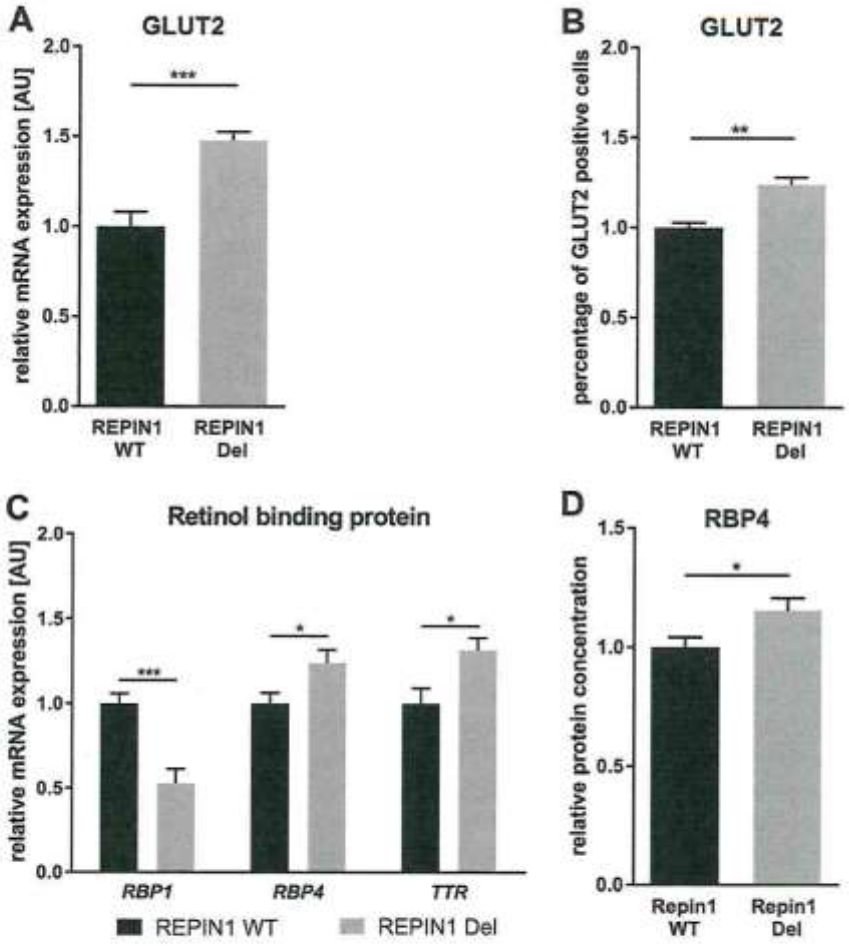

Fig. 3 A: Relative mRNA expression of glucose transporter 2 (*GLUT2*) related to *18S rRNA* is in *REPIN1* 12 bp del cells significantly higher than in control cells. B: Detection of GLUT2 positive cells using FACS. The percentage of positive cells is given. The *REPIN1* 12 bp del cells had more GLUT2 positive cells. C: Relative mRNA expression of the retinol binding proteins (RBP) *RBP1*, *RBP4* and transthyretin (*TTR*) in both cell lines. *RBP1* is in *REPIN1* 12 bp del significantly lower expressed while *RBP4* and *TTR* are higher expressed compared to control cells. D: Relative circulating protein concentration of RBP4 measured by ELISA in relation to total protein. Cells with *REPIN1* 12 bp del have a significant higher concentration of RBP4 in the cell culture supernatant than cells transfected with *REPIN1* wildtype. $*p < 0.05$, $**p < 0.01$, $***p < 0.005$

higher signal of AdipoRed normalized to Hoechst compared to *REPIN1* wildtype transfected cells ($p = 0.01$; Fig. 2c).

Furthermore, cells with the *REPIN1* 12 bp del variant had a higher expression of REPIN1 target transcription factors such a peroxisome proliferator activated receptor α (*PPARA*; 50% higher than wildtype *REPIN1* cells), *PPARG-Isoform 2* (59%), and sterol regulatory element-binding protein 1c (*SREBP-1c*; 30%), suggesting that these cells exhibited stronger lipid accumulation than wildtype transfected cells. No gene variant-related difference was seen for *PPARG isoform 1* (Fig. 2d).

Fatty acid and glucose transporter genes

The 12 bp del resulted in a significantly higher mRNA expression of fatty acid transport protein 4 (*FATP4*; 20%) and *CD36* (88%), whereas apolipoprotein M (*APOM* -33%) was significantly downregulated in cells transfected with the deletion variant (Fig. 2e). No differences were found for *FATP2* and *FATP5*.

Glycerol levels in HepG2 cells with the 12 bp del were twice as high as in the wildtype form (Fig. 2f).

Furthermore, the 12 bp del resulted in a higher expression of glucose transporter protein 2 (*GLUT2*; 48% above the control) (Fig. 3a). Consistently, the percentage of GLUT2-positive cells was significantly higher in cells with the *REPIN1* 12 bp del variant in comparison to the *REPIN1* wildtype variant (Fig. 3b).

Finally, mRNA expression of retinol binding protein 1 (*RBP1*) was 48% lower in wildtype overexpressing cells compared to cells expressing the *REPIN1* 12 bp del (Fig. 3c). In contrast, the expression of *RBP4* and transthyretin (*TTR*) (Fig. 3c) was significantly higher in these cells (by 26% and 32%, respectively). In line with this, ELISA measurements showed 16% higher circulating RBP4 levels in media of cells with the 12 bp del (Fig. 3d).

Discussion

Repin1 is a zinc finger protein highly expressed in liver and adipose tissue [3]. The *Repin1* resides within a QTL for body weight and triglyceride levels in the rat [2], and its hepatic deletion in mice results in improved insulin

sensitivity and lower body weight [9], most likely to be explained by its influence on genes of the fatty acid and glucose metabolism in adipocytes [6]. Here, we analyzed the consequences of human genetic variation within *REPIN1* on glucose and lipid metabolism.

Sequencing of the coding region of *REPIN1* revealed nine representative genetic variants including a 12 bp del (rs3832490). Our data show that common genetic variation in *REPIN1* moderately associates with traits related to glucose and lipid metabolism, such as insulin sensitivity measured by hyperinsulinemic-euglycemic clamps, HbA1c, total and LDL cholesterol, as well as serum triglycerides. One of the most promising functional variants found by sequencing, the 12 bp deletion (rs3832490) is a rare variant with minor allele frequency (MAF) 0.062, which significantly constrained the statistical power of association analyses with metabolic traits. In both study cohorts including 1402 subjects with NGT, we only found three subjects homozygous for the deletion variant. They tend to have lower serum glucose and insulin levels, as well as HOMA IR, suggesting that the deletion might be associated with improved insulin sensitivity, which ultimately results in a reduced risk of T2D. It is noteworthy that the carriers of the deletion also show lower BMI, WHR, and less body fat, as well as smaller adipocytes, which could, at least partially, mediate the observed beneficial effects on glucose metabolism. Despite the lack of statistical power, these data are congruent with the findings from animal studies demonstrating that liver-restricted Repin1 deficiency improves whole-body insulin sensitivity, alters lipid metabolism, and causes secondary changes in adipose tissue in the *LRep1*$^{(-/-)}$ mice [6]. Moreover, mRNA as well as protein expression of GLUT2, representing the main transporter (independent of insulin stimulation) in hepatocytes [17], was significantly increased in vitro in cells expressing *REPIN1* with the 12 bp del. In line with this, the cells with REPIN1 12 bp del have a tendency for higher basal glucose uptake, which is independent from insulin stimulation (data not shown). Consistently, Kern et al. showed a higher Glut2 expression in a *Repin1* knockout mouse model [9], which further implies that the observed associations of the 12 bp del with improved metabolic phenotypes might be attributed to Repin1 effects on Glut2 regulation.

Whereas the Repin1 deletion seems to be associated with improved glucose metabolism, carriers of the 12 bp del variant tend to have a higher total cholesterol and LDL cholesterol, but lower serum triglycerides. Our *in vitro* studies further show that the 12 bp del induces higher expression of the fatty acid transporter *CD36* and higher circulating glycerol levels. The higher expression of *CD36* in the cells with the 12 bp del in *REPIN1* most likely reflects higher *REPIN1* expression, because *Repin1* knockout mice have lower *Cd36* expression [9], and Miquilena-Colina et al. suggested a link between higher expression of CD36 (mRNA and protein) and decreased insulin sensitivity [18]. FATP4 is a membrane protein of the endoplasmatic reticulum metabolizing fatty acids [19]. Higher expression of *FATP4* caused by the 12 bp del might indicate an increased rate of metabolism associated with a decrease in fatty acid concentration in the cell.

In contrast, we show that PPARα, controlling β-oxidation in liver, skeletal muscle, and heart [20], was overexpressed in cells transfected with the *REPIN1* 12 bp deletion. Increased expression of *SREBP-1C* in these cells further suggests a role of REPIN1 in regulating genes of lipogenesis, as well as adipogenesis through SREBP-1C and PPARγ [21–23]. Further investigations are warranted to clarify whether the effects on mRNA expression of fatty acid transporters and transcription factors might ultimately explain the higher cell glycerol content elicited by the 12 bp del.

Interestingly, overexpression of *REPIN1* with the 12 bp del decreased the expression of apolipoprotein M (*APOM*), a reverse transport protein of cholesterol [24]. Since APOM has been shown to be negatively associated with total cholesterol [25], one might expect higher cholesterol levels in subjects carrying the *REPIN1* deletion. In line with this, we observed increased cholesterol in subjects homozygous for the 12 bp del. Nevertheless, studies with larger human cohorts will be inevitable to test whether the REPIN1 deletion effects on APOM would translate into higher cholesterol levels in individuals carrying the deletion.

Finally, whereas, both in vivo and in vitro data seem to be consistent with regard to glucose metabolism, they are inconclusive regarding lipid metabolism and obesity. These data were achieved in *in vitro* experiments using only one cell culture system that, due to the substantially lower molecular complexity, cannot entirely resemble the *in vivo* situation. Also of note, well-acknowledged differences in the physiology between species (mice vs. humans) have to be taken into account. Therefore, we interpret these findings with caution and acknowledge that further functional studies using different cell types are warranted to elucidate the precise molecular mechanisms by which genetic variation in REPIN 1 affects obesity-related traits. Although such studies will undoubtedly shed more light on molecular mechanisms whereby the 12 bp del propagates its metabolic effects, the GTEx Portal [26] (https://www.gtexportal.org) does report rs3832490 as an eQTL in skeletal muscle and other variants (rs1051760, rs3735170, rs6971465, rs9640161) as eQTLs in sc and/or vis adipose tissue. These data implicate a possible regulatory role of the 12 bp deletion in gene transcription. Accordingly, the Regulome database [27] (www.regulomedb.org/) indicated minimal evidence for binding, binding of RNA polymerase II subunit and enhancer for chromatin modification, which however, has not been reported for liver or adipose tissue.

In conclusion, our data suggest that genetic variation in *REPIN1* may contribute to changes in parameters of glucose and lipid metabolism, most likely due to specific and Repin1 genotype-related regulation of target gene expression in glucose metabolism, insulin sensitivity, fatty acid transport, and adipogenesis.

Acknowledgements We thank all those who participated in the studies. We would like to acknowledge excellent technical assistance by Ines Müller, Beate Gutsmann, Manuela Quandt, and Viola Döbel. This work was supported by grants from the Deutsche Forschungsgemeinschaft (DFG) (SFB 1052 "Obesity mechanisms', projects B01, B03, B04, C01), from the Deutsche Diabetes Stiftung (DDS- Funktionelle Charakterisierung Adipositas- und Typ 2 Diabetes-assoziierter Varianten im Repin1-Gen), Deutsche Diabetes Gesellschaft (DDG 934300-003) and Deutsches Zentrum für Diabetesforschung (DZD 8200601). IFB Adiposity Diseases is supported by the Federal Ministry of Education and Research (BMBF), Germany, FKZ: 01EO1501 (AD2-060E, AD2-06E95, AD2-06E99). The authors declare no conflict of interest.

Compliance with ethical standards

Conflict of interest The authors declare no conflict of interest.

References

1. Locke AE, Kahali B, Berndt SI, Justice AE, Pers TH, Day FR, et al. Genetic studies of body mass index yield new insights for obesity biology. Nature. 2015;518:197–206.
2. Kovács P, Klöting I. Quantitative trait loci on chromosomes 1 and 4 affect lipid phenotypes in the rat. Arch Biochem Biophys. 1998;354:139–43.
3. Klöting N, Wilke B, Klöting I. Triplet repeat in theRepin1 3'-untranslated region on rat chromosome 4 correlates with facets of the metabolic syndrome. Diabetes Metab Res Rev. 2007;23:406–10.
4. Caddle MS, Dailey L, Heintz NH. RIP60, a mammalian origin-binding protein, enhances DNA bending near the dihydrofolate reductase origin of replication. Mol Cell Biol. 1990;10:6236–6243.
5. Houchens CR, Montigny W, Zeltser L, Dailey L, Gilbert JM, Heintz NH. The dhfr oribeta-binding protein RIP60 contains 15 zinc fingers: DNA binding and looping by the central three fingers and an associated proline-rich region. Nucleic Acids Res. 2000;28:570–81.
6. Ruschke K, Illes M, Kern M, Klöting I, Fasshauer M, Schön MR, et al. Repin1 maybe involved in the regulation of cell size and glucose transport in adipocytes. Biochem Biophys Res Commun. 2010;400:246–51.
7. Kunath A, Hesselbarth N, Gericke M, Kern M, Dommel S, Kovacs P, et al. Repin1 deficiency improves insulin sensitivity and glucose metabolism in db/db mice by reducing adipose tissue mass and inflammation. Biochem Biophys Res Commun. 2016;478:398–402.
8. Hesselbarth N, Kunath A, Kern M, Gericke M, Mejhert N, Rydén M, et al. Repin1 deficiency in adipose tissue improves whole-body insulin sensitivity, and lipid metabolism. Int J Obes (Lond). 2017;41:1815–23.
9. Kern M, Kosacka J, Hesselbarth N, Bruckner J, Heiker JT, Flehmig G, et al. Liver-restricted repin1 deficiency improves whole-body insulin sensitivity, alters lipid metabolism, and causes secondary changes in adipose tissue in mice. Diabetes. 2014;63:3295–309.
10. Saltiel AR, Kahn CR. Insulin signalling and the regulation of glucose and lipid metabolism. Nature. 2001;414:799–806.
11. Standards of medical care in diabetes--2010. Diabetes Care American Diabetes Association 2010;33 (Suppl 1):S11–61.
12. Blüher M, Michael MD, Peroni OD, Ueki K, Carter N, Kahn BB, et al. Adipose tissue selective insulin receptor knockout protects against obesity and obesity-related glucose intolerance. Dev Cell. 2002;3:25–38.
13. Tönjes A, Koriath M, Schleinitz D, Dietrich K, Böttcher Y, Rayner NW, et al. Genetic variation in GPR133 is associated with height: genome wide association study in the self-contained population of Sorbs. Hum Mol Genet. 2009;18:4662–8.
14. Tönjes A, Zeggini E, Kovacs P, Böttcher Y, Schleinitz D, Dietrich K, et al. Association of FTO variants with BMI and fat mass in the self-contained population of Sorbs in Germany. Eur J Hum Genet. 2010;18:104–10.
15. Veeramah KR, Tönjes A, Kovacs P, Gross A, Wegmann D, Geary P, et al. Genetic variation in the Sorbs of eastern Germany in the context of broader European genetic diversity. Eur J Hum Genet. 2011;19:995–1001.
16. Krowczynska AM, Coutts M, Makrides S, Brawerman G. The mouse homologue of the human acidic ribosomal phosphoprotein PO: a highly conserved polypeptide that is under translational control. Nucleic Acids Res. 1989;17:6408.
17. Mueckler M, Thorens B. The SLC2 (GLUT) family of membrane transporters. Mol Aspects Med. 2013;34:121–38.
18. Miquilena-Colina ME, Lima-Cabello E, Sanchez-Campos S, Garcia-Mediavilla MV, Fernandez-Bermejo M, Lozano-Rodriguez T, et al. Hepatic fatty acid translocase CD36 upregulation is associated with insulin resistance, hyperinsulinaemia and increased steatosis in non-alcoholic steatohepatitis and chronic hepatitis C. Gut. 2011;60:1394–402.
19. Krammer J, Digel M, Ehehalt F, Stremmel W, Fuellekrug J, Ehehalt R. Overexpression of CD36 and Acyl-CoA synthetases FATP2, FATP4 and ACSL1 increases fatty acid uptake in human hepatoma cells. Int J Med Sci. 2011;8:599–614.
20. Contreras AV, Torres N, Tovar AR. PPAR-alpha as a key nutritional and environmental sensor for metabolic adaptation. Adv Nutr. 2013;4:439–52.
21. Sato R. Sterol metabolism and SREBP activation. Arch Biochem Biophys. 2010;501:177–81.
22. White UA, Stephens JM. Transcriptional factors that promote formation of white adipose tissue. Mol Cell Endocrinol. 2010;318:10–4.
23. Diraison F, Parton L, Ferré P, Foufelle F, Briscoe CP, Leclerc I, et al. Over-expression of sterol-regulatory-element-binding protein-1c (SREBP1c) in rat pancreatic islets induces lipogenesis and decreases glucose-stimulated insulin release: modulation by 5-aminoimidazole-4-carboxamide ribonucleoside (AICAR). Biochem J. 2004;378:769–78.
24. Borup A, Christensen PM, Nielsen LB, Christoffersen C. Apolipoprotein M in lipid metabolism and cardiometabolic diseases. Curr Opin Lipidol. 2015;26:48–55.
25. Xu N, Nilsson-Ehle P, Ahrén B. Correlation of apolipoprotein M with leptin and cholesterol in normal and obese subjects. J Nutr Biochem. 2004;15:579–82.
26. The Genotype-Tissue Expression (GTEx) project. GTEx Consortium Nat Genet. 2013;45:580–5.
27. Boyle AP, Hong EL, Hariharan M, Cheng Y, Schaub MA, Kasowski M, et al. Annotation of functional variation in personal genomes using RegulomeDB. Genome Res. 2012;22:1790–7.

Supplemental material

Table S1: Main characteristics of the study cohorts

	Leipzig cohort Total	**Leipzig cohort** NGT	**Sorbs cohort** Total	**Sorbs cohort** NGT
N	1982	578	1031	824
Men/Women	967/1218	207/379	424/622	366/547
Age (years)	56.2±15.4	44.4±14.8	48.01±16.25	46.1±15.7
BMI (kg/m^2)	28.9±6.2	26.6±5.9	26.9±4.9*	26.5±4.6$^{\#}$
WHR	0.99±0.19	0.88±0.14	0.86±0.14*	0.86±0.11$^{\#\#}$
Body fat (%)	29.9±10.6	24.6±7.5	21.3±9.2	20.5±8.7
Traits related to glucose metabolism and insulin sensitivity				
Fasting plasma glucose (mmol/l)	6.14±1.79	5.21±0.52	5.55±1.19*	5.3±0.5$^{\#}$
Fasting plasma insulin (pmol/l)	158.8±230.5	48.0±82.9	42.4±28.0*	38.8±23.5$^{\#}$
120 min plasma glucose (mmol/l)	8.57±3.78	5.95±0.95	5.74±2.5*	5.4±1.7$^{\#\#}$
HOMA B	197.1±361.9	90.4+213.7	61.9±76.0*	64.7±42.3$^{\#\#}$
HOMA IR	6.78±10.31	1.64±2.88	1.57±1.32*	1.3±0.8$^{\#}$
HbA1c (%)	6.51±1.54	5.34±0.35		
GIR (µmol/kg/min)	57.3±33.5	85.5±18.2		
Traits related to lipid metabolism and adipocyte size				
Total cholesterol (mmol/l)	5.14±0.96	4.97±0.94	5.32±1.03	5.3±1.0$^{\#\#}$
LDL-cholesterol (mmol/l)	3.15±1.05	2.86±0.86	3.37±0.96	3.37±0.97$^{\#\#}$
HDL- cholesterol (mmol/l)	1.39±0.40	1.33±0.41	1.63±0.10	1.65±0.39$^{\#\#}$
Triglycerides (mmol/l)	2.43±1.91	1.25±0.54	1.31±0.89	1.25±0.81
Free Fatty acids (mmol/l)	0.47±0.41	0.27±0.23	-	-
maximun adipocyte size vis (µm)	270.8±114.7	269.2±121.2	-	-

maximum adipocyte size sc (µm)	285.2±133.0	278.4±135.8	-	-

The data are given as mean ± standard deviation; NGT- subjects with normal glucose tolerance; BMI- Body Mass Index; HOMA IR- Homeostatic model assessment for insulin resistance ; HOMA B- Homeostatic model assessment for β-cell function ; WHR- waist- to-hip- ratio; ; HbA1c- glycated hemoglobin; FPG- fasting plasma glucose; FPI- Fasting plasma insulin; HDL-cholesterol- high density lipoprotein cholesterol; LDL-cholesterol – Low density lipoprotein cholesterol; TG- Triglycerides; FFA- Free fatty acids; max. adipocyte size vis= the maximum of adipocyte size in visceral fat; max. adipocyte size sc= the maximum of adipocyte size in subcutaneous fat; T—test for the comparison of Leipzig and Sorb cohort in total *$p<0.001$ and in NGT subjects $^{\#}p<0.01$, $^{\#\#}p<0.001$

Table S2: Primers for sequencing *REPIN1* gene and sequencing conditions

Rep1_Ex1_for:	Hs	AGTGGCTTGAGTGACCCG
Rep1_Ex1_rev:	Hs	GCAGATCCAGCAGCGTC
Rep1_Ex2_for:	Hs	GGTTGTGGCTGGTGAGGAC
Rep1_Ex2_rev:	Hs	CCCAGGATATGAGAAAGGGC
Rep1_Ex3_for:	Hs	GTCACCTTGGGCAGGTCTC
Rep1_Ex3_rev:	Hs	CAGTGTCAGACAGGGAGTAAATG
Rep1_Ex4_1_for:	Hs	ATGGCAGCTCCTGTCCG
Rep1_Ex4_1_rev:	Hs	GCAGATGCAGAACCAGGG
Rep1_Ex4_2_for:	Hs	CCCTTCTTAGCACTGCACC
Rep1_Ex4_2_rev:	Hs	CGATCAAGTTGGGCTTGTG
Rep1_Ex4_3_for:	Hs	ACGTAGCTGAGGCCCTGG
Rep1_Ex4_3_rev:	Hs	GTCGCAGCTGTAGAGGGAG
Rep1_Ex4_4_for:	Hs	AGATTCACAAGCGATCCGAG
Rep1_Ex4_4_rev:	Hs	ACTTCTGGCTGAAGGCTTTG
Rep1_Ex4_5_for:	Hs	CTCCCAGGGCAGCCATC
Rep1_Ex4_5_rev:	Hs	GCACTAGGCAGGCACCC
Rep1_Ex4_6_for:	Hs	AGCACGATGTCTGAGACGG
Rep1_Ex4_6_rev:	Hs	GCCCAGAGCATTCATTTACAG
Rep1_Ex4_7_for:	Hs	AAGGAAGACCCTCCATCCTC
Rep1_Ex4_7_rev:	Hs	GCAGTCCTTGCCGTGAC
Rep1_Ex4_8_for:	Hs	GTCAGCAGCACTGTGTCCAG
Rep1_Ex4_8_rev:	Hs	CGTCCTTCTAGGGAGGAGAG

primer pairs:					
Rep1_Ex4_7	Initial denaturation	94	°C	3 min	
	Denaturation	94	°C	30 sec	30 cycles
	Annealing	58	°C	45 sec	
	Extension	72	°C	1 min	
	Final Extension	72	°C	10 min	
		10	°C	∞	

primer pairs:					
Rep1_Ex2 Rep1_Ex1 Rep1_Ex4_1 Rep1_Ex3	Initial denaturation	94	°C	3 min	
	Denaturation	94	°C	30 sec	

	Rep1_Ex4_4 Rep1_Ex4_2	Annealing	60	°C	45 seck	30 cylces
	Rep1_Ex4_6 Rep1_Ex4_3	Extension	72	°C	1 min	
	Rep1_Ex4_8	Final Extension	72	°C	10 min	
			10	°C	∞	
primer pairs:	Rep1_Ex4_5	Initial denaturation	94	°C	3 min	
		Denaturation	94	°C	30 sec	
		Annealing	62	°C	30 sec	30 cycles
		Extension	72	°C	1 min	
		Final Extension	72	°C	10 min	
			10	°C	∞	

Table S3: Protocol for genotyping of the 12 bp deletion in the *REPIN1* gene

Amplification	PCR Program	
3µl DNA (30µg)	95°C -15min	
1µl Rep1_Ex4_4_for	95°C -25min	
1µl Rep1_Ex4_4_rev	52°C -35min	35 cycles
10µl Hot Star plus	72°C -75min	
1µl DMSO	72°C - 5min	
4µl H_20		

Digestion	
10µl PCR product	37°C -20min
2µl Green Buffer	65°C - 5min
1µl Apa I	
17µl H_2O	

Table S4: Primer sequences and corresponding product length

Gene	Primer sequences (5'-3')	Product length
APOM	fw: GGAAGGAGTTCCCAGAGGTC bw: CAGAGCCCATCTTTCATGCG	201 bp
CD36	fw: CATGTCTTGCTGTTGATTTGTGAAT bw: TTCTTGTTCAGGAGGTGAATTAGTGT	115 bp
FATP2	fw: CACAGGTCTTCCAAAAGCAGC bw: CAAGAGTAGCACCAGCCACAA	176 bp
FATP4	fw: CTCAGCAGGAAACATCGTGG bw: GTGGCTGGTTCAGGAGGTAG	167 bp
FATP5	fw: GTTGTCGCAGGTGGACTTCT bw: CTTACCCTCACAACCTGGCA	70 bp
GLUT2	fw: TGGTTCATGGTGGCTGAGTTT bw: GTCCACAGAAGTCCGCAATGT	130 bp
PPARA	fw: AGGCCAGTAACAATCCACCTT bw: CAGGTCCAAGTTTGCGAAGC	212 bp
PPARG-Isoform1	fw: CGTGGCCGCAGATTTGA bw: AGTGGGAGTGGTCTTCCATTAC	178 bp

PPARG-Isoform2	fw: GAAAGCGATTCCTTCACTGAT bw: TCAAAGGAGTGGGAGTGGTC	146 bp
RBP1	fw: ATGACCGCAAGTGCATGACAAC bw: CTTCTCACCCTTCTGCACACA	71 bp
RBP4	fw: AAGATTGTAAGGCAGCGGCA bw: CATCGCAGTAACCGTTGTGG	79 bp
SREBP-1c	fw: ACACCATGGGGAAGCACACAG bw: GTGTCAGAAAATGCAAGGCCC	177 bp
TTR	fw: TCATTCTTGGCAGGATGGCT bw: GCCACATTGATGGCAGGACT	160 bp

apolipoprotein M (APOM); fatty acid transport proteins 2,4,5 (FATP2,4,5); glucose transporter protein 2 (GLUT2); peroxisome proliferator activated receptor A (PPARA, PPARG); retinol binding protein 1, 4 (RBP1,4); sterol regulatory element-binding protein 1c (SREBP-1c); Transthyretin (TTR); fw-forward primer; bw-backward primer

Table S5: Case Control Studies for type 2 diabetes (T2D) versus normal glucose tolerant (NGT) individuals and for lean (BMI<25kg/m²) versus obese (BMI>30kg/m²) individuals

Case Control Study for obesity in the Leipzig cohort						
rs3832490	BMI< 25kg/m² lean	BMI> 30kg/m² obese	MAF lean *vs.* obese	unadjusted *p*-value	adjusted *p*-value add model	adjusted *p*-value dom model
wt/wt	475 (87.6%)	593 (90%)	0.062/0.051	0.260	0.479 (0.870 [0.592-1.279])	0.410 (0.849 [0.575-1.253])
wt/del	67 (12.4%)	65 (9.9%)				
del/del	0 (0%)	1 (0.2%)				
Case Control Study for obesity in the Sorbs cohort						
wt/wt	341 (86.1%)	199 (85.0%)	0.073/0.079	0.932	0.422 (0.811 [0.487-1.351])	0.488 (0.825 [0.478-1.422])
wt/del	52 (13.1%)	33 (14.1%)				
del/del	3 (0.8%)	2 (0.9%)				

MAF- minor allele frequency; add- additive model of inheritance, dom- recessive model of inheritance for the minor allele

Table S6: Association of variants in the *REPIN1* gene with metabolic parameters in the Leipzig cohort

	rs1051760		rs3735170		rs4725336		rs6971465		rs9640161		rs10229175		rs10278590		rs17173703	
	A>G		T>C		A>C		C>T		C>A		G>T		G>T		C>T	
MAF	0.337		0.251		0.139		0.334		0.364		0.107		0.399		0.279	
	ED	p-value	ED	p-value	ED	p-value	ED	p-value	ED	p-value	ED	p-value	ED	p-value	ED	p-value
BMI	+	0.105	+	0.246	+	0.281	+	0.454	+	0.724	-	0.475	+	0.536	+	0.071
WHR	+	0.220	-	0.983	+	0.423	+	0.871	+	0.957	-	0.765	+	0.316	+	0.305
Body fat (%)	-	0.094	-	0.971	+	0.405	-	0.718	-	0.458	-	0.124	-	**0.033***	-	0.552
FPG	+	0.403	+	0.291	+	0.268	+	0.824	+	0.806	-	0.442	+	0.536	+	0.599
Glucose 120min	+	0.525	+	0.280	-	0.597	+	0.629	+	0.773	-	0.597	+	0.289	-	0.652
FPI	-	0.570	+	0.300	+	0.909	-	0.956	+	0.184	+	0.270	+	0.691	-	0.876
HOMA IR	-	0.812	+	0.406	-	0.676	+	0.952	+	0.099	+	0.086	+	0.493	-	0.847
HOMA B	-	0.720	+	0.611	-	0.407	+	0.908	+	0.104	+	0.069	+	0.536	-	0.900
GIR	+	**0.011***	+	0.051	-	0.081	+	**0.047***	+	0.178	-	0.567	+	**0.026***	+	**0.011***
HbA1c	+	**0.026***	+	**0.036***	-	0.145	+	0.087	+	0.052	+	0.958	+	0.192	+	**0.038***
FFA	+	0.809	+	0.071	+	0.946	+	0.597	+	0.993	-	0.147	+	0.701	+	0.556
Cholesterol	+	0.149	+	0.093	-	0.187	+	0.177	+	0.078	+	0.267	+	0.077	+	**0.012***
HDL-cholesterol	+	0.896	+	0.768	-	0.320	-	0.592	-	0.992	-	0.939	+	0.966	+	0.719
LDL-cholesterol	+	0.275	+	0.260	-	0.207	+	0.612	+	0.090	+	0.436	+	0.185	+	**0.022***
TG	+	0.132	+	0.441	-	0.842	+	0.124	+	**0.040***	+	**0.050***	+	0.195	+	0.562

MAF= Minor allele frequency; ED= effect direction for the minor allele ; *p*-values adjusted for sex, age and lnBMI except for BMI and WHR (adjusted for sex and age); $^{*}p<0.05$; all SNPs were in Hardy Weinberg equilibrium.

BMI= Body mass index; WHR= waist to hip ratio; FPG= fasting plasma glucose; Glucose 120min= glucose after 120min in oral glucose tolerance test; FPI= fasting plasma insulin; HOMA IR= Homeostasis model assessment for insulin resistance ; HOMA B= Homeostasis model assessment for beta cell function; GIR= glucose infiltration rate; HbA1c= glycosylated hemoglobin A1c ; FFA= free fatty acids; HDL= high density lipoprotein; LDL= low density lipoprotein; TG= triglycerides;

Table S7: Association of variants in the *REPIN1* gene with metabolic parameters in the Sorbs cohort

	rs1051760		rs3735170		rs4725336		rs6971465		rs9640161		rs10229175		rs10278590		rs17173703	
	A>G		T>C		A>C		C>T		C>A		G>T		G>T		C>T	
MAF	0.327		0.239		0.131		0.303		0.369		0.131		0.392		0.255	
	ED	p-value	ED	p-value	ED	p-value	ED	p-value	ED	p-value	ED	p-value	ED	p-value	ED	p-value
BMI	-	0.691	-	0.416	-	0.436	+	0.907	-	0.327	-	0.680	+	0.694	-	0.846
WHR	-	0.841	+	0.616	-	0.075	+	0.341	+	0.442	+	0.610	+	0.222	+	0.908
Body fat (%)	+	0.751	+	0.069	-	0.659	+	0.507	-	0.603	-	0.055	+	0.892	+	0.309
FPG	-	0.186	-	0.410	+	0.759	-	0.094	+	0.630	+	0.136	-	0.097	-	0.582
Glucose 120min	+	0.806	+	0.543	-	0.591	+	0.466	+	0.661	+	0.672	+	0.365	+	0.225
FPI	-	0.901	+	0.355	-	0.801	+	0.594	+	0.539	+	0.999	-	0.876	+	0.619
HOMA IR	-	0.742	+	0.424	-	0.856	+	0.851	+	0.517	+	0.869	-	0.693	+	0.710
HOMA B	+	0.385	+	0.096	-	0.536	+	0.120	+	0.513	-	0.473	+	0.480	+	0.286
Cholesterol	+	0.131	+	0.179	-	0.180	+	0.002*	+	0.970	-	0.275	+	0.241	+	0.096
HDL-cholesterol	+	0.195	+	0.335	-	0.396	+	0.539	+	0.410	+	0.740	+	0.068	+	0.309
LDL-cholesterol	+	0.138	+	0.203	-	0.193	+	0.005*	-	0.909	-	0.159	+	0.232	+	0.123
TG	-	0.834	+	0.534	+	0.668	+	0.360	-	0.517	-	0.150	-	0.374	+	0.736
Lipoprotein	-	0.592	-	0.469	+	0.287	-	0.593	+	0.952	+	0.648	-	0.399	-	0.183

MAF= Minor allele frequency; ED= effect direction for the minor allele; *p*-values adjusted for sex, age and lnBMI except for BMI and WHR (adjusted for sex and age); *$p<0.05$; all SNPs were in Hardy Weinberg equilibrium.

BMI= Body mass index; WHR= waist to hip ratio; FPG= fasting plasma glucose; Glucose 120min= glucose after 120min in oral glucose tolerance test; FPI= fasting plasma insulin; HOMA IR= Homeostasis model assessment for insulin resistance ; HOMA B= Homeostasis model assessment for beta cell function; HDL= high density lipoprotein; LDL= low density lipoprotein; TG= triglycerides; ED= effect direction for the minor allele

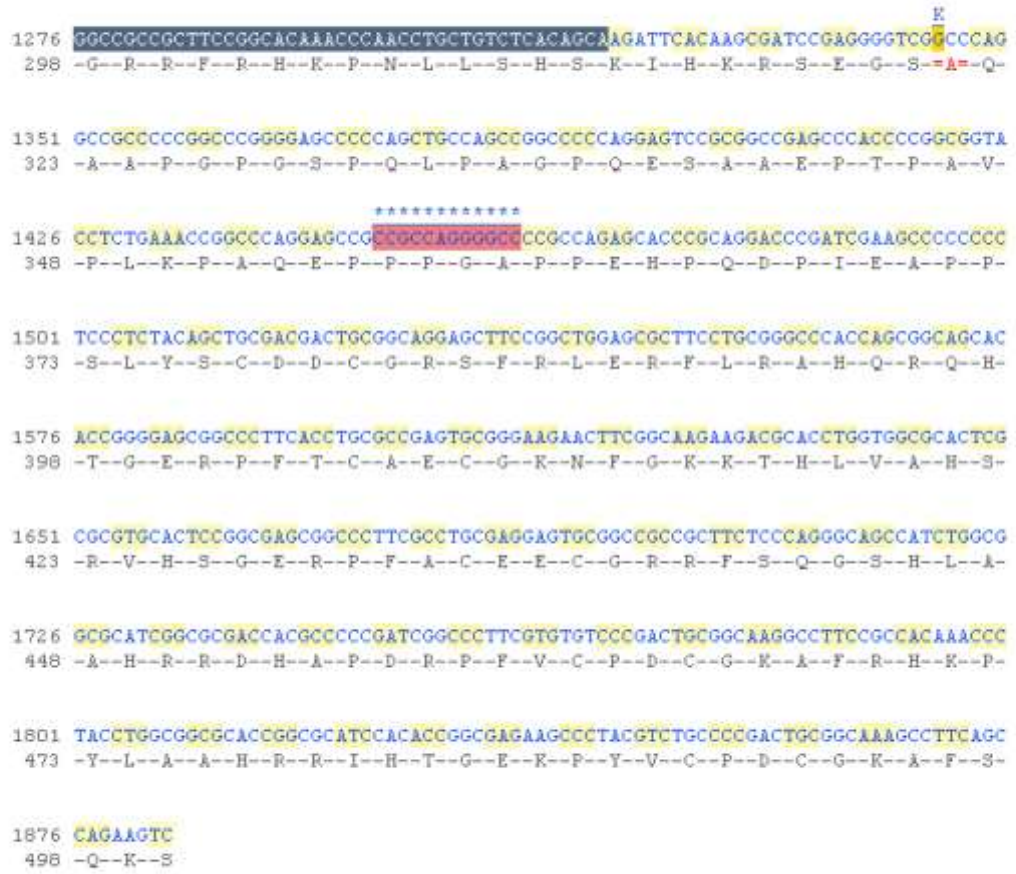

Figure S1: Sequence of *REPIN1*- region with the12 bp deletion marked in red.

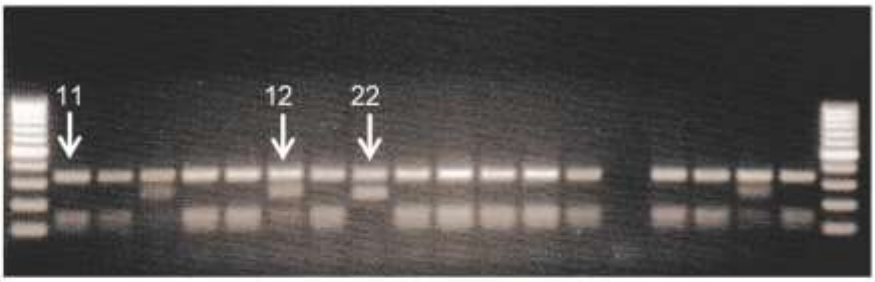

Figure S2. Agarose gel after RFLP for the human genotyping. 11- homozygote for wildtype (3 fragments), 12- heterozygote (4 fragments), 22- homozygote for 12 bp deletion (2 fragments).

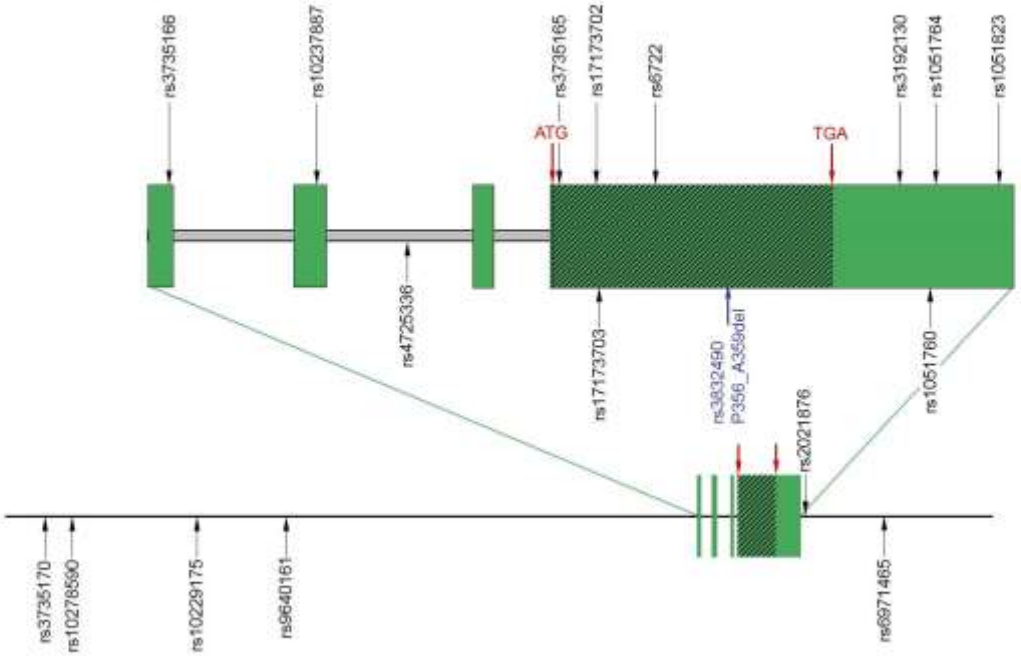

Figure S3: Map of the *REPIN1* gene with the schematic location of the polymorphisms.

Chapter 4

IRX3 and *IRX5* expression in subcutaneous and visceral adipose tissue in obesity

4.1. Abstract

Background

The strongest signal for BMI in genome wide association studies maps in introns 1 and 2 of the *FTO, alpha-ketoglutarate dependent dioxygenase* gene (*FTO*, also: *fat mass and obesity associated*). Recent studies show that the variants do not exert their regulatory effect on the gene itself, but rather on the neighbouring genes *IRX3* and *IRX5*. Therefore, we investigated the fat depot specific mRNA expression of *IRX3* and *IRX5* in relation to obesity and associated metabolic traits.

Results

IRX5 showed significantly higher expression in subcutaneous adipose tissue (ScAT) compared to visceral adipose tissue (VAT), whereas *IRX3* demonstrated no differences between both depots. Furthermore, the ScAT mRNA expression of *IRX3* was associated with obesity measures such as weight and BMI. No association was observed between the obesity-associated SNP rs8050136 and the expression levels of both genes.

Conclusion

Our analysis suggests a moderate relationship between the AT specific expression of *IRX3* and *IRX5* and obesity.

4.2. Introduction

In 2007 the strongest signal in GWAS for BMI pointed out intron 1 of the *fat mass and obesity associated gene (FTO)* gene [2,3]. Subsequently, numerous studies demonstrated that *FTO* polymorphisms were not only associated with BMI [4] but also with obesity related parameters and complications like the metabolic syndrome [5], hypertension [6] and atherosclerosis [7]. Despite the strong and robustly replicated associations, the direct molecular mechanisms behind the *FTO* associations remained poorly understood. However, recent studies suggested that the reported *FTO* SNPs exert regulatory effects not only on FTO itself, but also on nearby genes [8]. Initially, Smemo et al. showed a long range interaction between *FTO* and the *iroquios homebox 3 (IRX3)* [9]. The obesity-associated *FTO* SNPs in introns 1 and 2 interact directly with the promoters of *IRX3* as well as *FTO* in humans. *Irx3*-deficient mice showed a 25–30 % reduction of body weight, primarily through the loss of fat mass. At the same time, the basal metabolic rate was increased through browning of the white AT [9]. In line with findings by Smemo et al., Claussnitzer et al. [10] demonstrated a potential mechanistic pathway for the genetic variants in *FTO,* which seems to regulate the *IRX3* and *IRX5* expression in AT [10].

To gain more insights into the role of *IRX3* and *IRX5* in obesity, we investigated the fat depot specific mRNA expression of *IRX3* and *IRX5* in relation to obesity and associated metabolic traits.

4.3. Material and Methods

4.3.1. Subjects

Paired samples of ScAT and VAT were obtained from 551 participants who underwent open abdominal surgery. All AT samples were frozen immediately in liquid nitrogen and stored at -80°C. Phenotypic characterization of the study participants including anthropometric measurements (weight, height, waist, hip circumference, WHR), bioimpedance analyses or dual-energy X-ray absorptiometry (body fat), and metabolic parameters (fasting plasma glucose, fasting plasma insulin, 75-g oral glucose tolerance test (OGTT), HbA1c, lipoprotein-, triglyceride-, free fatty acid- and adipokine serum concentrations) was performed as previously described [11,12]. Measurement of abdominal VAT and ScAT areas was performed using computed tomography (CT) or MRI scans. For our analysis, data from 176 men and 375 women were available (mean age 50±13 years; mean BMI 44.1±13.1 kg/m²). 303 subjects had normal glucose tolerance (mean age 49±13 years; mean BMI 39.9±13.4 kg/m²), whereas 224 subjects manifested with T2D (mean age 52±11 years; mean BMI 49.4±10.4 kg/m²) (Table 1). The study

was approved by the ethics committee of the University of Leipzig and all participants gave written informed consent before taking part in the study.

Table 1. Anthropometric and metabolic characteristics of the study participants

	Total	NGT	T2D
N	551	303	224
Men/Women	176/375	93/210	77/147
Age (years)	50±13	49±15	52±11
BMI (kg/m^2)	44.1±13.1	39.9±13.4	49.4±10.4
Weight (kg)	127.7±41.4	115.2±42.9	142.9±33.2
Waist (cm)	126.9±29.2	114.0±29.6	143.3±21.4
WHR	0.94±0.10	0.90±0.08	1.03±0.08
Body fat (%)	42.6±11.5	38.1±13.9	45.89±8.15
Visceral fat area (cm²)	243.5±182.9	177.7±152.2	410.4±150.5
Subcutaneous fat area (cm²)	1094.21±807.7	945.0±835.1	1467.5±617.9
Fasting plasma glucose (mmol/l)	6.74±2.83	5.53±1.17	8.46±3.52
Fasting plasma insulin (pmol/l)	118.12±131.2	67.70±68.8	168.9±156.9
120 min plasma glucose (mmol/l)	6.72±2.14	6.26±0.99	12.72±6.93
HbA1c (%)	6.17±1.2	5.51±0.5	7.06±1.4
GIR (µmol/kg/min)	76.95±32.35	90.35±21.05	36.15±27.26
Total cholesterol (mmol/l)	5.07±1.09	5.05±1.08	5.05±1.05
LDL-cholesterol (mmol/l)	3.09±0.88	3.12±0.88	3.00±0.85
HDL-cholesterol (mmol/l)	1.25±0.37	1.37±0.43	1.15±0.31
Triglycerides (mmol/l)	1.96±1.24	1.54±1.12	2.30±1.21
Free fatty acids (mmol/l)	0.59±0.40	0.39±0.34	0.89±0.31
Leptin (ng/ml)	38.97±25.44	34.53±23.77	43.17±27.13
Adiponectin (µg/ml)	6.67±4.64	8.55±4.98	4.43±3.11
IL6 (pg/ml)	6.31±5.4	5.33±4.70	7.89±6.20

Table continued on the next page

	Total	NGT	T2D
Max. adipocyte size vis (µm)	200.21±23.4	198.37±27.13	202.22±18.28
Max. adipocyte size sc (µm)	203.3±21.9	200.75±25.11	206.42±17.26
Mean adipocyte size vis (µm)	126.56±17.7	122.15±19.68	131.74±13.37
Mean adipocyte size sc (µm)	130.5±17.6	124.77±18.71	137.56±13.5

BMI- body mass index, WHR- waist-to-hip ratio, IL-6- interleukin 6, HbA1c- Glycohemoglobin, GIR- glucose infusion rate during the steady state of an euglycemic hyperinsulinemic clamp, HDL- high density lipoprotein cholesterol, LDL- low density lipoprotein cholesterol , Vis mean- mean adipocyte size in visceral adipose tissue, Sc mean- mean adipocyte size in subcutaneous adipose tissue, Vis max- maximum adipocyte size in visceral adipose tissue, Sc max- maximum adipocyte size in subcutaneous adipose tissue

4.3.2. Measurement of human *IRX3 and IRX5* mRNA expression

The mRNA expression of *IRX3* and *IRX5* was measured with specific primers (IRX3-CTCTCCCTGCTGGGCTCT CAAGGCACTACAGCGATCTG; IRX5-GACCTGGAGAAGAACGACGA GCCTTCTGCTCAGCTCCTC) by qRT-PCR (Applied Biosystems, Darmstadt, Germany). Total RNA was isolated from AT samples using the Qiacube System (Qiagen, Hilden, Germany), and 2 µg RNA was reverse transcribed with standard reagents (Life Technologies). The expression levels of *IRX3* and *IRX5* were calculated relative to the mRNA expression of *hypoxanthine guanine phosphoribosyltransferase 1 (HPRT1)*, determined by the assay (Applied Biosystems, Darmstadt, Germany, Hs01003267_M1). Expression of *IRX3, IRX5* and *HPRT1* mRNA were quantified by using the second standard curve based method of the TaqMan Software (Applied Biosystems).

4.3.3. Genotyping of *FTO* SNP rs8050136

Genomic DNA was extracted from blood samples using the QuickGene DNA whole blood kit (Kurabo, Japan). Genotyping of the SNPs rs8050136 was performed using the TaqMan SNP Genotyping assay (Applied Biosystems; C_2031259_10). To assess genotyping reproducibility, a random ~5 % selection of the sample were re-genotyped for all SNPs; all genotypes matched initial designated genotypes. Rs8050136 belongs to one L.D. group, which includes the previously reported BMI-associated SNP rs9939609 [2].

4.3.4. Statistical analysis

Statistical analyses were done with SPSS (SPSS, version 24, Inc., Chicago, IL, USA). All non-normally distributed parameters were logarithmically transformed to approximate a normal distribution. To analyze differences in mRNA expression levels between *IRX3* and *IRX5*

expression in VAT and ScAT, paired two-tailed t-tests were applied. To test for group differences, two tailed t-tests was used. Pearson's correlation coefficients were used to assess bivariate correlation with phenotypes related to obesity, fat distribution and glucose and insulin metabolism. Linear regression models were used to control for confounders such as age, gender and BMI. Linear regression analysis adjusted for respective covariates was applied to analyze rs8050136 for genetic association with mRNA expression and metabolic traits.

4.4. Results and Discussion

4.4.1. Correlation of *IRX3* and *IRX5* mRNA expression with metabolic parameters

The mRNA expression of *IRX3* in ScAT was positively correlated with weight and BMI, and remained significant even after adjustment for sex and age. Although waist correlated with subcutaneous *IRX3* expression, the correlation did not withstand adjustments for age and sex. Similarly, the *IRX3* mRNA in VAT showed correlations with weight, BMI and waist only if the relevant covariates are not taken into account (Table 2).

Table 2. Correlation of *IRX3* mRNA expression in adipose tissue with metabolic traits

IRX3	**Subcutaneous AT**			**Visceral AT**		
Trait	R	unadj. p-value	adj. p-value	R	unadj. p-value	adj. p-value
Weight (kg)	0.168	**$2.49*10^{-3}$**	**0.021**$^{\#}$	0.116	**0.037**	0.355$^{\#}$
BMI (kg/m²)	0.180	**$1.22*10^{-3}$**	**0.015**$^{\#}$	0.130	**0.019**	0.248$^{\#}$
Waist (cm)	0.181	**0.037**	0.554	0.167	**0.049**	0.804$^{\#}$
WHR	-0.091	0.349	0.876$^{\#}$	-0.095	0.310	0.635$^{\#}$
% Body fat	0.077	0.546	0.624$^{\#}$	0.139	0.271	0.618$^{\#}$
Vis fat (cm²)	0.075	0.449	0.750	0.128	0.181	0.741
Sc fat (cm²)	0.155	0.116	0.929	0.117	0.224	0.686
FPG (mmol/l)	-0.103	0.070	0.061	-0.030	0.604	0.746
FPI (mmol/l)	0.004	0.974	0.421	0.130	0.227	0.793
oGTT2h (mmol/l)	-0.103	0.360	0.163	-0.072	0.511	0.374
GIR (µmol/kg/min)	0.295	0.017	0.128	0.103	0.392	0.910
HbA1c (%)	-0.079	0.305	0.182	-0.050	0.505	0.199
Chol (mmol/l)	-0.012	0.863	0.927	0.015	0.838	0.701
HDL (mmol/l)	0.007	0.939	0.109	0.001	0.992	0.096
LDL (mmol/l)	0.110	0.240	0.379	0.041	0.654	0.950
TG (mmol/l)	-0.008	0.906	0.340	0.034	0.635	0.907
FFA (mmol/l)	-0.030	0.788	0.103	0.108	0.324	0.806
Leptin (ng/ml)	0.249	**0.014**	0.392	0.196	0.052	0.526
Adiponectin (µg/ml)	-0.092	0.369	0.750	-0.156	0.121	0.606
IL6 (pg/ml)	0.280	**0.016**	0.061	0.119	0.295	0.746

Table continued on the next page

IRX3	Subcutaneous AT			Visceral AT		
Trait	R	unadj. p-value	adj. p-value	R	unadj. p-value	adj. p-value
Vis mean (cm²)	0.060	0.614	0.447	0.009	0.941	0.960[#]
Sc mean (cm²)	0.052	0.660	0.561	0.072	0.539	0.510[#]
Vis max (cm²)	0.037	0.757	0.557	-0.162	0.162	0.172[#]
Sc max (cm²)	-0.091	0.439	0.581[#]	-0.074	0.527	0.606[#]

The data are given as mean ± standard deviation, p-values are adjusted for sex, age and BMI, [#] p-value adjusted for sex and age, bold p-values indicate statistical significance.

R- correlation coefficient, AT- adipose tissue, BMI- body mass index, WHR- waist-to-hip ratio, TG- triglycerides, IL-6- interleukin 6, HbA1c- glycohemoglobin, oGTT- oral glucose tolerance test, FPG- fasting plasma glucose, FPI- fasting plasma insulin, GIR- glucose infusion rate during the steady state of an euglycemic hyperinsulinemic clamp, HDL- high density lipoprotein cholesterol, LDL- low density lipoprotein cholesterol , FFA- free fatty acids, Sc- subcutaneous, Vis- visceral, Vis mean- mean adipocyte size in visceral adipose tissue, Sc mean- mean adipocyte size in subcutaneous adipose tissue, Vis max- maximum adipocyte size in visceral adipose tissue, Sc max- maximum adipocyte size in subcutaneous adipose tissue.

For the subcutaneous *IRX5* mRNA levels no significant correlations with metabolic parameters were found. The mRNA expression of *IRX5* in VAT showed significant correlations with BMI and waist but only in the unadjusted model (Table 3).

Table 3. Correlation of *IRX5* mRNA expression in adipose tissue with metabolic traits

IRX5	Subcutaneous AT			Visceral AT		
Trait	R	unadj. p-value	adj. p-value	R	unadj. p-value	adj. p-value
Weight (kg)	0.006	0.923	0.677[#]	0.112	0.053	0.107[#]
BMI (kg/m²)	0.021	0.725	0.932[#]	0.130	**0.025**	0.069[#]
Waist (cm)	-0.094	0.322	0.167[#]	0.227	**0.014**	0.128[#]
WHR	-0.043	0.692	0.782[#]	0.014	0.892	0.757[#]
% body fat	0.033	0.810	0.286[#]	0.283	**0.033**	0.644[#]
Vis fat (cm²)	-0.180	0.102	0.068[#]	0.169	0.111	0.294[#]
Sc fat (cm²)	-0.082	0.458	0.309[#]	0.111	0.299	0.816[#]
FPG (mmol/l)	-0.089	0.136	0.244	0.028	0.640	0.664
FPI (mmol/l)	-0.129	0.282	0.162	0.260	**0.025**	0.152
oGTT2h (mmol/l)	0.004	0.973	0.973	0.051	0.670	0.781
GIR (µmol/kg/min)	0.284	**0.044**	0.366	-0.039	0.775	0.514
HbA1c (%)	0.009	0.911	0.535	-0.019	0.816	0.232
Chol (mmol/l)	-0.20	0.790	0.919	0.092	0.219	0.158
HDL (mmol/l)	0.065	0.509	0.147	-0.093	0.332	0.654
LDL (mmol/l)	-0.032	0.744	0.700	0.136	0.157	0.303
TG (mmol/l)	-0.015	0.836	0.695	0.017	0.817	0.667
FFA (mmol/l)	0.032	0.800	0.659	0.108	0.372	0.661

Table continued on the next page

IRX5	Subcutaneous AT			Visceral AT		
Trait	R	unadj. p-value	adj. p-value	R	unadj. p-value	adj. p-value
Leptin (ng/ml)	0.013	0.905	0.112	0.209	0.055	0.309
Adiponectin (µg/ml)	0.064	0.565	0.756	-0.153	0.161	0.552
IL6 (pg/ml)	0.220	0.091	**0.033**	0.062	0.624	0.920
Vis mean (cm²)	-0.066	0.587	0.690	0.052	0.671	0.648
Sc mean (cm²)	0.033	0.782	0.812	0.026	0.831	0.860
Vis max (cm²)	-0.073	0.551	0.623	-0.132	0.276	0.305
Sc max (cm²)	0.089	0.459	0.341	-0.122	0.313	0.328

The data are given as mean ± standard deviation, p-values are adjusted for sex, age and BMI,[#] p-value adjusted for sex and age, bold p-values indicate statistical significance.

R- correlation coefficient , AT- adipose tissue, BMI- body mass index, WHR- waist-to-hip ratio, TG- triglycerides, IL-6- interleukin 6, HbA1c- glycohemoglobin, oGTT 2h- oral glucose tolerance test measurement after 2 hours, FPG- fasting plasma glucose, FPI- fasting plasma insulin, GIR- glucose infusion rate during the steady state of an euglycemic hyperinsulinemic clamp, HDL- high density lipoprotein cholesterol, LDL- low density lipoprotein cholesterol , FFA- free fatty acids, Sc- subcutaneous, Vis- visceral, Vis mean- mean adipocyte size in visceral adipose tissue, Sc mean- mean adipocyte size in subcutaneous adipose tissue, Vis max- maximum adipocyte size in visceral adipose tissue, Sc max- maximum adipocyte size in subcutaneous adipose tissue.

4.4.2. Differences of *IRX3* and *IRX5* mRNA expression in subcutaneous and visceral adipose tissue

We did not find a difference in the mRNA expression levels of *IRX3* between ScAT and VAT in our cohort (Figure 1A). The mRNA expression levels were near the same in both ATs in the subgroups of subjects with normal glucose tolerance (NGT) and also in the subgroup of subjects with T2D. There were also no differences observed in expression levels in lean or obese subjects (Figure 1B).

Figure 1. **mRNA expression levels of *IRX3* in subcutaneous (ScAT) and visceral (VAT) adipose tissue**. The analysis were done in the total cohort, in subjects with normal glucose tolerance (NGT) and subject with type 2 diabetes (T2D) **(A)** and in lean (BMI<25 kg/m²) and obese (BMI>30 kg/m²) subjects **(B).**

The mRNA expression levels for *IRX5* differ between both tissues. We observed significantly higher levels in the ScAT compared to the VAT and these findings were also observed in the subgroups of subjects with NGT and T2D (Figure 2A). Consistently, we found differential mRNA expression in ScAT vs. VAT in both, lean and obese subjects (Figure 2B).

Figure 2. mRNA expression levels of *IRX5* in subcutaneous (ScAT) and visceral (VAT) adipose tissue. The analysis were done in the total cohort, in subjects with normal glucose tolerance (NGT) and subject with type 2 diabetes (T2D) **(A)** and in lean (BMI<25 kg/m²) and obese (BMI>30 kg/m²) subjects **(B)**.***p<0.001

4.4.3. Association of rs8050136 with metabolic traits

Rs8050136 showed only a moderate association with BMI (p=0.057). Furthermore, it was associated with obesity measures such as weight, waist and hip (Table 3). The SNP was not associated with the mRNA expression levels of *IRX3* and *IRX5*, although a tendency was observed for the *IRX3* mRNA expression in VAT with a p value of 0.077 (Table 4).

Table 4. Association of rs8050136 with metabolic traits

	rs8050136			
Trait	AA	AC	CC	adj. p-value
BMI (kg/m²)	44.5±12.0	40.0±14.0	39.0±13.1	0.057#
% body fat	44.6±8.9	40.5±12.8	42.3±12.0	0.323
Weight (kg)	127.9±37.9	116.3±43.9	112.6±41.4	**0.034#**
Waist (cm)	126.4±25.1	115.5±28.6	112.5±29.9	**$1.23x10^{-3}$#**
Hip (cm)	140.0±27.0	129.0±30.	125.0±30.5	**$3.00x10^{-3}$#**
WHR	0.90±0.08	0.89±0.10	0.90±0.10	0.290
FPG (mmol/l)	5.43±0.78	5.34±0.66	5.43±0.79	0.678
FPI (mmol/l)	91.5±61.5	85.7±72.7	103.49±78.1	0.360
GIR (µmol/kg/min)	84.4±17.9	92.0±21.6	90.3±26.9	0.179
HbA1c (%)	5.53±0.46	5.43±0.44	5.43±0.38	0.452
Chol (mmol/l)	4.77±0.95	4.84±1.05	4.71±1.05	0.447
HDL (mmol/l)	1.28±0.34	1.32±0.44	1.33±0.47	0.464
LDL (mmol/l)	3.07±0.81	3.14±1.00	2.91±1.02	0.273
TG (mmol/l)	1.41±0.70	1.31±0.52	1.21±0.58	0.067
FFA (mmol/l)	0.46±0.35	0.35±0.32	0.35±0.29	0.558
Vis fat (cm²)	194.0±154.6	181.9±138.0	165.1±131.3	0.305#
Sc fat (cm²)	1194.7±821.2	1011.0±830.5	905.1±806.7	0.102#
Vis mean (cm²)	121.3±17.2	113.4±24.4	122.7±14.8	0.323
Sc mean (cm²)	128.0±14.9	119.7±21.0	127.9±16.4	0.187
Vis max (cm²)	218.0±77.8	209.8±76.8	204.0±33.7	0.649
Sc max (cm²)	220.9±80.3	219.7±85.0	205.7±58.7	0.902
log*IRX3* sc	3.29±1.23	3.45±1.19	3.30±1.18	0.282
log*IRX3* vis	3.22±1.06	3.40±1.24	3.64±1.27	0.077
log*IRX5* sc	6.49±1.54	6.37±1.44	6.18±1.83	0.637
log*IRX5* vis	3.81±1.19	4.01±1.44	3.98±1.50	0.712

The data are given as mean ± standard deviation, p-values are adjusted for sex, age and BMI,# p-value adjusted for sex and age, bold p-values indicate statistical significance.

AT- adipose tissue, BMI- Body mass index, WHR- waist-to-hip ratio, TG- triglycerides, IL-6- interleukin 6, HbA1c- glycohemoglobin, oGTT 2h- oral glucose tolerance test measurement after 2 hours, FPG- fasting plasma glucose, FPI- fasting plasma insulin, GIR- glucose infusion rate during the steady state of an euglycemic hyperinsulinemic clamp, HDL- high density lipoprotein cholesterol, LDL- low density lipoprotein cholesterol , FFA- free fatty acids, Sc- subcutaneous, Vis- visceral, Vis mean- mean adipocyte size in visceral adipose tissue, Sc mean- mean adipocyte size in subcutaneous adipose tissue, Vis max- maximum adipocyte size in visceral adipose tissue, Sc max- maximum adipocyte size in subcutaneous adipose tissue.

.

4.5. Summary

In the present study we investigated the fat depot specific mRNA expression levels of *IRX3* and *IRX5* as plausible candidate genes for obesity and their link to related traits. We showed differential expression profiles for *IRX5* in ScAT and VAT but not for *IRX3*. We confirmed an association between *IRX3* expression levels in ScAT but found no association in VAT. We did not find a significant correlation between the mRNA expression of *IRX3* and *IRX5* with the obesity related SNP rs8050136. One explanation might be the restricted statistical power due

to the limited sample size caused by the fact that the overlap of the study group with expression data and the group of genotyped subjects was rather small (N=155). Further limitation of our study was that the mRNA expression was only measured in the whole extracted AT, since the adipocytes and the stroma vascular fraction (SVF) were not separated after the biopsies. Landgraf et al. showed an association between the *FTO* variant and *IRX3* and *IRX5* expression in adipocytes, but none were found in SVF or in the whole AT [13]. Thus, lacking the separation of adipocytes might explain the missing associations in our study. Moreover, it would also be desirable to elucidate the role of *IRX3* and *IRX5* in the process of browning of AT as has been shown recently by Zou et al.[14].

In conclusion, our analysis suggests a moderate relationship between the AT specific expression of *IRX3* and *IRX5* and obesity. Further experiments focusing on specific cell types such as adipocytes as well as on processes like AT browning are warranted to better understand the role of these genes in the pathophysiology of human obesity.

4.6. References

1 World Health Organisation, Obesity and overweight. http://www.who.int/mediacentre/factsheets/fs311/en/.

2 Frayling TM, Timpson NJ, Weedon MN, Zeggini E, Freathy RM, Lindgren CM *et al.* A common variant in the FTO gene is associated with body mass index and predisposes to childhood and adult obesity. *Science (New York, N.Y.)* 2007; **316**: 889–894; doi:10.1126/science.1141634.

3 Scuteri A, Sanna S, Chen W-M, Uda M, Albai G, Strait J *et al.* Genome-wide association scan shows genetic variants in the FTO gene are associated with obesity-related traits. *PLoS genetics* 2007; **3**: e115; doi:10.1371/journal.pgen.0030115.

4 Tönjes A, Zeggini E, Kovacs P, Böttcher Y, Schleinitz D, Dietrich K *et al.* Association of FTO variants with BMI and fat mass in the self-contained population of Sorbs in Germany. *European journal of human genetics : EJHG* 2010; **18**: 104–110; doi:10.1038/ejhg.2009.107.

5 Elouej S, Belfki-Benali H, Nagara M, Lasram K, Attaoua R, Sallem OK *et al.* Association of rs9939609 Polymorphism with Metabolic Parameters and FTO Risk Haplotype Among Tunisian Metabolic Syndrome. *Metabolic syndrome and related disorders* 2016; **14**: 121–128; doi:10.1089/met.2015.0090.

6 He D, Fu M, Miao S, Hotta K, Chandak GR, Xi B. FTO gene variant and risk of hypertension: a meta-analysis of 57,464 hypertensive cases and 41,256 controls. *Metabolism: clinical and experimental* 2014; **63**: 633–639; doi:10.1016/j.metabol.2014.02.008.
7 Äijälä M, Ronkainen J, Huusko T, Malo E, Savolainen E-R, Savolainen MJ *et al.* The fat mass and obesity-associated (FTO) gene variant rs9939609 predicts long-term incidence of cardiovascular disease and related death independent of the traditional risk factors. *Annals of medicine* 2015; **47**: 655–663; doi:10.3109/07853890.2015.1091088.
8 Loos RJ. The genetics of adiposity. *Current opinion in genetics & development* 2018; **50**: 86–95; doi:10.1016/j.gde.2018.02.009.
9 Smemo S, Tena JJ, Kim K-H, Gamazon ER, Sakabe NJ, Gómez-Marín C *et al.* Obesity-associated variants within FTO form long-range functional connections with IRX3. *Nature* 2014; **507**: 371–375; doi:10.1038/nature13138.
10 Claussnitzer M, Dankel SN, Kim K-H, Quon G, Meuleman W, Haugen C *et al.* FTO Obesity Variant Circuitry and Adipocyte Browning in Humans. *NEW ENGLAND JOURNAL OF MEDICINE* 2015; **373**: 895–907; doi:10.1056/NEJMoa1502214.
11 Blüher M, Klöting N, Wueest S, Schoenle EJ, Schön MR, Dietrich A *et al.* Fas and FasL expression in human adipose tissue is related to obesity, insulin resistance, and type 2 diabetes. *The Journal of clinical endocrinology and metabolism* 2014; **99**: E36-44; doi:10.1210/jc.2013-2488.
12 Klöting N, Fasshauer M, Dietrich A, Kovacs P, Schön MR, Kern M *et al.* Insulin-sensitive obesity. *American journal of physiology. Endocrinology and metabolism* 2010; **299**: E506-15; doi:10.1152/ajpendo.00586.2009.
13 Landgraf K, Scholz M, Kovacs P, Kiess W, Körner A. FTO Obesity Risk Variants Are Linked to Adipocyte IRX3 Expression and BMI of Children - Relevance of FTO Variants to Defend Body Weight in Lean Children? *PloS one* 2016; **11**: e0161739; doi:10.1371/journal.pone.0161739.
14 Zou Y, Lu P, Shi J, Liu W, Yang M, Zhao S *et al.* IRX3 Promotes the Browning of White Adipocytes and Its Rare Variants are Associated with Human Obesity Risk. *EBioMedicine* 2017; **24**: 64–75; doi:10.1016/j.ebiom.2017.09.010.

Chapter 5

KLF13 is a new candidate gene for the regulation of body fat distribution

5.1. Abstract

Background

In 2015 Shungin et al. reported 49 loci associated with waist-to hip-ration (WHR), suggesting that they might be involved in the regulation of body FD. One of these loci carries the rs8042543 in *KLF13*. To better understand its role in the regulation of body fat composition, *KLF13* mRNA expression was measured in paired samples of human subcutaneous (ScAT) and visceral (VAT) adipose tissue from metabolically well-characterized subjects. Furthermore, the rs8042543 variant was genotyped in all study participants. Finally, *Klf13* was silenced by siRNA in murine inguinal and epididymal preadipocytes to investigate the effect of *Klf13* on adipogenesis.

Results

The mRNA expression of *KLF13* was significantly higher in ScAT compared to VAT. The variant rs8042543 was significantly associated with WHR (adjusted for BMI), maximum adipocyte size in ScAT and VAT and with the subcutaneous *KLF13* mRNA expression. The *Klf13* siRNA mediated knockdown in murine inguinal and visceral preadipocytes showed moderate effects on the expression of *Pparg* and *Cebpb*.

Conclusion

The present data suggest a link between KLF13 and body FD, which might be driven by its regulatory role in adipocyte differentiation.

5.2. Introduction

In 2015 Shungin et al. reported a GWAS showing 49 loci associated with WHR, which carry potential candidate genes influencing the body FD [1]. Most of the candidate genes are implicated in adipose tissue (AT) pathways. For instance PPARG and CCAAT/enhancer binding protein alpha (C/EBPA) are essential for adipocyte differentiation [2] and bone morphogenic protein 2 (BMP2) is crucial in mesenchymal stem cells fate towards adipogenesis or osteogenesis [3]. Moreover, a number of genes encoding transcriptional regulators such as KLF13 seem to map to the WHR-associated loci. Adipogenesis contributes to specific fat depot mass and might thereby influence body FD. PPARG and C/EBPs are master regulators of these processes but many other factors play an important role in adipocyte differentiation, including members of the KLF family [4].

The KLF family members share homology in their Cys2/His2 zinc finger-DNA binding domains allowing them to bind to GC-rich sequences and related CT or CACCC boxes in regulatory regions of target genes [5,6]. 17 members have been identified in mammalian cells and classified as KLF1 - KLF17 [7]. It is known that multiple KLF's involved in the regulation of the same metabolic processes although they can also have opposing effects. One example is the adipogenesis regulation; *KLF2* is required for the maintenance of preadipocytes and is downregulated during the differentiation [5]. On the other hand *KLF5* and *KLF15* serve as positive regulators of adipogenesis [8,9]. KLF13 was first identified as an activator of RANTES (CCL5) expression, a chemokine involved in the activated T-cell response [10]. Jiang et al. showed that the *Klf13* mRNA expression increased during differentiation in porcine adipocytes [11]. In porcine adipocytes KLF13 binds directly to *PPARG* and promotes the adipogenesis through this pathway.

Based on the GWAS by Shungin et al., *KLF13* is a candidate gene for the body FD [1]. Moreover, there is a strong evidence that KLF family members including *KLF13* are involved in adipogenesis [5,11]. To better understand its role in the regulation of body fat composition, I measured *KLF13* mRNA expression in paired samples of human ScAT and VAT from metabolically well-characterized subjects. Furthermore, I genotyped the rs8042543 variant in all study participants to assess its possible link to the mRNA expression pattern. Finally, I employed siRNA mediated knockdown of *Klf13* in murine inguinal and epididymal preadipocytes to investigate its effect on adipogenesis.

5.3. Materials and Methods

5.3.1. Subjects

KLF13 mRNA expression was measured in paired ScAT and VAT samples obtained from 463 German subjects. The samples were taken from individuals undergoing different types of abdominal surgeries. All patients gave their written informed consent and the study was approved by the ethical committee of the University of Leipzig. The mean age of the cohort was 48±13 years and the mean BMI was 46.0±11.9 kg/m². In the analysis 211 subjects (mean age 47±15 years, mean BMI 42.1±13.0) with normal glucose tolerance (NGT) and 212 subject (mean age 50±11 years, mean BMI 50.1±9.7) with type 2 diabetes (T2D) were included. Characterization of the study participants including anthropometric measurements, (weight, height, WHR), body fat analysis using bioimpedance analyses or dual-energy X-ray absorptiometry and metabolic parameters such as fasting plasma glucose and insulin, a 75 g oral glucose tolerance test (OGTT), HbA1c, lipoprotein-, triglyceride-, free fatty acid- and adipokine serum concentrations was performed as previously described [12,13]. Measurement of abdominal VAT and ScAT areas was performed using CT or MRI scans.

5.3.2. Measurement of *KLF13*

The human *KLF13* mRNA expression was measured by qRT-PCR using TaqMan Gene Expression Assay (Applied Biosystems, Darmstadt, Germany) and normalized to *HPRT1*. Total RNA was isolated from AT samples using the Qiacube System (Qiagen, Hilden, Germany), and 2 µg RNA were reverse transcribed with standard reagents (Life Technologies). Expression of *KLF13* and *HPRT1* mRNA were quantified by using the second derivative maximum method of the TaqMan Software (Applied Biosystems).

5.3.3. Genotyping of rs8042543

Genomic DNA was extracted from blood using the QuickGene DNA whole blood kit (Kurabo, Japan). Genotyping of rs8042543 (C/T), which is located in the intron 2 of *KLF13*, was performed using the TaqMan SNP Genotyping assay (Applied Biosystems; C_2911174_10). A random ~5 % selection of the sample were re-genotyped for all SNPs to assess genotyping reproducibility; all genotypes matched initial designated genotypes.

5.3.4. Cell culture

For cell culture experiments SV40 T-antigen immortalized murine preadipocytes isolated from inguinal and epididymal white AT of C57BL/6 mice were used [14]. The cells were kindly

provided by Prof. Dr. Johannes Klein and Dr. Nina Perwitz from the University of Lübeck. The murine inguinal and epididymal preadipocytes correspond to human subcutaneous and visceral preadipocytes and were therefore used for the further experiments. Both cell types were grown in growth medium (DMEM high; 20 % FBS) in humidified atmosphere of 5 % CO_2 at 37 °C. The medium was normally changed every second day. At a confluence of 80-90 %, the cells were harvested and transfected with siRNA. When the cells became 100 % confluent the adipocyte differentiation was induced by changing medium to induction medium containing 0.5 mM IBMX, 2 µg/ml dexamethasone, 0.125 mM indomethacin, 20 mM insulin and 1 nM T3 for 48 h. Subsequently cells were additionally differentiated in differentiation medium (growth medium, 20 nM insulin and 1 nM T3) for six days.

5.3.5. siRNA knockdown of *Klf13*

The cells were transfected using the Neon Transfection system (Invitrogen). Cells were detached using trypsin and cell density was adjusted to $1x10^6$ cells per 100 µL. 10 µl of 20 mM siRNA (GE Dharmacon, Freiburg, Germany) were added to cell suspension and transfection was carried out with two 20 ms pulses of 1300 V. Three different preparations were used: *Klf13*-siRNA (ON-TARGETplus siRNa-SMARTpool Mouse Klf13 [50794]), non- targeting Control siRNA (ON TARGETplus Non-targeting Control Pool) and *Gapdh*- siRNA (ON-TARGETplus Gapdh Control) as a positive control. Two transfections for every preparation were done. The treated cells were resuspended in growth medium and distributed on plates accordingly (Table 1). After 72 h the cells were 100 % confluent and induced for differentiation. This differentiation timeline was done in triplicate.

Table 1. Cell amount per well for different conditions

condition	Plate	Cell amount
RNA	12 well plate	80000 cells per well
AdipoRed measurement	96 well plate	4500 cells per well
Microscopy	24 well	40000 cells per well

5.3.6. Lipid staining

The intracellular lipid accumulation during the differentiation was measured by the AdipoRed™ assay (Lonza, Basel, CH). The cells were differentiated in 96 well plates and at the respective time point washed with PBS. Subsequently a mixture of 200 µl PBS ($+Ca^{2+}$,$+Mg^{2+}$, pH 7.4) and 5 µl AdipoRed was added to each well. The nuclei were stained with Hoechst (1µg/ml in MilliQ water) to normalize the AdipoRed signal. The fluorescence was measured in the FLUOstar OPTIMA (BMG LAPTECH) and the amount of

AdipoRed/Hoechst was analyzed subsequently. For microscopy the cells were also stained with AdipoRed™ at day eight. A mixture of 1ml PBS and 60 µl AdipoRed were added to each well of the 12 well plate.

5.3.7. RNA isolation and reverse transcriptase PCR (RT-PCR) analysis

The cells were treated with TRIzol® reagent (Invitrogen) according to the manufacturer´s instructions. To optimize the quality of RNA the RNase-free DNase Set from Qiagen and subsequently the RNeasy MinElute Cleanup Kit from Qiagen were used. 1 µg total RNA was reverse transcribed using SuperScript III First Strand Synthesis SuperMix for qRT-PCR (Thermo Fisher Scientific). cDNA was amplified and measured by qPCR using the TaqMan PCR system with selective TaqMan gene assays (*KLF13*[human]- Hs00429818_m1; *HPRT1*[human]-Hs01003267_m1; *Klf13*[mouse]-Mm00727486_s1; *Hprt1*[mouse]-Mm01545399_m1; *Pparg* [mouse]-Mm01184322_m1; *Gapdh* [mouse]-Mm99999915_g1; *Leptin* [mouse]-Mm00434759_m1; *Cebpb* [mouse]-Mm00843434_s1). Specific mRNA expression was calculated relative to *Hprt1* and was quantified by efficiency based calculation of relative gene expression as described by *Pfaffl* [15].

5.4. Results and Discussion

5.4.1. mRNA expression levels in AT correlate with metabolic traits and with rs8042543

KLF13 showed significantly lower mRNA levels in ScAT compared to VAT in analysis with the total cohort and also in the subgroup of subjects with normal glucose tolerance (Figure 1A). In addition, the subjects with obesity had higher *KLF13* mRNA expression levels in VAT than lean subjects (Figure 1B).

Figure 1. The mRNA expression of *KLF13* in ScAT and VAT. A The expression levels are shown in the total cohort, in subjects with normal glucose tolerance (NGT) and in subjects with type 2 diabetes (T2D). *** $p < 0.001$. **B** The KLF13 mRNA expression in both adipose tissues in comparison of lean (BMI< 25 kg/m²) and obese (BMI> 30 kg/m²) subjects. * $p < 0.05$

The mRNA expression of *KLF13* in both ATs correlated significantly with age. In VAT no further correlations were found. A significant correlation for the ScAT with weight (p=0.011) and BMI (p=0.013) (Table 2) was identified.

Table 2. Correlation of *KLF13* mRNA expression in ScAT and VAT with metabolic traits

KLF13	**Subcutaneous AT**			**Visceral AT**		
Trait	R	unadj. *p*-value	adj. *p*-value	R	unadj. *p*-value	adj. *p*-value
Age (years)	-0.143	**0.037**		-0.165	**0.017**	
Weight (kg)	-0.082	0.235	**0.011**[#]	0.128	0.065	0.451
BMI (kg/m²)	-0.068	0.322	**0.013**[#]	0.120	0.084	0.578[#]
Waist (cm)	-0.245	0.114	0.184[#]	0.153	0.332	0.386[#]
WHR	-0.302	0.223	0.334[#]	0.253	0.327	0.405[#]
% Body fat	0.167	0.302	0.856[#]	0.246	0.127	0.291[#]
Vis fat (cm²)	0.080	0.794	0.784[#]	-0.246	0.440	0.525[#]
Sc fat (cm²)	0.096	0.756	0.783[#]	-0.016	0.960	0.993[#]
FPG (mmol/l)	-0.166	**0.020**	0.117	-0.033	0.646	0.944
FPI (mmol/l)	-0.537	**7.01×10^{-5}**	0.147	-0.098	0.501	0.644
oGTT 2h (mmol/l)	-0.001	0.996	0.620	-0.039	0.886	0.590
GIR (µmol/kg/min)	-0.177	0.581	0.768	0.190	0.554	0.665
HbA1c (%)	0.125	0.350	0.083	0.073	0.590	0.516
Chol (mmol/l)	0.024	0.780	0.624	0.068	0.426	0.449
HDL (mmol/l)	0.142	0.154	0.443	-0.027	0.788	0.958
LDL (mmol/l)	-0.055	0.581	0.888	0.088	0.377	0.355
TG (mmol/l)	-0.021	0.805	0.675	0.044	0.604	0.548
FFA (mmol/l)	-0.195	0.566	0.112	-0.171	0.616	0.266
Leptin (ng/ml)	-0.385	0.103	0.910	-0.427	0.077	0.057
Adiponectin (µg/ml)	0.066	0.789	**0.048**	0.304	0.219	0.394
IL6 (pg/ml)	-0.390	0.236	0.133	-0.280	0.434	0.487
Vis mean (cm²)	0.083	0.582	0.805[#]	0.000	0.998	0.811[#]
Sc mean (cm²)	0.142	0.346	0.601[#]	-0.048	0.752	0.429[#]
Vis max (cm²)	0.107	0.478	0.955[#]	-0.005	0.976	0.669[#]
Sc max (cm²)	0.209	0.164	0.390[#]	-0.139	0.356	0.275[#]

The data are given as mean± standard deviation, p-values are adjusted for sex, age and BMI,[#] p-value adjusted for sex and age, bold p-values indicate statistical significance.

R- correlation coefficient, AT- adipose tissue, BMI- body mass index, WHR- waist-to-hip ratio, TG- triglycerides, IL-6- interleukin 6, HbA1c- glycohemoglobin, oGTT- oral glucose tolerance test, FPG- fasting plasma glucose, FPI- fasting plasma insulin, GIR- glucose infusion rate during the steady state of an euglycemic hyperinsulinemic clamp, HDL- high density lipoprotein cholesterol, LDL- low density lipoprotein cholesterol , FFA- free fatty acids, Sc- subcutaneous, Vis- visceral, Vis mean- mean adipocyte size in visceral adipose tissue, Sc mean- mean adipocyte size in subcutaneous adipose tissue, Vis max- maximum adipocyte size in visceral adipose tissue, Sc max- maximum adipocyte size in subcutaneous adipose tissue.

Moreover, the *KLF13* SNP rs8042543 was associated with WHR (p=0.035 adj. sex, age) and the reported association with WHR (p=0.044 adj. BMI) was confirmed as well [1]. However, whereas the ancestral allele C was associated with higher WHR in the study by Shungin et al., in my work the C allele was related to lower WHR. This inconsistent effect direction might be attributed to the character of study populations, with an obvious tendency towards extreme obesity in the present study cohort, which might significantly bias the measurement of WHR. Furthermore, I found an association of the T allele with higher maximum size of adipocytes in ScAT (p= 0.001) and VAT (p= 0.044) (Table 3). Finally, in a subgroup of individuals with both mRNA expression and genotyping data (N=79) I identified a significant association (p=0.042, Figure 2) between the *KLF13* mRNA expression in ScAT and the SNP. Homozygous carriers of the minor allele T showed higher *KLF13* mRNA expression level, suggesting rs8042543 SNP effects the *KLF13* gene regulation in ScAT. In databases like RegulomeDB [16], HaploReg [17] or GTex [18] no eQTL or link to other transcription factors have been reported so far.

Table 3. Association of rs8042543 with metabolic traits

	rs8042543			
Trait	CC	CT	TT	adj. p-value
BMI (kg/m²)	40.9±13.3	41.1±13.6	40.4±15.1	0.704[#]
% body fat	42.0±11.9	43.8±11.2	42.5±11.7	0.848[#]
Weight (kg)	117.4±39.3	121.1±46.5	114.3±44.9	0.555[#]
Waist (cm)	112.3±26.9	118.3±29.7	120.0±35.2	0.084[#]
Hip (cm)	126.8±30.5	131.4±30.3	127.4±34.9	0.434[#]
WHR	0.88±0.09	0.90±0.08	0.94±0.13	**0.035[#]**
WHRadjBMI				**0.044**
FPG (mmol/l)	5.3±0.8	5.2±0.8	5.2±0.8	0.543
FPI (mmol/l)	82.0±67.9	109.1±75.4	83.5±72.5	0.115
GIR µmol/kg/min)	93.0±22.1	88.2±24.6	91.0±16.7	0.438
HbA1c (%)	5.54±0.41	5.46±0.46	5.49±0.52	0.946
Cholesterol (mmol/l)	4.8±0.9	4.7±1.0	4.7±1.2	0.727
HDL (mmol/l)	1.3±0.3	1.3±0.4	1.4±0.6	0.608
LDL (mmol/l)	3.0±0.8	3.0±1.0	2.9±1.0	0.346
TG (mmol/l)	1.3±0.6	1.2±0.5	1.2±0.6	0.329
FFA (mmol/l)	0.36±0.32	0.39±0.33	0.52±0.43	0.998
Leptin (ng/ml)	9.1±4.9	9.2±4.7	8.1±5.5	0.839
Adiponectin (µg/ml)	36.1±24.7	35.0±18.6	42.9±31.6	0.208
Vis fat (cm²)	171.5±129.6	195.8±153.2	192.4±171.5	0.409[#]
Sc fat (cm²)	1014.0±836.0	1069.8±800.9	1044.7±923.3	0.234[#]
ln*KLF13* sc	5.5±1.1	5.7±1.3	6.7±0.3	**0.042**
ln*KLF13* vis	0.5±0.9	0.5±0.4	0.9±0.3	0.947

Table continued on the next page

	rs8042543			
Trait	CC	CT	TT	adj. *p*-value
Vis mean (cm²)	119.1±18.0	117.4±23.3	117.7±16.5	0.596[#]
Sc mean (cm²)	122.7±17.1	124.5±20.4	127.0±21.0	0.534[#]
Vis max (cm²)	199.9±32.0	218.1±85.6	244.0±111.7	**0.044**[#]
Sc max (cm²)	198.7±46.2	227.0±93.1	259.9±123.1	**0.001**[#]

The data are given as mean ± standard deviation, p-values are adjusted for sex, age and BMI,[#] p-value adjusted for sex and age, bold p-values indicate statistical significance.

AT- adipose tissue, BMI- body mass index, WHR- waist-to-hip ratio, TG- triglycerides, IL-6- interleukin 6, HbA1c- glycohemoglobin, oGTT- oral glucose tolerance test, FPG- fasting plasma glucose, FPI- fasting plasma insulin, GIR- glucose infusion rate during the steady state of an euglycemic hyperinsulinemic clamp, HDL- high density lipoprotein cholesterol, LDL- low density lipoprotein cholesterol , FFA- free fatty acids, Sc- subcutaneous, Vis- visceral, Vis mean- mean adipocyte size in visceral adipose tissue, Sc mean- mean adipocyte size in subcutaneous adipose tissue, Vis max- maximum adipocyte size in visceral adipose tissue, Sc max- maximum adipocyte size in subcutaneous adipose tissue.

Figure 2. Association of variant rs8042543 with *KLF13* expression in human ScAT and VAT. Scatter dot plots represent KLF13 mRNA expression in ScAT (**A)** and VAT **(B)** grouped by genotype for rs8042543. Indicated are p-values of linear regression analysis using the additive model of inheritance and adjusted for sex, age and BMI.

5.4.2. *Klf13* knockdown affects the mRNA expression of *Cebpb* and *Pparg* in adipocytes

The siRNA mediated knockdown of *Klf13* appeared to be more efficient in the epididymal cells (downregulated to 25 %) than in the inguinal cells (38 %; Figure 3). In the inguinal cells the *Klf13* mRNA expression rapidly recovered at day six. In the epididymal cells the *Klf13* mRNA levels remained lower during the differentiation compared to the non-targeting control (Figure 3).

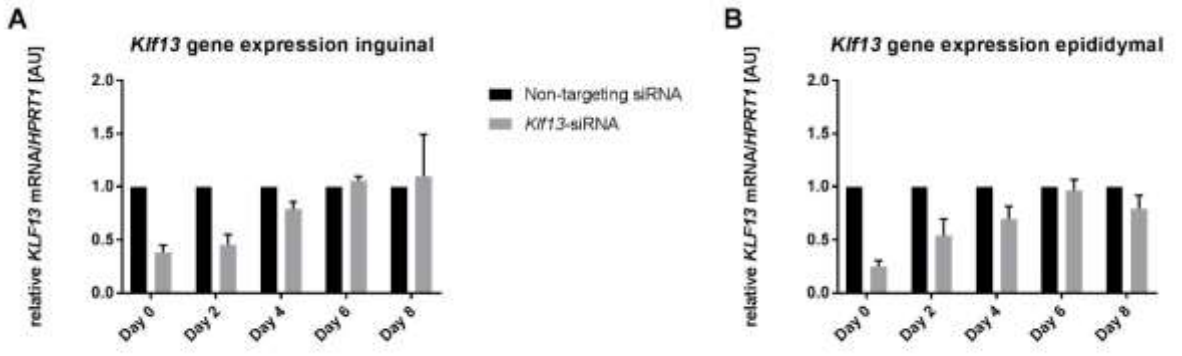

Figure 3. The mRNA expression of *Klf13* after *Klf13*-siRNA knockdown during adipogenesis. Relative *Klf13* mRNA expression are plotted against time of differentiation in murine inguinal (**A**) and epididymal (**B**) cells. *Klf13* mRNA level was normalized to *Hprt1* as a reference gene and is presented relative to gene expression in non-targeting control cells.

In both fat cell types the control as well as *Klf13* siRNA knockdown cells were differentiated (Figure 4) and filled with lipids as quantified by AdipoRed/Hoechst (Figure 5). However, compared to control cells, *Klf13* siRNA treated cells did not differ in the amount of the AdipoRed in inguinal or epididymal adipocytes.

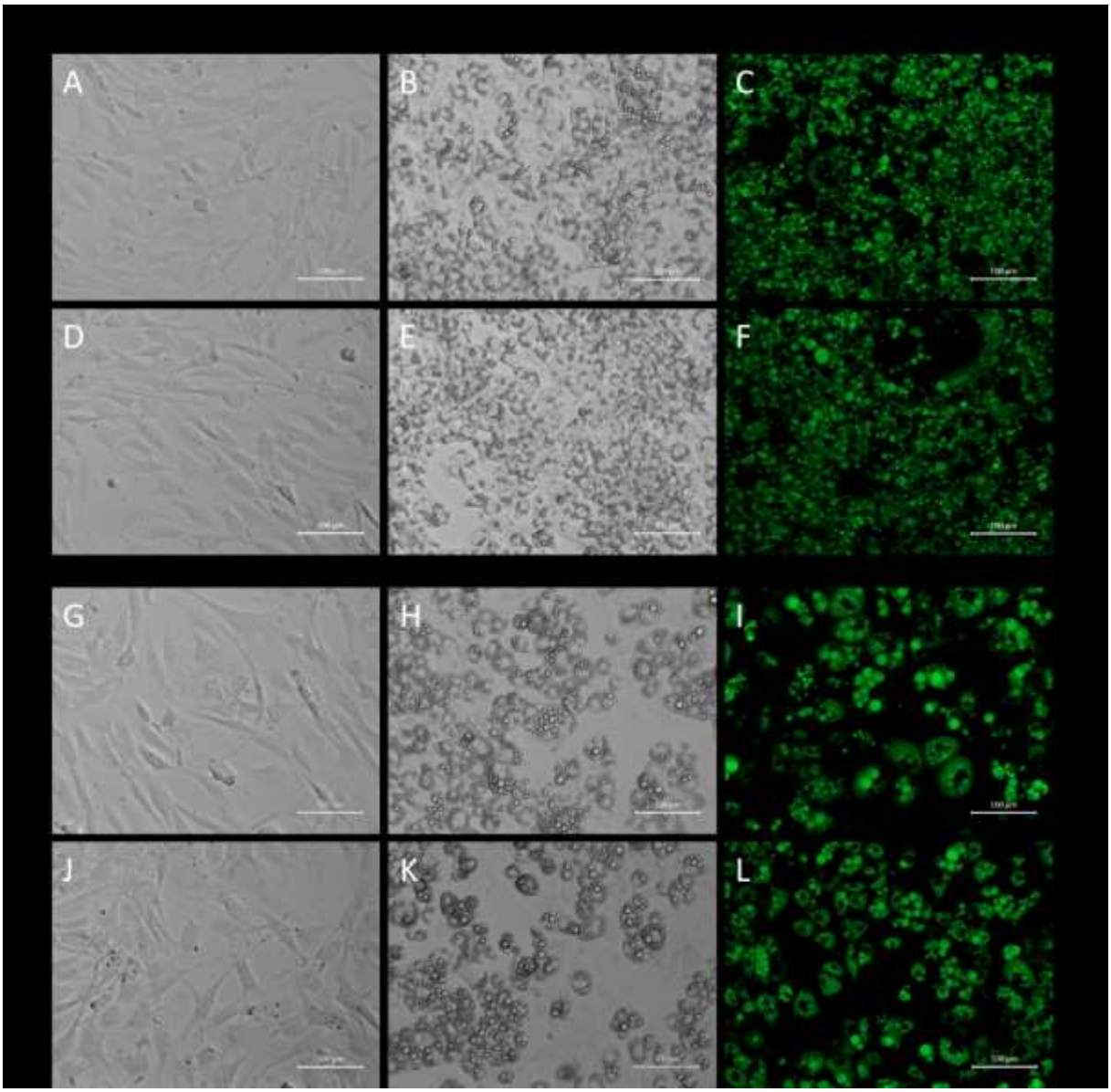

Figure 4. Microscopy of inguinal and epididymal cells in course of differentiation after transfection with siRNA. Epididymal (**A-F**) and inguinal (**G-L**) preadipocytes were transfected with *Klf13* siRNA (**D-F** and **J-L**) or for control with non-targeting control siRNA (**A-C** and **G-I**). At the day of induction of differentiation (**A, D, G** and **J**) and at day four (**B, E, H** and **K**) bright field pictures were made under the microscope (10 x magnification). At day eight lipids were stained with AdipoRed® and fluorescence images were taken (**C, F, I** and **L**; 10 x magnification, FITC channel; exposure time 1000 ms).

Figure 5. AdipoRed signal during the differentiation after transfection with siRNA. Relative fluorescence signal of AdipoRed normalized to signal of Hoechst during the differentiation in inguinal (**A**) and epididymal (**B**) adipocytes.

PPARγ and CEBPβ are transcription factors representing key regulators of the adipogenesis. Therefore, I measured the mRNA expression of these genes in *Klf13* knockdown and control cells. In the inguinal cells the *Pparg* expression was significantly higher in *Klf13* knockdown cells compared to the control cells on day zero and day six (Figure 6 A). Albeit not statistically significant, also on the other days of differentiation the mRNA levels of *Pparg* remained higher in knockdown cells. In epididymal adipocytes the mRNA expression of *Pparg* was significantly higher in *Klf13* knockdown cells compared to control cells at day six (Figure 6 B). The leptin mRNA expression showed no differences between treated cells and control cells neither in inguinal nor epididymal adipocytes (Figure 7 A-B). The mRNA expression of *Cebpb,* was found to be significantly higher in *Klf13* knockdown cells compared to control cells during the differentiation in both cell lines (Figure 7 C-D). In porcine adipocytes *PPARG* has been shown to be the target gene of *KLF13* [11]. Accordingly, it was speculated that *Pparg* is also the target gene for *Klf13* in murine adipocytes, but based on the present results it seems that contrary to the effects on *Cebpb* mRNA expression, *Klf13* knockdown does not influence the *Pparg* expression during murine adipocyte differentiation.

Figure 6. The mRNA expression of *Pparg* after *Klf13*-siRNA knockdown during the adipogenesis. Relative *Pparg* mRNA expression are plotted against time of differentiation in murine inguinal (**A**) and epididymal (**B**) cells. *Pparg* mRNA level was normalized to *Hprt1* as a reference gene and is presented relative to gene expression in non-targeting control cells. **p<0.01; ***p<0.001

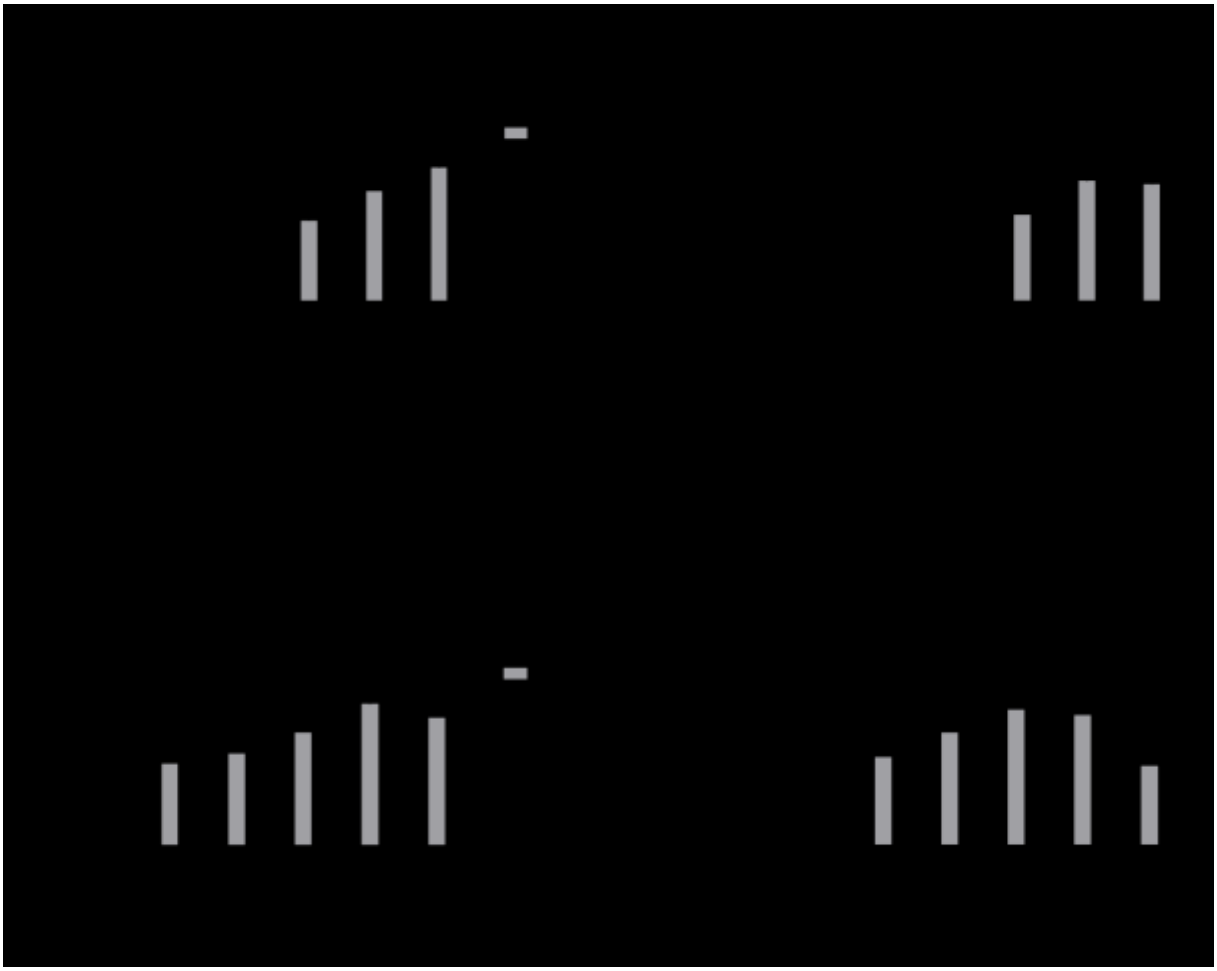

Figure 7 . The mRNA expression of *Leptin* and *Cebpb* after *Klf13*- siRNA knockdown during adipogenesis. Relative *Leptin* and *Cebpb* mRNA expression are plotted against time of differentiation in murine inguinal (**A**) and epididymal (**B**) cells. *Leptin* and *Cebpb* mRNA level was normalized to *Hprt1* as a reference gene and is presented relative to gene expression in non-targeting control cells. *** p<0.001

5.5. Summary

In the present study, I measured in paired samples of ScAT and VAT the mRNA expression of *KLF13* as a plausible candidate gene involved in the regulation of body FD. I show depot specific mRNA levels of *KLF13* with significantly higher mRNA expression in VAT compared to ScAT. Moreover, the subcutaneous *KLF13* mRNA levels correlate with weight and BMI. Although inconsistent in allele effect direction, I also confirm the reported association of the variant rs8042543 with WHR[1]. Additionally I report a significant association between rs8042543 and the maximum size of adipocytes in both ScAT and in VAT. In a subgroup of subjects (N=79), the rs8042543 T-allele is significantly associated with a higher mRNA expression of *KLF13* in ScAT.

It was shown by Jiang et al. that in porcine adipocytes, *KLF13* has an influence on adipogenesis through the activation of *PPARG* [11] . SiRNA mediated knockdown of *Klf13* in murine inguinal and epididymal preadipocytes in the present study did not result in differences in the AdipoRed signal (stain the intracellular lipid droplets). The mRNA expression of *Pparg* and *Cebpb*, two master regulators of the adipogenesis, were higher in *Klf13* knockdown cells compared to control cells at some time points of the differentiation.

In conclusion, this work suggests a relationship between the AT specific expression of *KLF13* and body FD. Although further experiments with isolated human adipocytes are inevitable to get more insights into the role of these genes in the regulation of body FD, my findings strongly suggest that the link with FD might be mediated by the functional role of KLF13 in adipogenesis.

5.6. References

1 Shungin D, Winkler TW, Croteau-Chonka DC, Ferreira T, Locke AE, Mägi R *et al.* New genetic loci link adipose and insulin biology to body fat distribution. *Nature* 2015; **518**: 187–196; doi:10.1038/nature14132.

2 Nakagami H. The Mechanism of White and Brown Adipocyte Differentiation. *Diabetes & Metabolism Journal* 2013; **37**: 85–90; doi:10.4093/dmj.2013.37.2.85.

3 Li H, Li T, Wang S, Wei J, Fan J, Li J *et al.* miR-17-5p and miR-106a are involved in the balance between osteogenic and adipogenic differentiation of adipose-derived mesenchymal stem cells. *Stem cell research* 2013; **10**: 313–324; doi:10.1016/j.scr.2012.11.007.

4 Wu Z, Wang S. Role of kruppel-like transcription factors in adipogenesis. *Developmental biology* 2013; **373**: 235–243; doi:10.1016/j.ydbio.2012.10.031.

5 Pearson R, Fleetwood J, Eaton S, Crossley M, Bao S. Krüppel-like transcription factors: a functional family. *The international journal of biochemistry & cell biology* 2008; **40**: 1996–2001; doi:10.1016/j.biocel.2007.07.018.

6 Kaczynski J, Cook T, Urrutia R. Sp1- and Krüppel-like transcription factors. *Genome biology* 2003; **4**: 206.

7 Suske G, Bruford E, Philipsen S. Mammalian SP/KLF transcription factors: bring in the family. *Genomics* 2005; **85**: 551–556; doi:10.1016/j.ygeno.2005.01.005.

8 Oishi Y, Manabe I, Tobe K, Tsushima K, Shindo T, Fujiu K *et al.* Krüppel-like transcription factor KLF5 is a key regulator of adipocyte differentiation. *Cell metabolism* 2005; **1**: 27–39; doi:10.1016/j.cmet.2004.11.005.

9 Mori T, Sakaue H, Iguchi H, Gomi H, Okada Y, Takashima Y *et al.* Role of Krüppel-like factor 15 (KLF15) in transcriptional regulation of adipogenesis. *The Journal of biological chemistry* 2005; **280**: 12867–12875; doi:10.1074/jbc.M410515200.

10 Zhou M, McPherson L, Feng D, Song A, Dong C, Lyu S-C *et al.* Kruppel-like transcription factor 13 regulates T lymphocyte survival in vivo. *Journal of immunology (Baltimore, Md. : 1950)* 2007; **178**: 5496–5504.

11 Jiang S, Wei H, Song T, Yang Y, Zhang F, Zhou Y *et al.* KLF13 promotes porcine adipocyte differentiation through PPARγ activation. *Cell & bioscience* 2015; **5**: 28; doi:10.1186/s13578-015-0016-z.

12 Blüher M, Klöting N, Wueest S, Schoenle EJ, Schön MR, Dietrich A *et al.* Fas and FasL expression in human adipose tissue is related to obesity, insulin resistance, and type 2 diabetes. *The Journal of clinical endocrinology and metabolism* 2014; **99**: E36-44; doi:10.1210/jc.2013-2488.

13 Klöting N, Fasshauer M, Dietrich A, Kovacs P, Schön MR, Kern M *et al.* Insulin-sensitive obesity. *American journal of physiology. Endocrinology and metabolism* 2010; **299**: E506-15; doi:10.1152/ajpendo.00586.2009.

14 Wagner IV, Perwitz N, Drenckhan M, Lehnert H, Klein J. Cannabinoid type 1 receptor mediates depot-specific effects on differentiation, inflammation and oxidative metabolism

in inguinal and epididymal white adipocytes. *Nutrition & diabetes* 2011; **1**: e16; doi:10.1038/nutd.2011.12.

15 Pfaffl MW. A new mathematical model for relative quantification in real-time RT-PCR. *Nucleic acids research* 2001; **29**: e45.

16 Boyle AP, Hong EL, Hariharan M, Cheng Y, Schaub MA, Kasowski M *et al.* Annotation of functional variation in personal genomes using RegulomeDB. *Genome research* 2012; **22**: 1790–1797; doi:10.1101/gr.137323.112.

17 Kundaje A, Meuleman W, Ernst J, Bilenky M, Yen A, Heravi-Moussavi A *et al.* Integrative analysis of 111 reference human epigenomes. *Nature* 2015; **518**: 317–330; doi:10.1038/nature14248.

18 The Genotype-Tissue Expression (GTEx) project. *Nature genetics* 2013; **45**: 580–585; doi:10.1038/ng.2653.

Chapter 6 Zusammenfassung der Arbeit

Dissertation zur Erlangung des akademischen Grades Dr. rer. nat.

Functional significance of genes associated with fat distribution

Eingereicht von

Jacqueline Herold (geb. Krüger)

Angefertigt an

Universität Leipzig, IFB AdiposityDiseases

Betreut von

Professor Dr. rer. med. Peter Kovacs

Dr. rer. nat. Dorit Schleinitz

Eingereicht im

Februar 2019

Obesity is a growing health problem characterized by a variety of related complications like fatty liver disease, T2D and cardiovascular diseases. One of the major organs relevant for obesity is the AT, which is not only a passive reservoir for fat. In the last decades it has been shown that AT is an endocrine organ located in different sites of the body. The AT is mainly distributed in two depots, the ScAT and VAT. It is well acknowledged that fat stored prominently in VAT makes subjects more prone for metabolic complications. In the clinical practice waist circumference and WHR are common measures of the regional FD but the gold standard are the imaging techniques such as CT or whole body MRI scans. It is also known that obesity as well as FD are controlled by genetic factors including single nucleotide

polymorphisms, deletions or insertions of nucleotides or sequences; but also the altered mRNA expression or epigenetic modifications like DNA methylation play a role. There is clear evidence that the majority of obesity cases have a polygenic character. This thesis aims to identify and characterize novel candidate genes to gain further insights into different types of obesity and into causes and consequences of adverse FD, including related comorbidities, which are described more in detail in **Chapter 1**.

Chapter 2 deals with the first candidate gene of this thesis – the *hypoxia inducible factor 3 subunit alpha* (*HIF3A*). *HIF3A* was recently shown in an EWAS as a plausible candidate gene whose DNA methylation and mRNA expression in ScAT strongly correlated with BMI. In this study, I measured the mRNA expression of *HIF3A* in paired samples of ScAT and VAT and correlated these with parameters of obesity and FD. I found higher mRNA levels in ScAT compared to VAT, which was true for both AT and isolated adipocytes. I confirmed the correlation of *HIF3A* expression levels with BMI in ScAT and showed for the first time the same pattern in VAT. The mRNA expression of *HIF3A* in both fat depots correlated with different parameters of obesity and FD like BMI, waist and WHR. In subgroups of individuals I investigated the effects of reported *HIF3A* genetic variants on its mRNA expression in AT and methylation on reported CpG-sites (*cg22891017*). The methylation levels in VAT correlated with hip, subcutaneous fat mass, CT ratio and adiponectin levels. For the investigated cohort I found higher HIF3A methylation levels in VAT compared to ScAT, which is in accordance with mRNA expression that was found to be lower in VAT compared to ScAT. Therefore, a regulation of gene expression through DNA methylation could be hypothesized. The *HIF3A* variant rs8102595 was associated with the methylation levels in ScAT as reported by Dick *et al*., but I also observed a significant association between the variant and the methylation levels in VAT. Furthermore, I showed significant associations of the variant with HDL, glucose infiltration rate and maximum fat cell size of ScAT. For the second reported variant rs3826795 I suggest its effects on the methylation level, but also on the total cholesterol and the mean fat cell size of VAT.

In conclusion, my data not only support previously reported results, but also reveal that the mRNA expression and the methylation level of *HIF3A* cg22891017 are fat depot specific and related to obesity and AT dysfunction. In the meantime, other groups have replicated my results in their studies, thus demonstrating that *HIF3A* is an attractive candidate involved in the regulation of AT function, and is potentially providing a link to metabolic complications of obesity and FD.

GWAS/EWAS became possible with the development of high-throughput DNA/RNA technologies as an approach to identify new candidate loci. In 1998 Kovacs et al. identified a QTL for serum fasting insulin, TG and body weight in rats on chromosome 4, which carries the *zinc finger protein replication initiator 1* (*REPIN1*) gene. In the coming years different analyses in mice and rats showed that *Repin1* influences the lipid and glucose metabolism and turns out to be a candidate gene for obesity and related complications. In my study, presented in **Chapter 3**, I showed for the first time a strong relationship between genetic variants in *REPIN1* with metabolic traits in humans. *REPIN1* was sequenced (four exons, exon-intron boundaries, 5′ and 3′ UTRs) in 48 unrelated Caucasian subjects and the detected variants were summarized in eight L.D. groups. Additionally, a 12 bp deletion was found in exon 4. Eight so called tagging variants representing the L.D. groups and the 12 bp deletion were analyzed in two independent cohorts (Leipzig cohort and Sorb cohort). I found associations with traits related to obesity and glucose metabolism (e.g., total and low density lipoprotein cholesterol, serum TG, glucose infiltration rate and HbA1c). The 12 bp deletion (rs3832490) is very rare, so that only heterozygote carriers were detected in the Leipzig cohort. The genotype-phenotype analyses revealed nominal associations with % body fat, 120 minute plasma glucose levels and the maximums size of adipocytes in VAT and ScAT. In a second independent cohort, only three homozygous carriers of the 12 bp deletion have been identified and they had lower fasting plasma glucose and HOMA B, which is consistent with the lower risk for T2D, which was observed in a case-control study. These three subjects also had a lower BMI, WHR, % body fat and serum TG but on the other hand they had higher HDL, LDL and total cholesterol levels. Based on these interesting findings we investigated the 12 bp deletion in HepG2 cells. The HepG2 cells were transfected with plasmids carrying the *REPIN1* sequence with or without the 12 bps and we analyzed the glucose and lipid metabolism. We showed that cells transfected with the *REPIN1* 12 bp deletion had more lipid droplets and an higher mRNA expression of transcription factors such as *peroxisome proliferator activated receptor α* (*PPARA*), *PPARG-Isoform 2* and *sterol regulatory element binding protein 1c* (*SREBP-1c*) as compared to the wildtype transfected cells. Furthermore, HepG2 cells transfected with this *REPIN1* variant also had significantly higher mRNA expression levels for *fatty acid transport protein 4* (*FATP4*) and *CD36*, whereas *apolipoprotein M (APOM*) was significantly downregulated in these cells and the glycerol levels were twice as high as in the wildtype transfected cells. Further, the glucose transporters were influenced by the 12 bp deletion so that the mRNA expression of *glucose transporter protein 2 (GLUT2)* was higher and more GLUT2 positive cells were observed in this case. These findings suggest that genetic variation in *REPIN1,* especially the

12 bp deletion (rs3832490), may contribute to changes in parameters of glucose and lipid metabolism, most likely due to specific *REPIN1* genotype related regulation of target gene expression in glucose metabolism, insulin sensitivity, fatty acid transport and adipogenesis.

Dissecting the causal gene(s)/variant(s) in loci shown to be associated with diseases or complex traits remains a major challenge. In the last decade, the *FTO* locus has been studied extensively, however the molecular mechanisms underlying the reported associations are still not fully understood. Recent studies suggest that the BMI-associated variants in *FTO* not only affect the FTO itself, but also the nearby genes like *iroquios homeobox 3 (IRX3)* and *IRX5*. Therefore, I measured the mRNA expression of *IRX3* and *IRX5* in paired samples of VAT and ScAT and correlated these with parameters related to obesity and lipid and glucose metabolism. The results are summarized in **Chapter 4**. Although I did not find fat depot specific mRNA expression for *IRX3*, the mRNA expression of *IRX5* was significantly higher in ScAT compared to VAT. Moreover, the subcutaneous mRNA levels of *IRX3* were significantly correlated with weight and BMI. The correlation with waist, leptin and interleukin 6 levels, however, did not withstand adjustments for sex, age and BMI. The visceral mRNA expression of *IRX3* correlated with weight, BMI and waist, and the visceral *IRX5* mRNA expression correlated with weight, BMI, waist, % body fat and fasting plasma glucose. However, none of these correlations withstood the adjustments for adequate covariates. The obesity SNP rs8050136 at *FTO* was associated with weight, waist and hip, but no significant association with the mRNA expression of *IRX3* and *IRX5* was observed. In summary, my data demonstrated for the first time associations of *IRX3* with obesity related traits as well as a depot specific mRNA expression of *IRX5*, thus supporting the role of these genes in the pathophysiology of obesity.

Multiple GWAS uncovered a number of loci, which are associated with WHR. One of them, *KLF13*, was analyzed as described in **Chapter 5**. The *KLF13* mRNA expression was higher in VAT compared to ScAT. The mRNA expression in both AT correlated significantly with age and additionally the *KLF13* levels in ScAT correlated with weight and BMI. I confirmed the reported association between rs8042543 and WHR and showed that carriers with the minor allele T had higher maximum size of adipocytes in ScAT and VAT and correlated with higher mRNA expression of *KLF13* in ScAT as well. In further cell culture experiments I transfected inguinal and epididymal preadipocytes with *Klf13* siRNA and NTC siRNA as control and differentiated these to adipocytes. The *Klf13* knockdown cells showed no significantly different AdipoRed signal compared to control cells. However, at specific timepoints during the differentiation of the preadipocytes, there were significantly higher mRNA expression of *Pparg*

and *Cebpb* in *Klf13* siRNA treated cells, which are the main regulators of the adipogenesis, suggesting the role of Klf13 in the adipogenesis.

In summary, the above mentioned studies added successfully further pieces to the puzzle of polygenic obesity, contributing to better understanding of the role of genetic and epigenetic factors involved in FD distribution and of the link between obesity and its metabolic sequelae. I demonstrated that various approaches can be employed to identify novel candidate genes for FD and obesity. The elucidation of the involved pathways and processes is now the next big challenge, which was also addressed in my studies. *HIF3A* was initially identified in an EWAS for the trait BMI and my data suggested that this gene is involved in AT dysfunction via epigenetic regulation of its expression. For *REPIN1*, identified in a QTL analysis, I showed that its genetic variation has an impact on glucose and lipid metabolism, which in turn seems to influence Repin1 itself. However, as I showed in my study on *IRX3* and *IRX5* not only genes within the next proximity of the associated genetic variants but also structurally adjacent genes need to be considered for elucidation of causality behind the observed associations. Also reported loci from GWAS can be possible candidate genes and can help to find the link between AT dysfunction and adipogenesis as I showed in my study on *KLF13.*

Despite recent advances in our understanding of the obesity genetics, it is evident that many big challenges are yet to come in near future. For instance, we will need to understand how genes interact between each other as well as with the environment, which can ultimately shape the genes impact on a specific trait or disease. Better knowledge of mechanisms underlying or mediating gene-environment interaction will be essential to pave the road to the precision medicine, i.e. to tailor medical treatment to the individual characteristics of each patient.

Darstellung des eigenen Beitrags zur Publikation „Hypoxia- inducible factor 3A gene expression and methylation in adipose tissue is related to adipose tissue dysfunction“

Eigener Beitrag bei geteilter Erstautorenschaft einer Publikationspromotion

Der von Jacqueline Krüger geleistete wissenschaftliche Beitrag zu der Publikation „Hypoxia-inducible factor 3A gene expression and methylation in adipose tissue is related to adipose tissue dysfunction“ umfasst folgende Bereiche:

Datenbankpflege

Auswertung der Methylierungsdaten und anschließende Korrelationsanalysen

Genotypisierung des SNP rs3826795 und anschließende eQTL-Analysen sowie Assoziationen mit Methylierungsleveln and metabolischen Parametern

Korrelationsanalysen für subkutane und viscerale mRNA Expression von HIF3a mit Expression von Differenzierungsmarkern und metabolischen Paramentern

Schreiben des Manuskriptes und Erstellen und Bearbeitung von Graphen und Tabellen

Susanne Pfeiffer		Anna Maierhofer	
Yvonne Böttcher		Nora Klöting	
Nady El Hajj		Dorit Schleinitz	
Michael R. Schön		Arne Dietrich	
Mathias Fasshauer		Tobias Lohmann	
Miriam Dreßler		Michael Stumvoll	
Thomas Haaf		Matthias Blüher	
Peter Kovacs			

Darstellung des eigenen Beitrags zur Publikation „Metabolic effects of genetic variation in the human REPIN1 gene"

Eigener Beitrag bei geteilter Erstautorenschaft einer Publikationspromotion

Der von Jacqueline Krüger (Jacqueline Herold) geleistete wissenschaftliche Beitrag zu der Publikation „Metabolic effects of genetic variation in the human REPIN1 gene" umfasst folgende Bereiche:

- Genetische Analysen inklusive
  - DNA- Vorbereitung und Datenbankpflege
  - Genotypisierung der genetischen Varianten in REPIN1
  - Statistische Analysen, Assoziationsstudien mit metabolischen Parametern
- Anfertigung des Manuskriptes sowie Anfertigung und Bearbeitung von Graphen und Tabellen

Claudia Berger

Kerstin Weidle

Dorit Schleinitz

Anke Tönjes

Michael Stumvoll

Matthias Blüher

Peter Kovacs

Nora Klöting

Erklärung über die eigenständige Abfassung der Arbeit

Hiermit erkläre ich, dass ich die vorliegende Arbeit selbstständig und ohne unzulässige Hilfe oder Benutzung anderer als der angegebenen Hilfsmittel angefertigt habe. Ich versichere, dass Dritte von mir weder unmittelbar noch mittelbar eine Vergütung oder geldwerte Leistungen für Arbeiten erhalten haben, die im Zusammenhang mit dem Inhalt der vorgelegten Dissertation stehen, und dass die vorgelegte Arbeit weder im Inland noch im Ausland in gleicher oder ähnlicher Form einer anderen Prüfungs-behörde zum Zweck einer Promotion oder eines anderen Prüfungsverfahrens vorgelegt wurde. Alles aus anderen Quellen und von anderen Personen übernommene Material, das in der Arbeit verwendet wurde oder auf das direkt Bezug genommen wird, wurde als solches kenntlich gemacht. Insbesondere wurden alle Personen genannt, die direkt an der Entstehung der vorliegenden Arbeit beteiligt waren. Die aktuellen gesetzlichen Vorgaben in Bezug auf die Zulassung der klinischen Studien, die Bestimmungen des Tierschutzgesetzes, die Bestimmungen des Gentechnikgesetzes und die allgemeinen Datenschutzbestimmungen wurden eingehalten. Ich versichere, dass ich die Regelungen der Satzung der Universität Leipzig zur Sicherung guter wissenschaftlicher Praxis kenne und eingehalten habe.

....

Datum Unterschrift

Curriculum Vitae

Dipl. troph. Jacqueline Herold (née Krüger)

Date of Birth	21.04.1988
Nationality	German
Institutional Address	University of Leipzig, IFB Adiposity Diseases Division of Endocrinology, Nephrology and Rheumatology Liebigstraße 19, 04103 Leipzig

Education

Since 01/2013	PhD student in the Group of Prof. Dr. Peter Kovacs (IFB, "Genetics of Obesity and Diabetes"), Faculty of Medicine, University of Leipzig
09/2012-12/2012	Research fellow in the Group of Prof. Dr. Peter Kovacs (IFB, "Genetics of Obesity and Diabetes")
09/2012	Diploma of nutrition science (grade: 1.9)
09/2011-08/2012	Diploma thesis in the Group of Prof. Dr. Peter Kovacs (IFB, "Genetics of Obesity and Diabetes") entitled "Functional characterization of obesity and type 2 diabetes associated variant in Repin1"
10/2007-10/2011	Study of Nutrition Science (Diploma) at the Friedrich-Schiller-University of Jena, Germany
09/2010-10/2010	Internship Institut Dr. Appelt GmbH&Co.KG Leipzig
08/2009-10/2009	Internship in clinic „Lüneburger Heide- Kompetenzzentrum für Essstörungen"
09/1998-07/2007	Abitur Gymnasium Carolinum Neustrelitz (grade: 1.8)

Grants

02/2017	Research grant of the German Diabetes Association ("Einfluss von WHR-assoziierten genetischen Varianten auf die Adipozytenbiologie", 7.500€)
05/2016 **05/2015** **05/2014**	Travel grant of the German Diabetes Association
09/2016 **09/2014** **09/2013**	Travel grant European Association for the Study of Diabetes

Publications

1. Keller M, Klös M, Rohde K, **Krüger J**, Kurze T, Dietrich A, Schön MR, Gärtner D, Lohmann T, Dreßler M et al. (2018) DNA methylation of SSPN is linked to adipose tissue distribution and glucose metabolism. FASEB journal : official publication of the Federation o American Societies for Experimental Biology: fj201800528R. DOI:10.1096/fj.201800528R

2. **Krüger J**, Berger C, Weidle K, Schleinitz D, Tönjes A, Stumvoll M, Blüher M, Kovacs P, Klöting N (2018) Metabolic effects of genetic variation in the human REPIN1 gene. International journal of obesity . DOI:10.1038/s41366-018-0123-0

3. **Krüger J,** Schleinitz D (2017) Genetic Fingerprinting Using Microsatellite Markers i a Multiplex PCR Reaction: A Compilation of Methodological Approaches from Primer Design to Detection Systems. Methods in molecular biology (Clifton, N.J.) 1492: 1–15. DOI:10.1007/978-1-4939-6442-0_1

4. Ma L, Murea M, Snipes JA, Marinelarena A, **Krüger J**, Hicks PJ, Langberg KA, Bostrom MA, Cooke JN, Suzuki D et al. (2013) An ACACB variant implicated in diabetic nephropathy associates with body mass index and gene expression in obese subjects. PloS on 8(2): e56193. DOI:10.1371/journal.pone.0056193

5. Pfeiffer S, **Krüger J**, Maierhofer A, Böttcher Y, Klöting N, El Hajj N, Schleinitz D, Schön MR, Dietrich A, Fasshauer M et al. (2016) Hypoxia-inducible factor 3A gene expression and methylation in adipose tissue is related to adipose tissue dysfunction. Scientific reports 6: 27969. DOI:10.1038/srep27969

6. Tönjes A, Scholz M, Krüger J, Krause K, Schleinitz D, Kirsten H, Gebhardt C, Marzi C, Grallert H, Ladenvall C et al. (2018) Genome-wide meta-analysis identifies novel determinants of circulating serum progranulin. Human molecular genetics 27(3): 546–558. DOI:10.1093/hmg/ddx413

Oral presentations at scientific meetings

Krüger J, Weidle K, Kern M, Enigk B, Prellberg M, Müller l, Schleinitz D, Breitfeld J, Tönjes A, Stumvoll M, Blüher M, Kovacs P, Klöting N

Functional characterization of the type 2 diabetes associated variant rs3832490 in repin1, DDG 2013, Leipzig, Germany

Krüger J, Quandt M, Gutsmann B, Schleinitz D, Breitfeld J, Kern M, Klöting N, Tönjes A, Blüher M, Stumvoll M, Kovacs P

VEGFA is a candidate gene for regulation fat distribution,
DAG 2015, Berlin; Germany

Poster presentations at scientific meetings

Krüger J, Weidle K, Kern M, Enigk B, Prellberg M, Müller l, Schleinitz D, Breitfeld J, Tönjes A, Stumvoll M, Blüher M, Kovacs P, Klöting N

Functional analyses of the type 2 diabetes associated 12bp deletion in repin1,
EASD 2013, Barcelona, Spain

Krüger J, Prellberg M, Gutsmann B, Schleinitz D, Breitfeld J, Kern M, Klöting N, Blüher M, Stumvoll M, Kovacs P

Adipose tissue mRNA expression of WHR-associated genes exhibit inter-depot variability and correlates with fat distribution,
DDG 2014, Berlin, Germany

Krüger J, Prellberg M, Gutsmann B, Schleinitz D, Breitfeld J, Kern M, Klöting N, Blüher M, Stumvoll M, Kovacs P

Adipose tissue mRNA expression of WHR-associated genes exhibit inter-depot variability and correlates with fat distribution,
EASD 2014, Vienna, Austria

Krüger J, Quandt M, Gutsmann B, Schleinitz D, Breitfeld J, Kern M, Klöting N, Tönjes A, Blüher M, Stumvoll M, Kovacs P

VEGFA is a candidate gene for regulation fat distribution,
DDG 2015, Berlin; Germany

Krüger J, Quandt M, Gutsmann B, Schleinitz D, Breitfeld J, Kern M, Klöting N, Tönjes A, Blüher M, Stumvoll M, Kovacs P

The role of *VEGFA* in regulation of fat distribution,
EOS 2016, Gotheborg; Sweden

Krüger J, Fischer-Rosinsky A, Gieger C, Grallert H, Groop L, Kovacs P, Ladenvall C, Marzi C, Pfeiffer A, Scholz M, Spranger J, Stumvoll M, Thiery J, Thorand B, Toenjes A

Genome wide meta-analysis identifies novel regulators of circulating serum progranulin,
EASD 2016, Munich, Germany

Danksagung

Mein großer Dank geht an meinen Mentor Professor Peter Kovacs für die Chance, an vielen interessante Themen zu arbeiten. Vielen Dank für dein Vertrauen, deine Ideen, deine Freiheit und vor allem deine Unterstützung während der ganzen Zeit. Du hast es mir ermöglicht auf viele spannende internationale und nationale Kongresse zu fahren und so konnte ich meine Ergebnisse präsentieren und meine eigenen wissenschaftlichen Kenntnisse erweitern. Als Teil deiner Arbeitsgruppe bin ich in den letzten Jahren persönlich aber auch als Wissenschaftlerin gewachsen. Vielen herzlichen Dank.

Ich bedanke mich herzlich bei jedem Einzelnen der Arbeitsgruppe: Jana Breitfeld, Manuela Quandt, Esther Guiu Jurado , Beate Gutsmann und im Besonderen bei Dorit Schleinitz. Ich konnte jederzeit auf eure Hilfe zählen, egal ob bei der Durchführung eines Experimentes, einer helfenden Hand im Labor, bei wissenschaftlichen Fragen oder in Vorbereitung auf Vorträgen und Posterpräsentationen. Aber auch auf persönlicher Ebene habe ich die Zeit mit euch in vollen Zügen genossen.

In den letzten Jahren durfte ich mit vielen Kollegen zusammenarbeiten. Vielen Dank: Matthias Blüher, Nora Klöting, Claudia Berger, Matthias Kern, Anke Tönjes, Kerstin Krause, Ines Müller, Yvonne Böttcher, Kerstin Rohde, Maria Keller, Tobias Wohland, Luise Müller und Susanne Pfeiffer.

Ein letzter großer Dank für eure Liebe, Unterstützung, Kraft, Motivation und Rückhalt gilt meiner Familie, meinen langjährigen Freunden und vor allem meinem Mann Markus.